The Role of the Fas Receptor in Adipocyte Metabolism

Dissertation

zur

Erlangung der naturwissenschaftlichen Doktorwürde (Dr. sc. nat.)

vorgelegt der

Mathematisch-naturwissenschaftlichen Fakultät

der

Universität Zürich

von

RETO ANDREAS RAPOLD

von

Rheinau ZH

Promotionskomitee

Prof. Dr. François Verrey (Vorsitz)

PD Dr. Daniel Konrad (Leitung der Dissertation)

Prof. Dr. Marc Donath

Prof. Dr. rer. nat. Jürgen Eckel

Zürich 2010

Table of Contents

Acknowledgement

This is the summary of the work that I was able to do to serve my project. The following pages should not be read as witnesses of triumph or success or some kind of happy ending but rather as a farewell to the past 3.5 years. A period in my life which gave me a lot of experience introduced me to fascinating topics and brought me together with very interesting and nice people - and a period in my life which deprived me of self-esteem, motivation and belief in science. Euphemistically spoken, it is hard for me to assess the value of my achievements with which I apply for a PhD title. However, a PhD title is just an academic degree that does not honour someone for being an intellectual. An intellectual being is not defined by a certain amount of work or knowledge in an academic field. Knowledge is rather a tool for the intellectual to make better observations and clearer conclusions not only as a basis for his or her work but to base the whole life upon. Having the urge to be an intellectual I need a PhD title to sell myself and to have the chance to do something that is of value. I have always idealised the idea of a humble scientist - a scientist who is humbled by the complexity of nature and determined to find the absolute truth to serve mankind and not primary himself. But in this world the humble scientist has a hard time to receive applause let alone any grants! So at this point in my life looking back and into the future is not the easiest thing for me to do. My thesis is supposed to be great and amazing! Unfortunately, such thesis is hardly ever written. And as they are, I hope that the following pages carry some scientific importance.

I like to thank everybody who made this possible and supported me throughout these years, especially Daniel Konrad my supervisor and my dear colleague Stephan Wueest. I also like to thank Marc Donath and Markus Niessen for letting our group work in collaboration with their labs. Of course, I thank all of the nice technicians, master students, PhD students, postdocs and group leaders working and discussing on the same floor at University Hospital. I thank François Verrey and Jürgen Eckel the other members of my scientific committee for their valuable scientific advice.

Finally, I like to give a special and deeply felt “thank you” to my parents and to my brother for loving and supporting me no matter what. I love you.

Summary

Fas (FasR, CD95, Apo-1) is a member of the tumour necrosis receptor superfamily and plays a crucial role in the induction of apoptosis. In addition, depending on the cell type, activation of Fas can also induce non-apoptotic signalling pathways, including inflammation and proliferation. Recently, we demonstrated that Fas-deficient and adipocyte-specific Fas knockout mice are partly protected from insulin resistance induced by high-fat diet, but the mechanisms of this protective effect are incompletely understood. The aim of this study was to elucidate the molecular mechanisms behind this protective effect; in particular the impact of the Fas receptor on adipocyte metabolism.

Incubation of differentiating 3T3-L1 preadipocytes with 2 ng/ml Fas ligand (FasL) reduced the early induction of the p44/42 MAP kinases (ERK1/2), which is important for the initiation of differentiation. Furthermore, activation of the Fas receptor led to a decreased expression of the adipogenic markers C/EBPα, C/EBPβ and PPARγ.

Treatment with FasL also reduced C/EBPα and PPARγ in mature 3T3-L1 adipocytes. Moreover, activation of the Fas receptor in these cells influenced lipolysis in a time dependent fashion with an initial decrease after 2 hours and an approximately 2-fold increase after 12 hours. Fas activation induced phosphorylation of ERK1/2 with a peak after 6 hours and FasL-induced lipolysis was completely blocked by ERK1/2-inhibition. Additionally, the thiazolidinedione rosiglitazone inhibited both Fas-induced ERK1/2 activation and lipolysis.

We then aimed to determine upstream mediators and downstream effects of Fas-induced ERK1/2 activation to dissect the pathway(s) leading to increased lipolysis.

Fas activation reduced the PPARγ target perilipin. ERK1/2 dependent down-regulation of perilipin was shown to increase lipolysis. However, Fas-induced reduction of this lipid droplet coating protein was independent of ERK1/2 activation.

Furthermore, FasL treatment of adipocytes led to an increased secretion of the cytokines IL-6, KC (mouse IL-8 homologue) but not of TNFα. But neither IL-6 nor KC was found to be responsible for the ERK1/2-dependent induction of lipolysis.

Fas induced ERK1/2 activation and lipolysis could be partly reduced using extra- and intracellular calcium chelators and an inhibitor of calcium/calmodulin dependent

protein kinase II (CaMKII). However, we failed to demonstrate an increase in the enzyme's activity after FasL treatment.

Interestingly, FasL treatment reduced mRNA-expression and protein levels of the C/EBPα target lipin-1, a phosphatase involved in the generation of triacylglycerols. This effect was independent of ERK1/2 activation. It was previously shown that lack of lipin-1 leads to accumulation of its substrate phosphatidic acid (PA) in adipose tissue. We could show here that administration of PA to 3T3-L1 adipocytes increased phosphorylation of ERK1/2 and induced lipolysis.

In summary, we show that Fas activation inhibits adipocyte differentiation. In mature adipocytes, FasL treatment induces an inflammatory response and induces ERK1/2-dependent lipolysis. The latter is probably regulated by calcium-dependent pathways. Another possible mechanism involves Fas-mediated inhibition of triacylglycerol synthesis and subsequent activation of tryacylglycerol breakdown. These data underscore the role of the Fas receptor in the development of adipose tissue dysfunction and whole body insulin resistance.

Zusammenfassung

Fas (FasR, CD95, Apo-1) gehört zur Familie der Tumor Nekrosis-Faktor Rezeptoren und spielt eine tragende Rolle in der Auslösung der Apoptose. Des Weiteren kann die Aktivierung von Fas, je nach Zelltyp, eine Entzündungsreaktion oder eine Zellproliferation auslösen. Wir konnten vor kurzem zeigen, dass Fas-defiziente und fettzellspezifische Fas-Knockout-Mäuse unter einer Fett-angereicherten Diät weniger schnell insulinresistent werden. Der Mechanismus dieses protektiven Effekts ist aber weitgehend unklar. Ziel dieser Arbeit war es, die molekularen Hintergründe dieses protektiven Effekts genauer aufzuklären und dabei besonders den Einfluss des Fas-Rezeptors auf den Metabolismus der Adipozyten zu untersuchen.

Inkubation von differenzierenden 3T3-L1 Präadipozyten mit 2 ng/ml Fas Ligand (FasL) reduzierte die frühe Induktion der p44/42 MAP Kinasen (ERK1/2), welche wichtig für die Auslösung der Differenzierung ist. Des Weiteren reduzierte die Aktivierung des Fas-Rezeptors die fettzellspezifischen Markerproteine C/EBPα, C/EBPβ und PPARγ.

Auch in reifen 3T3-L1 Fettzellen wurden C/EBPα und PPARγ durch die Behandlung mit FasL reduziert. Zudem beeinflusste die Aktivierung des Fas-Rezeptors die Lipolyse zeitabhängig, mit einer Reduktion nach 2 Stunden und einer ca. 2-fachen Stimulation nach 12 Stunden. Die Aktivierung von Fas führte zur Phosphorylierung von ERK1/2 mit einem Höchstwert nach 6 Stunden. Die durch Fas ausgelöste Lipolyse konnte durch Inaktivierung von ERK1/2 komplett gehemmt werden. Auch das Thiazolidinedion Rosiglitazone hemmte sowohl die durch Fas ausgelöste ERK1/2 Aktivierung wie auch die Lipolyse.

Unser Ziel war es dann sowohl Auslöser wie auch Effekte der durch Fas ausgelösten ERK1/2 Aktivierung zu charakterisieren, um die Signalwege aufzuzeigen, die zu einer gesteigerten Lipolyse führen.

Die Aktivierung von Fas reduzierte das PPARγ-abhängige Protein Perilipin. Früher konnte gezeigt werden, dass eine ERK1/2-abhängige Reduktion von Perilipin die Lipolyse steigern konnte. Jedoch war die Fas-induzierte Reduktion dieses Fetttropfen-umhüllenden Proteins ERK1/2 unabhängig.

Des Weiteren führte eine Fas Aktivierung in Fettzellen zu einer gesteigerten Ausschüttung der Zytokine IL-6 und KC (Maus IL-8 Homolog) aber nicht von TNFα.

Hingegen konnten weder KC noch IL-6 für die ERK1/2-abhängige Steigerung der Lipolyse verantwortlich gemacht werden.
Die Fas-induzierte ERK1/2-Aktivierung und Lipolyse konnten teilweise durch das Verwenden von extra- und intrazellulären Kalziumchelatoren sowie einem Inhibitor der Kalzium/Kalmodulin-abhängigen Protein Kinase II (KaMK II) gehemmt werden. Wir konnten jedoch keine erhöhte Aktivierung dieses Enzyms nach der Behandlung mit FasL messen.
Interessanterweise reduzierte eine FasL-Behandlung die mRNA Expression und die Protein-Konzentration des C/EBPα-abhängigen Protein Lipin-1. Letzteres ist eine Phosphatase, welche in der Synthese von Triacylglycerinen involviert ist. Dieser Effekt war ERK1/2-unabhängig. Es ist bekannt, dass ein Fehlen von Lipin-1 zu einer Akkumulation seines Substrates Phosphatidsäure (PA) im Fettgewebe führt. Wir fanden, dass eine Behandlung von 3T3-L1-Adipozyten mit PA sowohl die Phosphorylierung von ERK1/2 wie auch die Lipolyse induziert.
Zusammenfassend zeigt die vorliegende Arbeit, dass die Aktivierung des Fas-Rezeptors die Differenzierung von Präadipozyten hemmt. Im reifen Adipocyten löst eine FasL-Behandlung eine Entzündungsreaktion aus und induziert die Lipolyse ERK1/2-abhängig. Letztere ist möglicherweise durch kalziumabhängige Signalwege reguliert. Ein anderer möglicher Mechanismus beinhaltet eine durch die Fas-Aktivierung gehemmte Triacylgycerinsynthese und eine dadurch induzierte Aufspaltung von Triacylglycerinen. Vorliegende Daten bestätigen eine mögliche Rolle des Fas-Rezeptors in der Differenzierung des Fettgewebes und der Entstehung der Insulinresistenz.

List of Figures

Figure

Abbreviations

ATP	adenosine triphosphate
ADP	adenosine diphosphate
BMI	body mass index
CaMKII	calcium/calmodulin dependent protein kinase II
ER	endoplasmatic reticulum
ERK	extracellular signal-regulated kinase
FFAs	free fatty acids
GLUT	glucose transporter
HSL	hormone-sensitive lipase
IL-6	interleukin-6
IR	insulin receptor
IRS	insulin receptor substrate
JAK	Janus protein tyrosine kinase
MAPK	mitogen-activated protein kinase
PA	phosphatidic acid, phosphatidate
PDE	phosphodiesterase
PPARγ	peroxisome proliferator activated receptor gamma
SOCS	silencer of cytokine signalling
TNFα	tumour necrosis factor alpha
WAT	white adipose tissue

Introduction

Glucose Metabolism

Glucose as an Energy Source

Glucose is a monosaccharide with the chemical formula $C_6H_{12}O_6$ and belongs to the family of carbohydrates with the chemical makeup $(CH_2O)_n$. Containing 4.1 kcal/g, glucose is a very important energy source for the human body. Enzymatic breakdown of the disaccharide maltose, sucrose or of higher molecular carbohydrates, such as starches, liberate glucose in the human digestive tract. The epithelial cells of the small intestine absorb glucose at their apical membrane with the sodium-dependent glucose transporter (SGLT1). Glucose exits the cells at the basolateral membrane through the glucose transporter 2 (GLUT2) into the blood. Insulin stimulates the uptake of glucose into adipose tissue and muscle by enabling the translocation of glucose transporter 4 (GLUT4) to the plasma membrane. Liver takes up glucose through the insulin independent GLUT2 (1). Glucose is stored as glycogen in liver and muscle. Glycogen is made up of glucose molecules linked together by α-1,4 linkages in the straight portions of the polymer, and by α-1,6 linkages at the frequent branch points. The human body can store up to approximately 1% of its weight as glycogen. If glycogen stores are full, the energy of glucose can be preserved by converting glucose to glycerol and fatty acids which are then stored as triacylglycerols in adipose tissue (1).

To make the chemical energy of glucose available for the cell, glucose is degraded in the cytosol to pyruvate by a process known as glycolysis. This process generates energy even in the absence of oxygen and yields 2 molecules of adenosine triphosphate (ATP) per molecule of glucose (anaerobic catabolism). In the absence of O_2, pyruvate is further metabolised to lactate. Aerobic catabolism on the other hand yields 30 to 32 molecule of ATP per molecule of glucose. In this case pyruvate is converted to acetyl CoA. Acetyl CoA enters the citric-acid-cycle in which the liberated energy is conserved as guanosine triphosphate (GTP) and the reduced electron carriers nicotinamide adenine dinucleotide (NADH) and flavin adenine dinucleotide ($FADH_2$). In the mitochondrial process of oxidative phosphorylation

these reduced nucleotides are used to generate a proton gradient that spurs the synthesis of ATP from adenosine diphosphate (ADP) (1).

The Endocrine Pancreas

The pancreas is a secretory organ with a weight of approximately 100 grams, which is located in the upper abdomen behind the stomach. The pancreas consists of two different parts: the exocrine pancreas, which secretes digestives enzymes and HCO_3^- into the digestive tract, and the endocrine pancreas. The major function of the endocrine pancreas is to keep the glucose concentration in the blood plasma at a constant level of around 5 mM (90 mg/dl). Such regulation is essential to provide fuel supply for the central nervous system which responses the most sensitive to a drop in glucose levels. Concentrations below 3 mM (hypoglycaemia) cause confusion, seizures or even coma. On the other hand, severe hyperglycemia (above 30 mM), as seen in the diabetic state, produces osmotic diuresis and can lead to severe dehydration, hypertension and vascular collapse. Furthermore, high glucose levels are detrimental to several tissues (glucotoxicity) (1,2).

The endocrine pancreas consists of four different secretory cell types: α-, β-, δ- and F-cells. These cells are organised in structures called “islets of Langerhans” that are dispersed within the pancreatic tissue. The islets form approximately 2 – 3 % of the whole pancreas and have a diameter ranging from 75 – 300 μm. Each islet consists of around 3000 secretory cells. α-cells secrete glucagon. β-cells secrete insulin, proinsulin, C peptide and a newly described protein called amylin. The product of δ-cells is somatostatin, and F-cells release pancreatic polypeptide. Around 70% of the cells in a human islet are β-cells and around 20% are α-cells. Blood supply of the islet is of portal origin and flows from the centre to the periphery. In humans, but even more pronounced in rats, β-cells are more abundant in the centre, whereas α- and δ-cells are more frequent in the periphery (1,2).

Insulin and Glucagon

The pancreatic β-cells are the only cells in the human body that make the peptide hormone insulin. Transcription of the insulin gene produces preproinsulin which is translated into the endoplasmatic reticulum (ER). During synthesis the leader sequence of the preprohormone is cleaved to yield proinsulin. Proinsulin consists of

the domains A, B and C. In the trans-Golgi where the protein is packed into secretory granules, proteases cleave proinsulin at two spots and excise the C domain (C-peptide). The resulting insulin consists of the domains A and B linked by disulfide bonds. Insulin is secreted together with C-peptide (1). The major trigger of insulin release from the β-cells is a rise in plasma glucose. Other monosaccharides (galactose, mannose) as well as certain amino acids and free fatty acids (FFAs) also stimulate insulin release. The gut hormones cholecystokinin (CCK), gastric inhibitory protein (GIP) and glucagon-like peptide 1 (GLP-1) are called incretins because they further increase the insulin response after a meal. Moreover, insulin secretion is under the control of the autonomous nervous system. Activation of β_2-adrenergic receptors increases insulin release whereas α_2-receptor activation inhibits it. Monosaccharides, amino and fatty acids have to be metabolised in the β-cell to have their ATP dependent stimulatory effect. Glucose enters the β-cell through GLUT2. The metabolism of glucose increases the amount of ATP in the cell. The increased concentration of ATP or the change in the ATP/ADP ratio inhibits a potassium channel and leads to depolarisation of the cell membrane. Depolarisation activates a voltage-gated calcium channel. This promotes calcium influx from the extracellular space which further promotes calcium release from intracellular stores. The elevated calcium concentration in the cell then leads to the exocytosis of insulin from secretory granules. Other modulators of insulin secretion act via the adenyl cyclase-cAMP-protein kinase A and the phospholipase C-phosphoinositide pathway (1,2).

The α-cells of the endocrine pancreas secrete glucagon, another very important hormone in fuel metabolism. Like insulin, glucagon is a polypeptide, but unlike insulin it consists of only one peptide chain. Glucagon with a length of 29 amino acids is processed from proglucagon in the α-cell. The intestinal L cells on the other hand also produce proglucagon but cleave it to yield the incretin GLP-1. Glucagon secretion from the α-cell is stimulated by amino acids released from protein digestion. The main target of glucagon is the liver and in many metabolic processes glucagon antagonises the effects of insulin. Glucagon is important in stimulating glycogenolysis, gluconeogensis, and ketogenesis (1,2).

Insulin Signalling

Insulin is a powerful anabolic hormone. Binding of insulin to the insulin receptor (IR) leads to a cascade of signalling events that lead to glucose uptake, glycogen synthesis, protein synthesis, gene expression and inhibition of apoptosis - depending on the cellular context (3).

The IR is a tetrameric membrane glycoprotein with intrinsic tyrosine kinase activity composed of two α and two β subunits. Insulin binds to the α subunit which contains a ligand binding domain and a cysteine-rich region. The β-subunit is a single-pass transmembrane protein with a cytoplasmic catalytic domain and an ATP-binding site. Disulfide-bounds connect the α and β subunits as well as the two α subunits. Insulin binding probably brings the two α subunits closer together and causes allosteric interactions between the two α and β pairs. The resulting conformational change allows ATP to bind to the β subunit which enables the autophosphorylation of the IR and, subsequently, the phosphorylation of intracellular protein substrates (1,3).

The IR substrate (IRS) proteins play an essential role in insulin signal transduction. They are phosphorylated by the IR on specific tyrosine residues. Once phosphorylated the IRSs serve as docking sites for additional signalling molecules. The IRS family is composed of 4 closely related members (IRS-1 to -4) and the more distantly related homolog, Gab-1. Knockout of IRS-1 cause severe growth retardation and mild insulin resistance. Ablation of IRS-2 induces peripheral insulin resistance and impaired growth of pancreatic β-cells. IRS-1 and IRS-2 have widely overlapping tissue distribution which points to specific roles of each protein. Ablation of IRS-3 does not cause a clear phenotype, whereas lack of IRS-4 is associated with modest growth retardation and insulin resistance. Gab-1 seems to be involved in hepatic growth rather than in insulin signalling (3-7).

Proteins that contain a *Src* homology domain 2 (SH2) get activated by docking to certain phosphorylated tyrosine residues on IRS. One of these proteins is phosphatidylinositol 3-kinase (PI 3-kinase). Activated PI 3-kinase generates phosphatidyl inositol-3,4,5-triphosphate (PIP_3) from phosphatidyl inositol-4,5-biphosphate (PIP_2). PIP_3 acts as an intracellular messenger, leading to the activation PI-dependent kinase (PDK). PDK is a Ser/Thr kinase which activates Akt (protein kinase B, PKB). Akt then phosphorylates its substrate of 160 kDa (AS160), which is a Rab-GTPase activating enzyme. This insulin dependent signalling pathway finally

leads to the insertion of GLUT4 into the plasma membrane and increased glucose uptake by the cell (1,8).

Akt activation can also lead to phosphorylation of glycogen synthase kinase-3 (GSK-3). Phosphorylation inactivates GSK-3 which in turn is no longer able to inactivate glycogen synthase through phosphorylation. Thus, activation of this insulin signalling pathway leads to the synthesis of glycogen in liver and muscle. In the adipocyte, Akt activates the cyclic nucleotide phosphodiesterase 3B (PDE 3B), thereby reducing cAMP levels in the cell and, consequently, decreasing lipolysis. Furthermore, Akt has the ability to phosphorylate proteins that regulate lipid synthesis, protein synthesis and cell survival (1,3,9).

Insulin achieves its effects not only via PI 3-kinase dependent pathways. Direct phosphorylation of SHC (Src homology, C terminus) by the IR and activation of growth factor receptor binding protein 2 (GRB2) through IRS leads to activation of the mitogen-activated protein kinase (MAPK) pathway (1).

Insulin Action in Different Organs

In general, insulin promotes anabolism and reduces catabolic processes. In the liver, insulin increases the formation of glycogen from glucose by inducing the transcription of glucokinase and through activation of glycogen synthase. The liver takes up glucose via GLUT2, which is not insulin responsive. However, by inducing glycogen synthesis insulin increases liver glucose uptake indirectly. Glycogen breakdown is inhibited by insulin through inhibition of glycogen phosphatase and glucose-6-phosphatase. Moderate increases in insulin levels allow gluconeogenesis to persist while the hepatocyte stores the newly formed glucose 6-phosphate as glycogen rather than releasing glucose to the blood. At high concentration however, insulin also inhibits the gluconeogenic pathway. Insulin stimulates pyruvate generation from glucose and pyruvate oxidation with the consequence that this substrate is no longer available for gluconeogenesis. Moreover, insulin diminishes transcription of the phosphoenolpyruvate carboxykinase gene which encodes for a key enzyme in gluconeogenesis. Insulin further promotes the formation of triacylglycerols in hepatocytes and their export in very-low-density lipoproteins (VLDL). Finally, insulin inhibits proteolysis and increases protein synthesis in the liver (1).

Striated muscle is the main tissue of insulin mediated glucose disposal. As described earlier, insulin promotes the insertion of GLUT4 into the plasma membrane of muscle

and adipose tissue. By this process insulin increases glucose uptake of muscle, and it favours the subsequent conversion of glucose to glycogen through activation of hexokinase and glycogen synthase. Furthermore, insulin increases glucose breakdown and oxidation. Like in the liver insulin also has an anabolic effect on protein metabolism in muscle (1).

In adipose tissue, similar to muscle, insulin stimulates glucose uptake via GLUT4. Insulin promotes glycolysis to generate glycerol-3-phosphate and stimulates pyruvate dehydrogenase and acetyl CoA carboxylase to synthesise fatty acids. Insulin enhances the esterification of these molecules to form triacylglycerols. As mentioned earlier, insulin also inhibits the breakdown of triacylglycerols (lipolysis) by decreasing the activity of hormone-sensitive lipase (HSL). Finally, insulin induces the synthesis of lipoprotein lipase (LPL). LPL is exported from the adipocytes to the surface of the endothelial cells. There LPL acts on triacylglycerols in chylomicrons and thereby liberates fatty acids for triacylglycerol built up in fat cells (1).

White Adipose Tissue

Function and Composition of White Adipose Tissue

The primary function of white adipose tissue (WAT) is to store energy in the form of triacylglycerols during times of energy excess. In times of energy requirement, stored lipids are released as FFAs and glycerol. As large energy reserve of the body and insulin responsive organ, adipose tissue has a major impact on energy flux and plasma lipid levels. Adipose tissue is now also appreciated to be an endocrine organ that secretes multiple factors controlling whole body metabolism (10).

WAT not only consists of adipocytes but also harbours other cell types. This so called stromal vascular fraction includes cells types such as preadipocytes, endothelial cells, pericytes, monocytes, macrophages, and others. All of these cells have an important function in maintaining adipose tissue homeostasis. For example, endothelial cells and pericytes make up the vasculature of adipose tissue and thereby enable adipose tissue growth and development. Macrophages are thought to be necessary for the clearance of necrotic adipocytes, which particularly seems to play a role in obesity and its associated complications (11).

Adipocyte Commitment and Differentiation

The adipose lineage arises from multipotent stem cells of mesodermal origin within the vascular stroma of WAT. In an initial commitment step, known as determination, the precursor cells become preadipocytes which are restricted to the adipocyte lineage but show no special morphological features (10,12).

Adipocyte differentiation consists of a coordinated cascade of transcriptional events, which turns preadipocytes into mature, lipid filled adipocytes. The most important members of the adipogenic program are the transcriptional factors of the CCAAT-enhancer-binding protein (C/EBP) family and the peroxisome proliferator activated receptor γ (PPARγ). The first transcriptional factors to be expressed are C/EBPβ and C/EBPδ. The transcriptional activation of C/EBPβ is controlled by the cAMP-response element binding protein (CREB). However, at first, C/EBPβ lacks DNA-binding capacity because it forms heterodimers with the dominant negative isoform CHOP-10 (C/EBPζ). CHOP-10 is subsequently down-regulated and C/EBPβ is freed.

Subsequent hyperphosphorylation enables C/EBPβ to bind DNA. Together with C/EBPδ it induces C/EBPα and PPARγ. PPARγ and C/EBPα positively regulate each other's expression. PPARγ is the central regulator of adipogenesis and responsible for the activation of genes involved in fatty acid binding, uptake and storage. C/EBPα was shown to be required for the acquisition of insulin sensitivity (10,12).
For the differentiation of 3T3-L1 preadipocytes, a process called mitotic clonal expansion (MCE) was shown to be crucial. MCE consist of about two rounds of mitosis after the postconfluent growth-arrested cells are induced to differentiate. The p42 and p44 MAPKs, also called extracellular signal-regulated kinase (ERK) 1 and 2, play an essential role in this process (13).

Adipose Tissue Distribution

In humans WAT begins to develop early in the second trimester and at the time of birth it is well developed. Human WAT is dispersed throughout the body with subcutaneous and intra-abdominal depots representing the main compartments for triacylglycerol storage. Subcutaneous WAT is localised directly under the skin with major depots in the buttocks, thighs, and abdomen. Intra-abdominal WAT represents the fat inside the peritoneal cavity and can be further divided into an omental, a retroperitoneal and a visceral compartment. The latter consists of a mesenteric and a perirenal depot. Women have a higher percentage of body fat than man. However, pre-menopausal women store only 6% of body fat as visceral adipose tissue whereas in men it accounts for around 20% of total body fat. Fat distribution changes with age. Subcutaneous fat decreases and intra-abdominal fat increases making sex-related differences less prominent (11,14,15).
In the context of obesity fat distribution can be estimated by measuring the ratio of waist to hip circumference (WHR). People with low WHR accumulated more subcutaneous adipose tissue and exhibit so called pear-shaped obesity. High WHR is an index for accumulation of more visceral adipose tissue named apple-shaped or visceral obesity. This classification gained considerable interest as people with visceral obesity are at high risk to develop the metabolic syndrome and diabetes whereas people with subcutaneous obesity are not. There are two possible not mutually exclusive explanations for this phenomenon. The first is based on the fact that visceral fat drains its products (FFAs, cytokines and adipokines) into the portal circulation where they act primary on the liver to affect metabolism. The second is

based on the concept that adipocytes from different depots have different properties making them more or less prone to cause metabolic complications in the obese state. Indeed, visceral and subcutaneous adipose tissues have a different gene expression profile and show several other differences. For example, visceral adipose tissue secretes more interleukin-6 (IL-6), a cytokine involved in the development of insulin resistance and diabetes. Diabetes can be treated with thiazolidinediones (TZDs), which are PPARγ agonists. Interestingly, amelioration of the metabolic profile during treatment is associated with a selective increase of subcutaneous adipose tissue whereas visceral fat is unchanged. Furthermore, visceral WAT is more responsive to β-adrenoreceptor-mediated lipolysis. Exercise, which is known to improve metabolism in diabetics, consequently leads to more visceral than subcutaneous fat loss. Thus, the human body not only stores triacylglycerols in different locations, but the amount of these individual depots and the balance between them play an important role in complications associated with obesity (14,15).

Adipose Tissue Expansion

From a thermodynamic point of view, an increase in adipose tissue results from a decrease of energy expenditure or an increase in energy intake with food. The surplus of energy is stored as glycogen in liver and muscle and as triacylglycerols in WAT. As glycogen deposition to liver and muscle is limited, the main energy storage organ in mammals is adipose tissue. The adipocyte is unique among cells in that more than 95% of the cell volume consists of stored triacylglycerols and its diameter can change from 25 to 200 μM. WAT is the only tissue in the body that can markedly change its mass in adulthood. Thus, fat mass can range from 2 to 3% of body weight in extremely well trained athletes to 60 – 70% in massively obese humans. Gain of fat mass consists of two possible processes: first, enlargement of adipocytes (hypertrophy) and second: commitment as well as proliferation of preadipocytes and their subsequent differentiation into new adipocytes (hyperplasia) (11,16-19). However, it was shown that total adipocyte number as well as the different amount of adipocytes between lean and obese humans is established during childhood and adolescence. During adulthood it was postulated that the total number of adipocytes does no longer change, even during weight gain. Of note, the authors of that study looked at subjects with early onset obesity and they could not role out that there is

recruitment of additional adipocytes from precursor cells with increasing weight gain in adult subjects (20).

Triacylglycerol Synthesis

Triacylglycerols are synthesized through step-wise addition of acyl groups to glycerol-3-phosphate. Since in adipocytes glycerol kinase activity is negligible, glycerol-3-phosphate is derived from glucose or produced by glyceroneogenesis from gluconeogenic substrates depending on nutritional status. The acyl moieties derive either from de novo fatty acid synthesis with glucose as the main source (lipogenesis) or from FFAs taken up from the plasma (21).

The first acyl group is transferred to glycerol-3-phosphate by glycerol-3-phosphat acyltranferase (GPAT) yielding lisophosphatidate (LPA). LPA is then converted to phosphatidate (PA) through addition of another acyl group by acylglycerol-3-phophate acyltransferase (AGPAT). PA phosphatidase-1 (PAP1), better known as lipin-1, dephosphorylates PA producing diacylglycerol (DAG). Diacylglycerol acyltransferase (DGAT) adds the last acyl group to diacylglycerol to form triacylglycerol. The acyl transferases constitutively reside in the ER whereas lipin-1 is cytosolic and only transiently associates with the ER membrane to perform the PAP1 reaction (22).

Among the mentioned enzymes lipin-1 is special as it can also act as a transcriptional coactivator. In this function nuclear lipin-1 amplifies the expression of genes involved in fatty acid oxidation. Moreover, lipin-1 plays an important role during adipocyte differentiation and in the maintenance of adipocyte-specific gene expression by interacting with PPARy (22,23).

Mutations in the lipin-1 gene cause lipodystrophy and insulin resistance in mice (24). Furthermore, these fatty liver dystrophy (fld) mice show an increase of the lipin-1 substrate PA in WAT (25) which might play an important role as second messenger in this tissue. Mice that over-express lipin-1 in their mature adipocytes show increased adiposity and accelerated diet-induced obesity. However, these animals have increased insulin sensitivity (26). The importance of lipin-1 is further underlined by the fact that in mice and healthy male humans, lipin-1 expression correlates with a better metabolic profile (27).

Triacylglycerol Storage

Adipocytes store triacylglycerols in the form of one or more lipid droplets. These organelles presumably emerge from the ER lipid bilayer or a subset of ER membranes. Their core of triacylglycerols is surrounded with a phospholipid monolayer and coating proteins of the perilipin family. Besides stabilisation these proteins likely execute coordinative functions in the metabolism of the lipid droplet (28). The family founding member perilipin for example is an effective shielding protein that reduces the access of cytosolic lipases to the triacylglycerols. But apart from that barrier function, perilipin also seems to be needed for hormonally stimulated lipolysis since β-adrenergic receptor agonists fail to maximally stimulate this process in perilipin null adipocytes (29).

Lipolysis

Lipolysis describes the step-wise hydrolysation of triacylglycerols to diacylglycerols, monoacylglycerols and glycerol and FFAs by lipases (esterases). One triacylglycerol molecule is usually completely broken down to one molecule of glycerol and three molecules of FFAs. Nevertheless glycerol and FFAs are not released from the cell in the ratio 1:3 since some FFAs are re-esterified. But, because of the low glycerol kinase activity in adipocytes, only insignificant amounts of glycerol are re-utilized (30).

Three enzymes that catalyse triacylglycerol breakdown are known so far. HSL hydrolyses triacylglycerols to diacylglycerols and diacylglycerols to monoacylglycerols. Monoglycerid lipase (MGL) breaks down monoacylglycerols to glycerol and FFAs. The function of the adipocyte-specific triglyceride lipase (ATGL) seems to be the catalysis of the first step of triacylglycerol catabolism. Importantly, only HSL is responsive to hormone stimulation (30).

HSL exists in three isoforms ranging from 84 to 130 kDa. The enzyme contains three domains, a catalytic domain, a regulatory domain with several phosphorylation sites, and a variable N-terminal domain that can interact with other proteins or with lipids. The activity of the enzyme is dependent on serine phosphorylation. Increased activity of HSL is induced through phosphorylation on the Ser-563 residue by protein kinase A (PKA). In contrast, Ser-565 is phosphorylated in the basal state and prevents phosphorylation on Ser-563, thus decreasing lipase activity. Ser-659 and Ser-660

were also found to be activity controlling sites. Furthermore, the MAPKs ERK1/2 can activate the enzyme through phosphorylation on Ser-600 (31).

Lipolysis is typically stimulated by beta$_{1,2,3}$-adrenergic receptor agonists. In the physiological context the catecholamine hormones noradrenaline and adrenaline are the most important of this class of substances. In cell culture the $\beta_{1,2}$-receptor agonist isoproterenol is often used as a positive control when looking at lipolysis. Adrenoreceptors are coupled to G_s-proteins that activate adenylate cyclase, so that the production of cyclic AMP (cAMP) increases upon receptor stimulation. Increased levels of cAMP activate PKA which phosphorylates HSL leading to breakdown of triacylglycerols. Insulin on the other hand is a powerful inhibitor of lipolysis. IR stimulation leads to increased activity of phosphodiesterase 3 which converts cAMP to 5'-AMP thereby decreasing PKA and, subsequently, HSL activity. Additionally, humans have α_2A-adrenoreceptors that decrease lipolysis through their interaction with G_i-proteins and subsequent inhibition of adenylate cyclase (30,31).

Besides the well established stimulation by beta adrenergic receptor agonists, lipolysis can also be increased by other compounds. The cytokine tumour necrosis factor alpha (TNFα) stimulates lipolysis through activation of ERK1/2 and down-regulation of the lipid droplet coating protein perilipin (32). Furthermore, the cytokine IL-6, which is secreted by working muscle, has lipolytic activity in humans (33). In experiments performed with stromal vascular fractions containing newly differentiated adipocytes from human donors IL-6 as well was shown to signal via the ERK1/2 pathway (34). Studies in primary cells and cell lines suggest that lipolysis can also be positively influenced by a rise in intracellular calcium (Ca) levels that induce different signalling pathways involving calcium/calmodulin dependent protein kinase II (CaMKII), protein kinase C (PKC) and ERK1/2 (31). On the other hand, increased Ca seems to inhibit lipolysis in human adipocytes through induction of PDE activation and a subsequent decrease in cAMP (35).

Adipose Tissue as an Endocrine Organ

Since the 1980s it became clear that adipose tissue not only acts as energy storing compartment but also as an endocrine organ. Several factors are highly expressed in the adipocyte and get secreted by the cell. These adipose tissue derived molecules are generally termed adipokines. Adiponectin is the adipokine with the most restricted expression pattern. There are very few reports of adiponectin being produced by

other cells than adipocytes. Other adipokines such as leptin, however, show expression patterns that are less fat cell-specific. Moreover, hormones like resistin, omentin, and visfatin are made by several other tissues, as well (11).

Leptin is a 16 kDa protein encoded by the *ob* gene. The levels of leptin in circulation correlate directly with adipose tissue mass. Control of appetite is the primary role of leptin. Mice as well as human subjects with a mutation in the leptin (*obese*, *ob/ob*) or the leptin receptor (*diabetes*, *db/db*) gene are massively obese. Binding of leptin to its receptor on neurons in the hypothalamus provides the brain with information regarding energy stores of the body. By modulation of several orexigenic (appetite stimulating) and anorexigenic (appetite suppressing) peptides leptin decreases food intake and promotes weight loss. Besides adipose tissue, leptin is released by the stomach. Thereby it also influences short-term regulation of appetite and meal size together with other satiety peptides. On the other hand, fasting was shown to significantly reduce leptin levels and this change was much greater than the loss in adipose tissue. Several other studies have further supported the importance of leptin in the neuroendocrine response to starvation. Leptin is involved in other biological processes as well, including reproduction (initiation of human puberty), haematopoiesis, angiogenesis, bone formation and wound healing. Furthermore, leptin exerts a proinflammatory role, while at the same time protecting against infections (36,37).

Adiponectin (ACRP30, adipoQ, apM1, or GBP28) is a 30 kDa protein induced during adipocyte differentiation. The adipokine consists of an N-terminal collagenase and a C-terminal globular domain. After being synthesised adiponectin forms trimers, which then aggregate to polymers. In circulation, adiponectin exists as either a trimer, a hexamer (called the low molecular weight (LMW) form), or as multimeric forms of 12 to 18 subunits (high molecular weight (HMW) form). There are three possible receptors for adiponectin. One is mainly in the liver (AdipoR2), one in skeletal muscle (AdipoR1), and one on endothelial cells and smooth muscle cells (T-cadherin). Adiponectin reduces glucose output of the liver and suppresses gluconeogenic genes. It was also shown to have potent cardioprotective effects, and hypoadiponectinemia is highly correlated with cardiovascular disease (11,38).

Adiponectin does not increase with increased body fat mass like leptin. On the contrary, adiponectin serum levels are inversely correlated with obesity. Furthermore, the adipokine is significantly decreased in patients with type II diabetes. However,

several insulin resistant populations exhibit this relationship independent of obesity. The mechanism linking decreased adiponectin levels to the insulin resistant state is not completely clear. Administration of adiponectin to mice results in decreased glucose, FFAs and triacylglycerol levels. Adiponectin partly seems to mediate its positive effects on metabolism through activation of the 5`-AMP-activated protein kinase (AMPK) in muscle and liver. This leads to increased fatty acid oxidation and glucose uptake in myocytes in vitro. In mice, this adiponectin effect inhibits expression of proteins involved in gluconeogenesis in liver and thereby decreases glucose levels. Increased oxidation of FFAs in muscle triggered by adiponectin might have a positive effect on insulin signalling in muscle and on whole body insulin sensitivity. The low-inflammatory state associated with obesity might have a negative impact on adiponectin, since the cytokines TNFα and IL-6, which are both increased in obese subjects, inhibit adiponectin gene expression. On the other hand, adiponectin has anti-inflammatory properties and reduces the production of IL-6 and TNFα, while inducing the anti-inflammatory cytokines IL-10 and IL-1 receptor antagonist (11,36,38,39).

Resistin is a 12 kDa protein that is predominantly expressed by adipocytes in mice whereas the primary source in humans seems to be macrophages. It belongs to a family of resistin-like molecules, RELM (also called “found in inflammatory zone”, FIZZ). The protein known as FIZZ-3 was called resistin because of its ability to induce mainly hepatic insulin resistance in mice. Resistin levels are elevated in both diet-induced obesity and genetic mouse models of obesity/diabetes (*ob/ob* and *db/db* mice). However there is no consistent link between resistin levels and either obesity or insulin resistance in humans. In human subjects resistin may act as a mediator of the insulin resistance associated with sepsis and possibly other inflammatory conditions (36,38).

Obesity and Type 2 Diabetes

The Epidemiology of Obesity

Obesity is generally defined as excess body fat. However, the definition of excess is not clear-cut. Accumulation of adipose tissue develops gradually and there is no clear separation into normal and abnormal. Because direct measurement of body fat content is difficult, the body mass index (BMI) is used as an indirect index to define obesity. The BMI is calculated as weight in kilograms divided by height in meters squared and thus, sets total body weight (not total body fat) in relation to height. Currently, a healthy weight in adults is defined as a BMI between 18.5 and 24.9 kg/m^2, overweight as a BMI of or greater than 25 kg/m^2, obesity as a BMI of or greater than 30 kg/m^2 and extreme obesity as a BMI of or greater than 40 kg/m^2. In the United States of America, overweight in children is defined as a BMI at or above the 85^{th} percentile and obesity as BMI at or above the 95^{th} of the 200 CDC growth charts (40).

In the USA the prevalence of adults that are overweight increased from 44.9 to 66.2% between 1960 and 2004. Among them, mainly the prevalence of obesity and extreme obesity increased from 13.3 to 32.9% and from 0.9% to 5.1% respectively, whereas the percentage of people that are overweight but not obese remained stable during that period. The prevalence of obesity changed little between 1960 and 1980. However, between 1980 and 2000 the percentage of obesity more than doubled from 15 to 30.9 %. Until 2004 obesity further increased to 31.7% in men and 34% in women. The dramatic increase of people with excess body weight is not limited to the adult population. In the USA the prevalence of overweight children (2 – 19 years of age) increased from 5.1 to 17.1% between 1974 and 2004 (40).

The increasing prevalence of obesity is not experienced by the USA alone but is becoming a worldwide phenomenon. By 2010 one out of ten school children in Europe is expected to be obese. Also in Switzerland obesity prevalence in adults and children has clearly increased in the past three decades. Between 1960 and 2002 the prevalence of overweight in Swiss children (6 – 12 years of age) increased from 5.1% in boys and 5.8% in girls to 19.9% and 18.9%, respectively. During the same time period obesity in Swiss children increased from 0.25 to 7.4% in boys and from 0.41 to

5.7% in girls. The percentage of obese Swiss adults by 2004 was 14.2% for men and 12.5% for women (40-43).

The onset and progression of obesity have multiple determinants such as genetic background, environmental factors (i.e. diet), behaviour factors (i.e. inactivity) and socioeconomic status. Likely a gene-environment interaction in which genetically susceptible individuals respond to the modern western environment with unlimited access to palatable energy-dense foods and reduced demand for energy expenditure, contributes to the current high prevalence of obesity. The clinical problem of overweight and especially obesity lies in its strong association with a number of chronic diseases such as hypertension, dyslipidemia, cardiovascular disease, non-alcoholic fatty liver disease, certain cancers, insulin resistance and diabetes mellitus, and others (40).

Adipose Tissue Dysfunction and Inflammation in Obesity

As described earlier, adipose tissue stores energy in form of triacylglycerols. Through sequestration of lipid molecules, especially FFAs, away from tissues, which are not suited for lipid storage, adipose tissue protects the body from toxic effects of these compounds (lipotoxicity). As outlined above, WAT plays also a role as endocrine organ. In healthy subject, factors secreted by adipocytes regulate whole-body metabolism and neuroendocrine control of food intake. During prolonged intake of excess energy and the resulting development of obesity, WAT becomes dysfunctional and inflamed. This pathological condition of WAT has a negative impact on many organs and tissues like muscle, liver, pancreas (44).

Hyperphagia induces increased energy deposition in WAT as triacylglycerols and consequently causes the adipocytes to enlarge (hypertrophy). Hypertrophied fat cells show a different pattern of secreted factors. For example, leptin and IL-6 are up-regulated as well as monocyte chemoattractant protein-1 (MCP-1). MCP-1 enhances macrophage infiltration into WAT. Lean subjects normally exhibit a macrophage content of under 10% in WAT. In obese humans however, nearly 40% of the cells in adipose tissue are macrophages (45). In obesity macrophages form crown-like structures around necrotic adipocytes. This gives rise to the hypothesis that adipocytes can enlarge to a certain size before they undergo cell death, and macrophages clear the resulting debris. Macrophages also secrete MCP-1 to attract more inflammatory cells. Furthermore, they secrete inflammatory cytokines like

TNFα, IL-6 and IL-1β as well as the adipokine resistin in humans. Macrophages are the major source of TNFα produced by WAT and the origin of around 50% of WAT-derived IL-6. Inflammatory cytokines negatively affect the secretion pattern of adipocytes. TNFα for example decreases the secretion of adiponectin. Moreover, inflammatory cytokines have a dramatic influence on adipocyte function resulting in insulin resistance, increased lipolysis and decreased lipogenesis (36,44,46).

TNFα down-regulates PPARγ on multiple levels. PPARγ is an essential regulator of adipogenesis and is required for the maintenance of mature adipocyte function. On the other hand, TNFα stimulates lipolysis through multiple mechanisms. TNFα reduces insulin signalling and thereby inhibits the antilipolytic actions of insulin in adipocytes. TNFα increases cAMP levels in the cell by down-regulation of inhibitory G-protein coupled receptors. Finally, TNFα decreases perilipin expression via an ERK1/2 mediated pathway and also down-regulates the function of this lipid-coating protein (32,44).

In obesity, as a result of permanent nutritional overflow, WAT additionally suffers from organelle dysfunction, impacting mitochondria an ER. The so called ER-stress leads to the activation of the unfolded protein response (UPR). Besides the attenuation of protein translation and the increased chaperone transcription, ER stress and the UPR are linked to major inflammatory and stress signalling networks. UPR induces inflammatory genes in many cell types. Furthermore, ER stress induces the activation of the enzyme c-Jun N-terminal kinase (JNK). JNK1 inhibits insulin signalling through serine phosphorylation of IRS-1. One possible action of JNK is also the phosphorylation and inhibition of PPARγ. However, the importance of ER-stress in adipocyte insulin resistance and inflammation warrants further investigation (47).

Besides the afore mentioned disturbances originating from increased cell volume, inflammation and ER dysfunction, the adipose tissue is also confronted with oxidative stress and probably metabolic stress. The latter is caused by the increased availability of glucose and fatty acids as well as by the resulting metabolites. All those stresses are connected to each other and lead to signalling through a network of stress-sensing kinases. These enzymes including JNK1/2, p38 MAPK, ERK1/2, IKKβ, mTOR and PKCs linking the state of overnutrition to cellular dysfunction (48).

From Insulin Resistance to Type 2 Diabetes

In obesity, WAT is not longer able to store energy properly resulting in increased FFA release. Additionally adipose tissue is a source of inflammatory cytokines. The excess circulating FFAs cause accumulation of lipids in skeletal muscle, the liver and β-cells of the pancreas. Besides the negative impact of this ectopic fat deposition, increased release of inflammatory cytokines impair the metabolic function of these organs. The combined action of both FFAs and cytokines produces whole body insulin resistance (44).

Skeletal muscle is the main insulin responsive tissue in the body. In muscle, FFAs activate several protein Ser/Thr kinases which phosphorylate IRS proteins on serine residues and thereby inhibit insulin signalling. Fatty-CoA and diacylglycerol for example activate protein kinase C theta (PKCθ). PKCθ then inactivates IRS signalling through phosphorylation. FFAs also inhibit Tyr phosphorylation of the IR and IRS proteins. Toll-like receptor (TLR) 2 and 4 may also play a role in FFA-induced insulin resistance in muscle. Ceramides are lipid metabolites which are increased in obesity in rodents and humans. Increased ceramide synthesis induced by TNFα or saturated FFAs inhibit insulin signalling on the level of AKT/protein kinase B (PKB) activation. Further, TNFα impairs insulin signalling by inducing Ser/Thr phosphorylation of IRS proteins. This effect of TNFα is mediated by JNK1 and MAP4K4 in muscle (44).

FFA overload of the liver causes triacylglycerol accumulation in hepatocytes termed hepatosteatosis, and consequently hepatic insulin resistance. The adipose tissue derived cytokine IL-6 may also play an important role in inducing hepatic insulin resistance (46).

In the insulin resistant state more insulin is needed to achieve normal glucose levels (normoglycemia). The secretion of adequate amounts of insulin depends on both β-cell mass and function. The pancreas reacts to the increased insulin demand through proliferation of β-cells. Multiple factors influence the balance of β-cell proliferation and apoptosis. For example, hyperglycemia induces production of the cytokine interleukin 1 beta (IL-1β) by β-cells. Low concentrations of IL-1β were shown to induce Fas/FLIP-mediated proliferation of β-cells and this is probably part of the adaptive response in the insulin resistant state. On the other hand, high concentrations of IL-1β induce apoptosis of β-cells. Saturated fatty acids are also highly toxic for β-cells.

TNFα in combination with other adipose tissue derived cytokines probably further potentate this effect. Insulin resistant individuals who fail to adopt properly finally develop type 2 diabetes mellitus. In the latter, glucose concentration in the blood is permanently elevated with detrimental effects for the body (49,50).

The Fas Receptor

Fas and its Ligand FasL

Fas was first described in 1989 as surface molecule on lymphocytes that triggers cell death (51). The gene that encodes the Fas receptor (FasR, CD95, Apo-1) is located on mouse chromosome 19 and on human chromosome 10 (52). Fas ligand (FasL, CD95L) is located on chromosome 1 in both mice and humans (53,54).

Fas is a type I transmembrane protein that belongs to the tumour necrosis factor (TNF)/nerve growth factor (NGF) receptor superfamily (55). Members of this family share characteristic extracellular cysteine-rich domains, which control ligand binding and spontaneous self-assembly into trimers (51). Fas is activated by Fas ligand, a type II membrane protein and typical member of the TNF ligand family (56). The ability of Fas to induce apoptosis upon ligand binding depends on a conserved part of the cytoplasmic domain termed death domain (DD). The death domain consists of six α-helices, which bind to other DD-containing proteins. Due to their death domains a subset of TNF receptor superfamily members including TNF receptor 1 are often termed death receptors. However, the term death domain as well as death receptor are misleading as those receptors can also induce pathways leading to proliferation and survival instead of death (51).

The human Fas gene consists of nine exons and several transcripts are derived from the gene through alternative splicing. The transcripts give rise to multiple soluble variants of Fas which have been shown in vitro to have a negative regulatory role on membrane expressed Fas. Furthermore, human thymocytes express a membrane-bound form of Fas that has been described to act as a decoy receptor for Fas. FasL can exist in membrane bound and soluble form but the Fas-stimulatory capacity of membrane-bound FasL is magnitudes higher compared to soluble FasL (57).

In the adult mouse Fas and FasL are expressed in several tissues including the thymus, lung, spleen, small intestine, large intestine, seminal vesicle, prostate, uterus and adipose tissue [(58), and own observation]. In mice naturally occurring mutations of Fas and FasL cause lymphoproliferation (*lpr*) and generalized lymphoproliferative disease (*gld*). These mutant animals are important for the determination of the biological role of Fas and FasL (59)

Fas Signalling

Fas monomers spontaneously self-assemble to trimers in the cell membrane. Binding to FasL or agonistic Fas antibodies presumably induces a conformational change of these trimers allowing the recruitment of DD-containing adaptor proteins. There are three Fas DD-binding molecules known so far: the Fas Associated Death Domain protein (FADD/MORT-1), the death associated protein Daxx, and the Receptor Interacting Protein (RIP) (51).

Fas-induced apoptosis is mediated with the help of the adaptor protein FADD. FADD binds to pro-caspase 8 and/or pro-caspase-10. The resulting complex is called death inducing signalling complex (DISC). At the DISC pro-caspase-8 (and/or -10) converts itself to active caspase 8 (also known as FADD-like interleukin-1 converting enzyme, FLICE). Caspases are cysteine proteases that cleave their substrates at aspartic acid residue. In cells of type I, DISC formation leads to the cytoplasmic caspase cascade in which the initially activated caspases activate other pro-caspases. In type II cells DISC formation is strongly reduced and the apoptotic signal is amplified through mitochondrial destabilisation and release of pro-apoptotic molecules including cytochrome c. Both pathways converge on caspase 3 activation and programmed cell death (51,60).

Fas activation can also have other consequences than the induction apoptosis. FADD binds to FLICE Inhibitory Protein (FLIP). FLIP is a caspase 8 homologue that lacks catalytic activity. Like caspase 8, FLIP is essential for embryonic survival (62). FLIP inhibits the induction of apoptosis by binding to FADD instead of caspase 8. Furthermore, FLIP seems to mediate Fas-induced proliferation through activation of ERK1/2. ERK1/2 on the other hand up-regulates FLIP which may create a positive feedback loop that favours proliferation and inhibits cell death (51).

Daxx is a transcriptional repressor that binds to Fas independent of FADD. Daxx is mainly localised in the nucleus. Apoptosis signalling kinase 1 (ASK1) is needed for cytoplasmic localisation of Daxx as well as for the interaction with Fas. Daxx can enhance Fas-induced apoptosis. However, during development Daxx seems to be required as survival factor. Further, studies using RNAi for Daxx in cell lines showed increased apoptosis as well sensitisation of cells to Fas-, UV- and TNFα-induced cell death, suggesting an anti-apoptotic role for Daxx (51,61).

The death domain containing RIPs (RIP, RIP2, RIP3, RIP4) possess serine/threonine kinase activity and associates with Fas or with FADD or FLIP. In the vivo context RIP

appears to be a survival factor rather than an inducer of proliferation or apoptosis. RIP2 can mediate Fas-induced differentiation through activation ERK. RIP may also play a role in Fas-induced inflammation since it activates caspase-1. Caspase-1 converts pro-interleukin 1β to active IL-1β, a potent inducer of inflammation (51).

Fas Deficient and Fas Knockout Mice

Fas deficient mice have an interesting metabolic phenotype. Under chow diet these mice are heavier than their wildtype counterparts. However, they have less epididymal fat mass. Under high fat diet, Fas deficient mice increase their epididymal adipose tissue mass to the same extent as wild type mice. But the mean diameter of their fat cells does not increase, pointing towards hyperplasia of the tissue. Fas deficient mice show reduced macrophage infiltration into adipose tissues under high fat diet. Furthermore, Fas deficient mice are partly protected from high fat diet induce insulin resistance.

Specific ablation of the Fas receptor in adipocytes also partly protects mice from high fat diet-induced insulin resistance. Under high fat diet these adipocyte specific Fas knockout (AFasKO) mice show a favourable inflammatory profile in adipose tissue and less hepatosteatosis as well as less ceramide accumulation in the liver. Protection from insulin resistance of the liver mainly due to reduced IL-6 production of adipose tissue is an explanation for the healthier metabolism of high fat diet fed AFasKO mice (for details see attached paper).

Aims of this Work

The data obtained from Fas deficient and Fas knockout mice suggest that Fas influences adipocyte physiology and plays a role in the development of high fat diet-induced insulin resistance. We aimed to investigate the molecular mechanisms and consequences of Fas signalling in adipocytes by using the well established 3T3-L1 preadipocyte cell line. Better understanding of the effects of Fas in adipocytes will help to understand the complex influence of Fas on whole body physiology in the context of obesity and insulin resistance.

Materials and Methods

Cell Culture

Cells were cultured in Dulbecco's modified Eagle's medium (DMEM) containing 25 mM glucose (high glucose), fetal bovine serum and antibiotics. 48 hours after reaching confluence, cells were treated with a mixture of methylisobutylxanthine (500 μM), dexamethasone (1 μM), insulin (1.7 μM) and rosiglitazone (1 μM) to induce differentiation (day 0, D0). Two days later (D2) the medium was changed to high glucose culture medium containing insulin (0.5 μM). Another 2 days later (D4) the medium was replaced with culture medium alone. The culture medium was replaced every other day and changed to culture medium containing 5.5 mM glucose (low glucose) after 4 days (D8). Cells were kept at least 2 days on low glucose before experiments with mature adipocytes were performed. Adipocytes were generally treated with 2 ng per ml FasL (Upstate, Lake Placid, NY, USA) in DMEM containing no FCS for the indicated time.

Experiments in Preadipocytes

Proliferation

Cells were seeded in two different cells densities with the indicated amounts of FasL in the medium. Proliferation was assessed by measuring the reduction of MTT (Sigma) 48 hours after the cells were seeded and on D0. In living cells MTT is reduced in the mitochondria to the purple coloured formazan. Cells were washed twice with PBS and incubated in DMEM containing 0.5 mg MTT per ml for 1 hour. Thereafter cells were washed again twice with PBS and formazan was extracted with DMSO during 10 minutes. Absorption of the extracts was determined at 550 and 650 nm and the lower reading (650 nm) was subtracted from the higher (550 nm).

Differentiation

Cells were treated with different concentrations FasL per ml during different periods of differentiation and lipid accumulation was measured using Oil Red O staining as follows. At day 8 cells were fixed with 10% formalin, rinsed with 70% ethanol, incubated in Oil Red O solution and washed with H2O. Further, preadipocytes were treated with or without 2 ng/ml FasL and lysates were taken at different time points during differentiation. The differentiation markers pERK1/2, C/EBPα, C/EBPβ and PPARγ were analyzed on the protein level.

Experiments in Mature Adipocytes

Measurement of Lipolysis

Mature adipocytes were incubated in DMEM containing no FCS with or without 2 ng/ml FasL and the different compounds listed below for the indicated time periods. Thereafter, cells were washed with PBS and FFAs and glycerol were collected in Krebs-Ringer-HEPES buffer supplemented with 0.1% fatty acid free BSA for one hour. FFAs in the supernatant were measured with the NEFA kit from Wako (Neuss, Germany) and glycerol with the free glycerol reagent from Sigma.

Measurement of Cytokine Secretion

Cells were treated with 2 ng/ml FasL for the indicated time periods. Thereafter, cells were washed with PBS and cytokines were collected in Krebs-Ringer-HEPES buffer supplemented with 0.1% fatty acid free BSA for one hour. KC and IL-6 were measured with Luminex xMAP Technology.

Western Blotting

Adipocytes were lysed in ice-cold lysis buffer containing 150 mM NaCl, 50 mM Tris-HCl (pH 7.5), 1 mM EGTA, 1% NP-40, 0.25% sodium deoxycholate, 1 mM sodium vanadate, 1 mM NaF, 10 mM sodium β-glycerolphosphate, 100 nM okadaic acid, 0.2 mM PMSF and a 1:1000 dilution of protease inhibitor cocktail (Sigma). Protein concentration was determined using a BCA assay (Pierce, Rockford, IL, USA). Equal amounts of protein were resolved by LDS-PAGE (4-12% gel; NuPAGE, Invitrogen, Basel, Switzerland) and electro-transferred onto nitrocellulose membranes (0.2 µm, BioRad, Reinach, Switzerland). Protein content on membranes was checked by Ponceau S staining. Blots were blocked in tris-buffered saline containing 0.1% Tween (TBS-T) supplemented with 5% non fat dry milk. Primary antibody was applied in the same buffer in a dilution of 1:1000, secondary antibody in a dilution of 1:5000. Primary antibodies against the following proteins were used: PPARγ, C/EBPα□□, C/EBPβ (Santa Cruz Biotechnology), phospho-ERK1/2, total ERK1/2, phospho-STAT3 (Ser727) (from Cell Signaling Technology), Perilipin A (MBL International) and lipin-1 (Novus). Signal was generated based on chemoluminiscence and detected with the Fuji LAS-3000 image reader.

RNA Extraction and Quantitative RT-PCR

Total RNA was extracted using the NucleoSpin Kit (Macherey-Nagel, Oensingen, Switzerland). RNA was analyzed with a bioanalyzer (Agilent Technologies, Santa Clara, CA, USA), and concentration was determined with a nanodrop. 0.5 µg of RNA was reverse transcribed with Superscript III Reverse Transcriptase (Invitrogen) using random hexamer primer (Invitrogen). Taqman (Applied Biosystems, Rotkreuz, Switzerland) was used for real-time PCR amplification. All primers were purchased from Applied Biosystems: Lipin-1 (Mm01276800_m1), IL-6 (Mm00446190_m1), HSL (Mm00495359_m1), 36BA (Mm00725448_s1). 36BA (acidic ribosomal phosphoprotein) was used as housekeeping gen. The reaction mixture consisted of 2 µl cDNA (diluted 1:5 after RT), 10 µl Master Mix (No AmpErase, Applied Biosystems), 1 µl primer and 7 µl H_20 to a final volume of 20 µl. The amplification protocol consisted of a 2 min period at 50° C to activate the Uracil-N-Glycosylase. Then, samples were heated to 95°C, followed by 40 cycles with denaturation at 95° C for 15 sec and annealing/elongation at 60°C for 1 min (Applied Biosystems). Relative gene

expression was obtained after normalization to 18S RNA (Applied Biosystems), using the formula $2^{-\Delta\Delta cp}$ (62).

Measurement of CaMKII Activity

Cells were treated with 2 ng/ml FasL or 5 nM TNFα for 6 hours or with 1 μM isoproterenol for half an hour. Additionally time course experiments were conducted with FasL treatment alone. Lysis was performed with a buffer that contained 50 mM HEPES, 1 mM EGTA, 10% glycerol, 1 mM sodium vanadate, 100 nM okadaic acid, 0.2 mM PMSF and a 1:1000 dilution of protease inhibitor cocktail (Sigma P8340). To test the influence of the lysis conditions the lysis buffer used for Western blotting was used in one experiment. Enzyme activity was analysed with the CaMKII Assay System V8161 from Promega and radioactive [γ-32P]ATP from PerkinElmer. The assay uses a biotinylated substrate that is phosphorylated by CaMKII. Biotin is captured onto a streptavidin coated membrane. The radioactivity of the membrane measured in a β-counter corresponds to the activity of the enzyme. The assay was performed following the manufactures instructions. A buffer supplemented with calcium and calmodulin was used as positive control.

MS Analysis of Phosphatidic Acid

Cells were incubated with 2 ng/ml FasL or 5 nM TNFα for 6 hours and lysed with 0.05 N NaOH. The PA fraction was extracted from 1 volume of lysate three times with one volume of butanol. Prior to analysis the extracts were buffered with 5 mM ammonium acetate and 1,2-Dioctanoyl-sn-glycerol 3-phosphate (Sigma) was added as internal standard. Masses were analyzed with a Q-Tof mass spectrometer in positive ion mode. Data were quantified using the MassLynx Software from Waters.

Compounds Used for Cell Treatment

MEK1/2 Inhibitor

The MEK1/2 inhibitor U0126 was purchased from Sigma (Buchs, Switzerland). Dilutions of a 50 mM stock solution in DMSO were used in the experiments. The inhibitor was added at the same time as FasL in a concentration of 50 μM.

Recombinant KC

Carrier free recombinant KC was bought from R&D Systems. The cytokine was dissolved in PBS containing 0.1% endotoxin free bovine serum albumin to form a stock solution with a concentration of 100 μg per ml. The cytokine was used in concentrations ranging from 0.1 to 100 ng per ml and for different time periods from 1 hour to 9 hours.

Inhibitors of IL-6 Signalling

The IL-6 receptor superantagonist 7 (Sant7, sigma-tau) was stored as a 50 μg/ml stock in 0.9% NaCl. Sant7 was applied to the cells in concentrations ranging from 2 ng to 2 μg per ml. The recombinant IL-6 antibody was from R&D Systems and a stock solution with a concentration of 100 μg per ml was prepared in PBS. The stock solution was dissolved to yield concentrations of 50, 500 and 5000 ng per ml in the culture medium. Inhibitors for the Janus protein tyrosine kinases (JAKs) were bought from Calbiochem. Pyridone 6 was stored as a 10 mM stock solution in DMSO and was used in concentrations ranging from 1 nM to 1 μM. AG490 and WHI-P131 were dissolved in DMSO to form 100 mM DMSO stocks. Concentrations of both AG490 and WHI-P131 in the culture medium were 10, 50 and 100 μM. When not stated differently, compounds were added to the cells at the same time as FasL.

Rosiglitazone

Rosiglitazone used for induction of differentiation and for treatment of mature adipocytes was from Alexis Biochemicals. The thiazolidinedione was stored as a 15 mM stock solution in DMSO. Mature adipocytes were pretreated for 48 hours with 5 μM of the compound. Thereafter FasL together with rosiglitazone was applied for another 12 hours.

Calcium Chelators and CaMKII Inhibitor

The calcium chelator EDTA was used in dilutions from a 0.5 M stock solution in H_2O. EDTA was applied to the cell culture medium in concentrations from 0.1 to 10 mM. The intracellular calcium chelator BAPTA/AM was purchased from Calbiochem and dissolved in DMSO to form a 50 mM stock. BAPTA/AM was used in concentrations of 10 and 50 μM. KN62, an inhibitor of CaMKII was from Sigma and used in 0.1, 1 and 10 μM dilutions from a 10 mM DMSO stock solution. Inhibitors were added to the cells at the same time as FasL.

Phosphatidic Acid

Phosphatidic acid (1,2-Dioctanoyl-sn-glycerol 3-phosphate) was purchased from Sigma. The compound was dissolved in sterile H_2O. Dilutions of a 10 mM stock solution were used in the experiments. Adipocytes were incubated with 10, 50 or 100 μM of PA for 3 hours.

Data Analysis

Data are presented as means ± SEM and if not stated differently were analyzed by one sample t test, *$p < 0.5$, **$p < 0.01$, $^{\#}p < 0.001$.

Results

Fas Expression in Preadipocytes and Adipocytes

As shown in Fig. 1, Fas is expressed in 3T3-L1 preadipocytes, during adipocyte differentiation (D1, 2, 4 and 6) and in mature adipocytes. Expression levels of the adipocyte specific proteins PPARγ, C/EBPα and perilipin reflect the respective stage of differentiation.

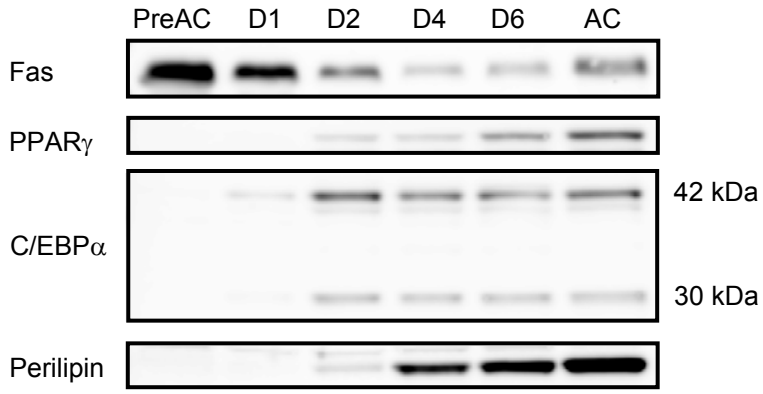

Fig. 1 The Fas receptor is expressed in 3T3-L1 cells. Lysates of 3T3-L1 preadipocytes (PreAC, D0), differentiating (D1, 2, 4 and 6) and mature adipocytes (AC) were resolved by LDS-PAGE and immunoblotted with an antibody against the Fas receptor, PPARγ, C/EBPα, and perilipin.

Influence of Fas on Preadipocytes

Fas Reduces Proliferation of Preadipocytes

In Fas deficient mice, adipocyte size did not increase under high fat-feeding, even though, epididymal adipose tissue mass increases to the same extent as in wild type mice. This indicates a hyperplastic adipose tissue response to a high fat diet in mice with Fas deficiency and an influence of Fas signalling on preadipocyte proliferation and differentiation.

Treatment of 3T3-L1 preadipocytes with FasL dose-dependently reduced MTT incorporation 48 hours after cells were seeded indicating that Fas inhibits the proliferation of these cells (Fig. 2).

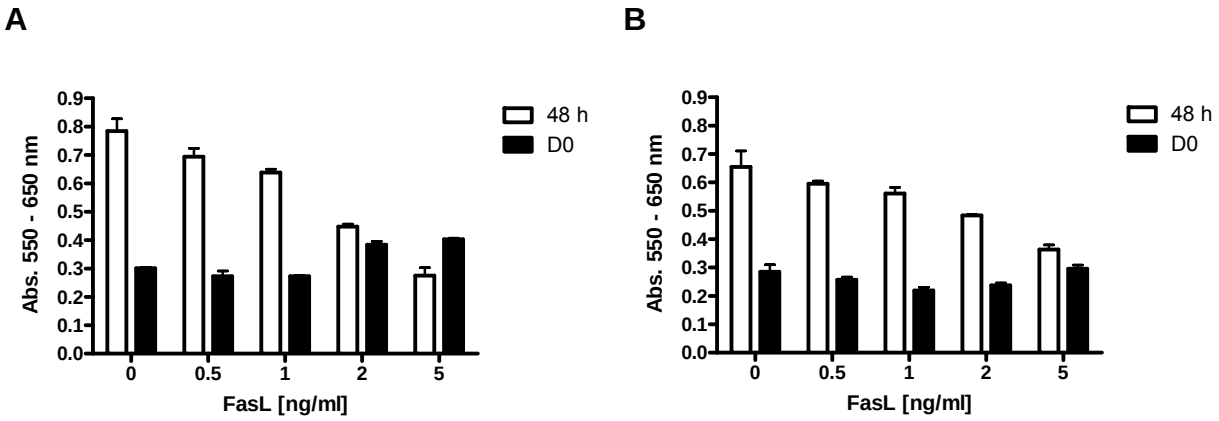

Fig. 2. Fas activation reduces proliferation of preadipocytes. Preadipocytes were seeded in two cell densities of 50'000 cells per well (A) or 80'000 cells per well (B) and treated with the indicated concentrations of FasL. MTT reduction was measured 48 hours after cells were seeded or on D0. Results are means ± SEM from 2 to 3 wells from the same plate.

Fas May Modulate Adipocyte Differentiation

To investigate the influences of Fas on the molecular chain of events during adipocyte differentiation, protein levels of key markers of differentiation were analyzed. FasL treatment reduced the early induction of pERK1/2 (Fig. 3A). Such early activation of the MAP kinases is important for mitotic clonal expansion of the cells and, thus, for differentiation. Furthermore, FasL treatment reduced protein levels of the transcription factors C/EBPβ, C/EBPα and PPARγ (Fig. 3B). Moreover, in experiments culturing primary adipocytes from the stromal vascular fraction of adipocyte-specific Fas-knockout or wild-type mice we found a trend towards increased differentiation in Fas-deficient preadipocytes (data not shown). Overall, these experiments hint towards an inhibitory role of Fas on adipocyte differentiation.

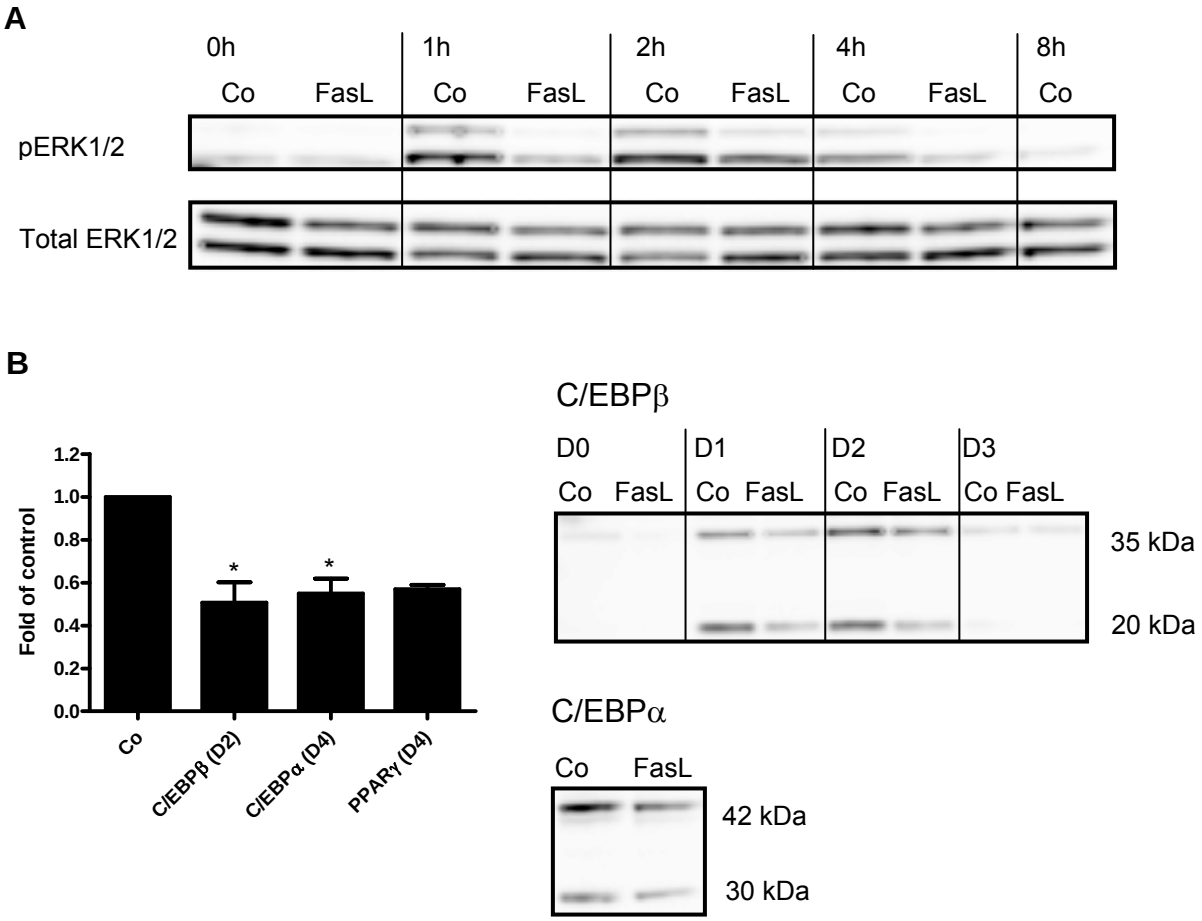

Fig. 3. Fas reduces markers of differentiation in differentiating 3T3-L1 preadipocytes. Cells were seeded with 2 ng/ml FasL in the culture medium. 48 hours after cells reached confluence differentiation was induced with isobutylmethylxanthine (IBMX), dexamethasone, insulin and rosiglitazone. At the indicated time points after induction of differentiation protein expression was analyzed. Total cell lysates were resolved by LDS-PAGE and immunoblotted with anti-phospho-ERK1/2 and total ERK (A), anti-C/EBPβ, anti-C/EBPα or anti-PPARγ (B) antibody. Results are the mean ± SEM of 2-3 independent experiments, *p < 0.5.

Fas Activation Induces Lipolysis in Mature Adipocytes

Fas-Induced Lipolysis is ERK1/2-Dependent

As described in the Introduction, total body and adipocyte-specific Fas-knockout mice were partly protected from high fat diet-induced adipocyte insulin resistance. Therefore, we intended to explore the effect of Fas stimulation on glucose uptake and lipolysis in adipocytes in culture. We previously observed that Fas activation

increased basal and decreased insulin-stimulated glucose uptake in 3T3-L1 adipocytes.

Furthermore, incubation of adipocytes with FasL regulated lipolysis in a time-dependent manner with an initial decrease after 2 hours and a significant increase after 6 to 12 hours (Fig. 4).

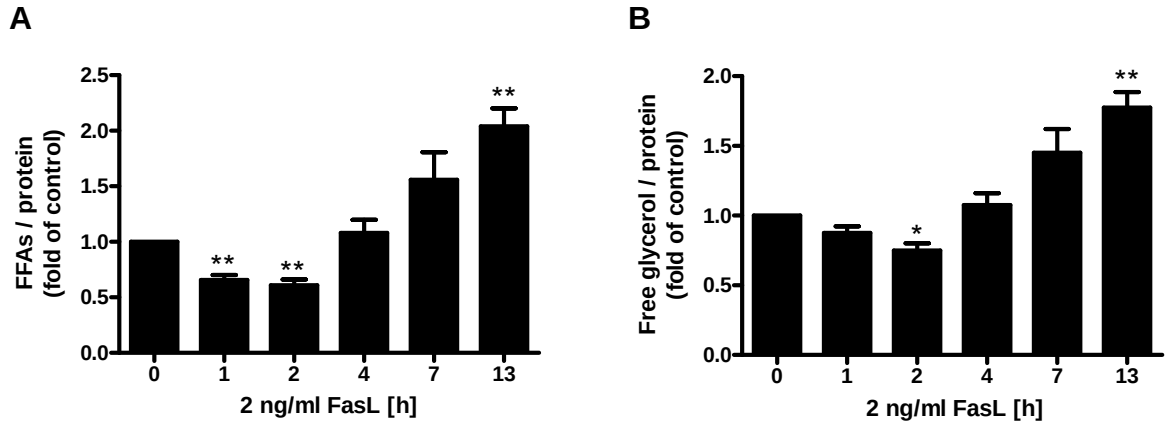

Fig. 4. FasL treatment induces lipolysis in 3T3-L1 adipocytes. Cells were incubated with FasL for the indicated time periods. Free fatty acid (A) and glycerol release (B) was determined after medium was removed and cells were incubated with KREBS buffer for another hour. Results represent the mean ± SEM of 5 (A) or 4 (B) independent experiments, *p < 0.5, **p < 0.01.

Like the TNF receptors, Fas belongs to the tumour necrosis receptor superfamily. TNFα was previously shown to induce lipolysis in 3T3-L1 cells via activation of the p44/42 MAP kinases (ERK1/2) (32), we therefore postulated that FasL-induced lipolysis is similarly dependent ERK1/2 activation. Incubation of mature 3T3-L1 adipocytes with 2 ng/ml FasL increased phosphorylation of ERK1/2 with a first peak after 15 minutes and a second, even higher peak after 6 hours (Fig. 5). Phosphorylation was still significantly increased after 12 hours of treatment. Total protein concentration of ERK1/2 was not affected by the treatment.

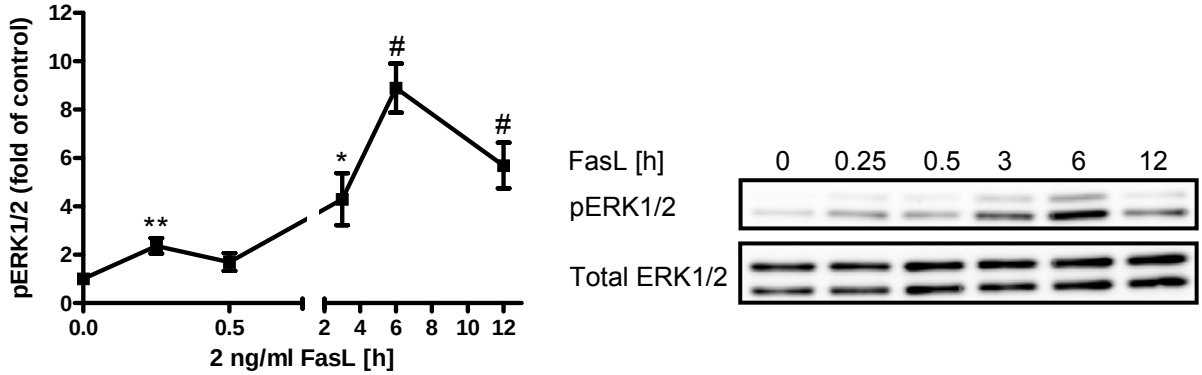

Fig. 5. FasL activates ERK1/2. Mature 3T3-L1 adipocytes were incubated with 2 ng per ml FasL for the indicated time periods. Total cell lysates were resolved by LDS-PAGE and immunoblotted with anti-phospho-ERK1/2 or anti-ERK1/2 antibodies. Results are the mean ± SEM of 6-10 independent experiments, *p < 0.5, **p < 0.01, #p < 0.001.

To assess whether Fas-stimulated lipolysis is dependent on ERK1/2 activation, we incubated 3T3-L1 cells in presence or absence of the MEK inhibitor U0126. U0126 inhibited Fas-induced ERK1/2 phosphorylation dose-dependently. In a concentration of 50 μM U0126 reduced the enzyme's activity to the level in the control (Fig. 6A). Inhibition of the MAP kinase pathway completely blocked Fas-induced lipolysis (Fig. 6B). Thus, Fas-stimulated lipolysis is dependent on ERK1/2 activation.

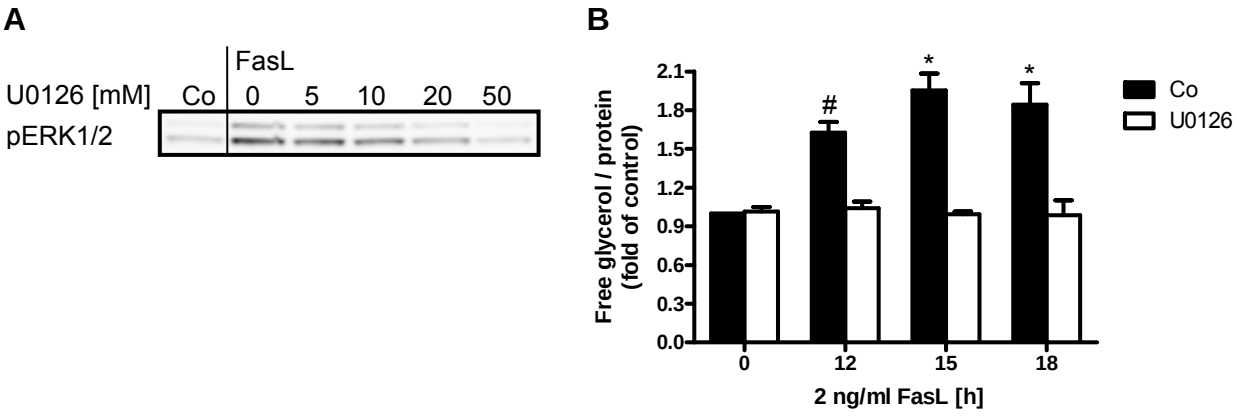

Fig. 6. Fas-induced lipolysis is dependent on ERK1/2 activation. 3T3-L1 adipocytes were treated with FasL and different concentrations of the MEK inhibitor U0126. Western blot analysis was performed with an antibody against pERK1/2 (A). Cells were incubated with or without FasL and 50 μM of U0126 for 12 hours. Glycerol release was determined after medium was removed and cells were incubated with KREBS buffer for another hour. Results are the mean ± SEM of 3 - 6 independent experiments, *p < 0.5, #p < 0.001.

Pretreatment with Rosiglitazone Partly Reverses FasL-Induced Lipolysis

As shown in preadipocytes, 12 hours of FasL treatment significantly down-regulated C/EBPα and PPARγ content in mature 3T3-L1 adipocytes (Fig. 7)

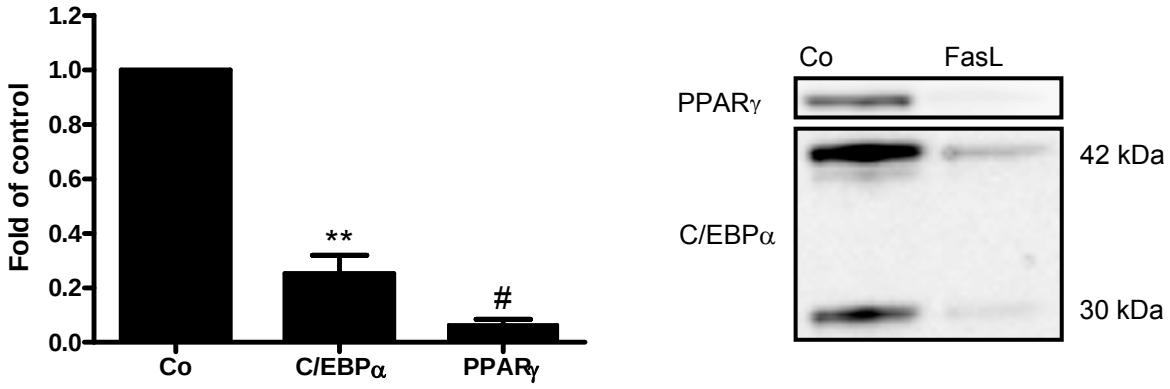

Fig. 7. FasL treatment down-regulates adipogenic markers in mature adipocytes. 3T3-L1 adipocytes were subjected to FasL treatment for 12 hours. Western blot analysis was performed with an antibodies against C/EBPα and PPARγ. The graphs show the mean ± SEM of 4 (C/EBPα) or 5 (PPARγ) independent experiments, **p < 0.01, #p < 0.001.

To test whether PPARγ activation modulates the effects of Fas activation, 3T3-L1 adipocytes were pre-treated with the PPARγ ligand rosiglitazone. Importantly, rosiglitazone pre-treatment reduced FasL-stimulated ERK1/2 phosphorylation without affecting total ERK1/2 protein content (Fig. 8).

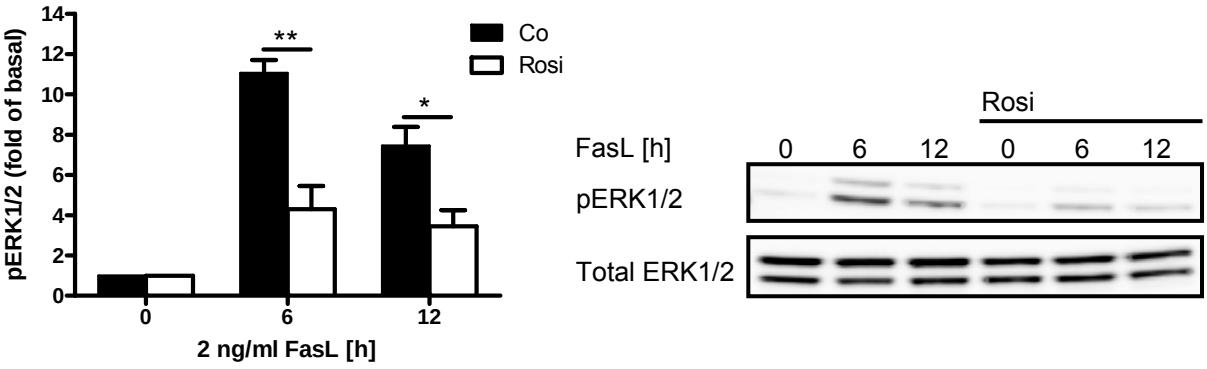

Fig. 8. Rosiglitazone pretreatment reduces Fas-induced ERK1/2 phosphorylation. Cells were incubated with or without 5 μM rosiglitazone for 60 hours. During the last 6 or 12 hours of this incubation period cells were treated with FasL. Total cell lysates were resolved by LDS-PAGE and immunoblotted with anti-phospho-ERK1/2 or anti-ERK1/2 antibodies. Results are the mean ± SEM of 4 independent experiments, *p < 0.5, **p < 0.01 (Student's t test).

Moreover, pre-treatment with rosiglitazone also reduced FasL-mediated lipolysis (Fig. 9). Thus, these sets of experiments further confirmed the importance of ERK-activation for FasL-induced lipolysis.

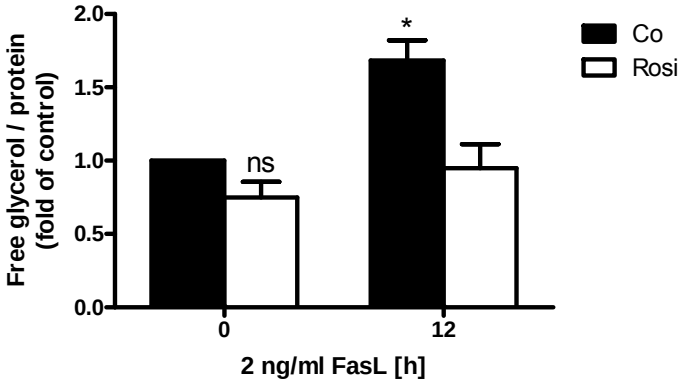

Fig. 9. Rosiglitazone reduces Fas-induced lipolysis. Cells were incubated with or without 5 μM rosiglitazone for 60 hours. During the last 12 hours of this incubation period cells were treated with FasL. Glycerol release was determined after medium was removed and cells were incubated with KREBS buffer for another hour. Results are the mean ± SEM of 4 independent experiments, *p < 0.5, ns: not significant.

Potential Downstream Effects of FasL-Induced ERK1/2 Activation

Fas Reduces Perilipin and HSL

So far we could demonstrate that FasL-induced lipolysis is dependent on the activation of the ERK1/2 MAP kinases.

The lipid droplet coating protein perilipin and the lipase HSL play an important role in lipolysis (30). Gene expression of both perilipin and HSL are regulated by PPARγ (63,64). Furthermore, MAP kinase-mediated serine phosphorylation of PPARγ was shown to reduce its activity (65). Interestingly, TNFα-induced lipolysis is associated with ERK1/2-dependent down-regulation of perilipin (32). Thus we postulated that FasL treatment may as well decrease expression of perilipin. Indeed, we found that FasL treatment also reduced perilipin protein content in adipocytes. Inhibition of ERK1/2 activation, however, could not rescue FasL-mediated decrease of perilipin content (Fig. 10A) whereas it prevented FasL-induced lipolysis as shown above (Fig. 6B). Therefore, the latter does not seem to be dependent on FasL-mediated reduction of perilipin.

Surprisingly, FasL treatment also decreased HSL mRNA, which is an important enzyme in the breakdown of triacylglycerols (Fig. 10B). Although activity of HSL is regulated through phosphorylation (30), we hypothesized that the Fas-induced increase in lipolysis would be mirrored by an increased expression of the lipase. HSL was shown to be activated by ERK1/2 through phosphorylation on serine 600 (66). Since there is no commercial antibody available against this specific form of HSL, we have no state anything about the activity of the enzyme after FasL treatment.

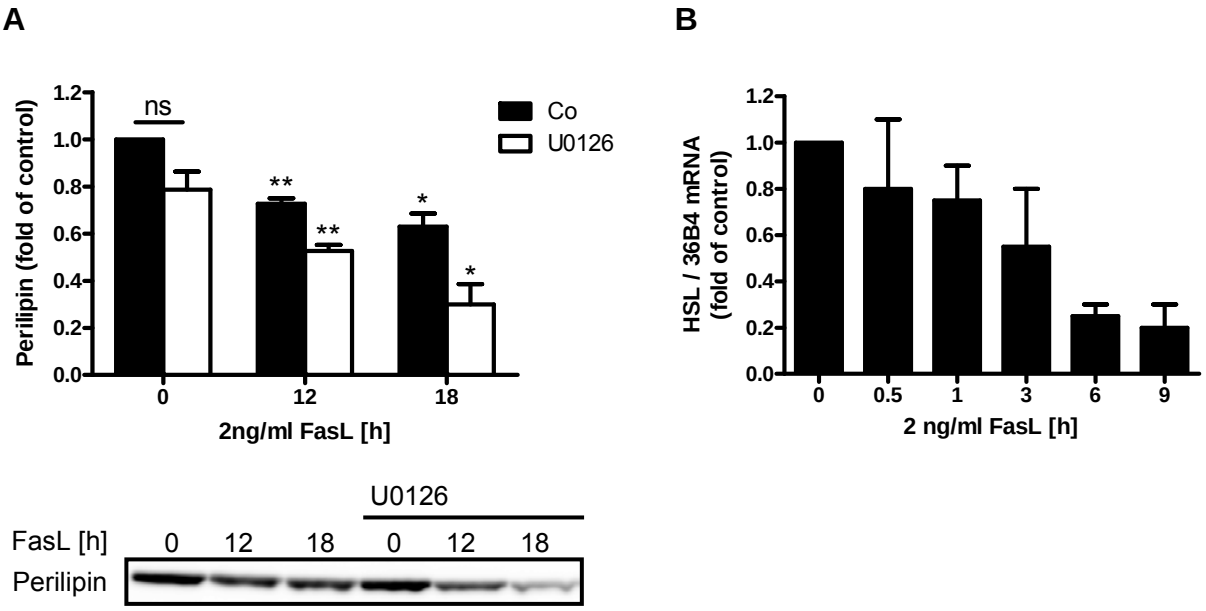

Fig. 10. Activation of Fas down-regulates perilipin and HSL. Cells were incubated for the indicated time periods with or without FasL (2 ng/ml) and the MEK inhibitor U0126. Perilipin protein levels in whole cell lysate were analyzed by Western blot analysis (A). Real-time PCR was performed to determine HSL mRNA levels (B). Results are the mean ± SEM of 3 (A) and 2 (B) independent experiments, *p < 0.5, **p < 0.01, ns: not significant.

Potential Upstream Mediators of FasL-Induced ERK1/2 Activation

Phosphatidic Acid

Interestingly, we found that Fas activation decreases both mRNA and protein levels of lipin-1 (Fig. 11). Lipin-1 is a phosphatase involved in the formation of triacylglycerols from glycerol-3-phosphate. Reduced lipin-1 protein levels could not be rescued through inhibition of the MAP kinase pathway either (Fig. 11B).

Suggesting that FasL-induced downregulation of lipin is either ERK-independent or upstream of ERK-activation.

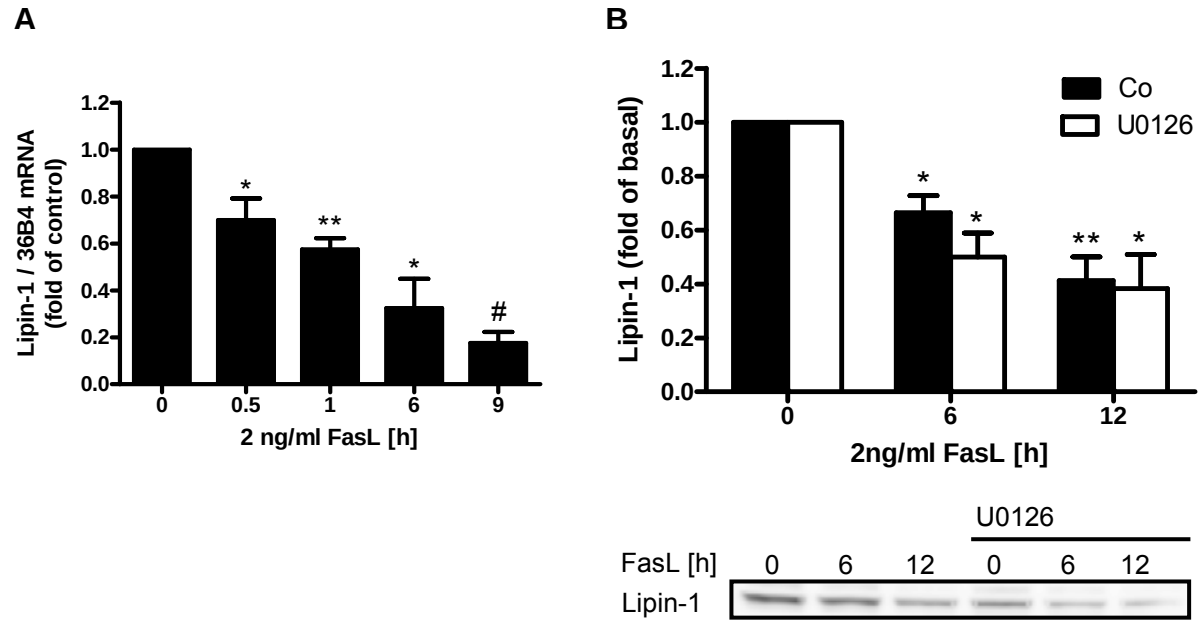

Fig. 11. Fas activation down-regulates lipin-1. Cells were incubated for the indicated time periods with or without FasL (2 ng/ml) and the MEK inhibitor U0126. Real-time PCR was performed to determine lipin-1 mRNA levels (A). Lipin-1 protein levels in whole cell lysate were analyzed by Western blot analysis (B). Results are the mean ± SEM of 4 independent experiments, *$p < 0.5$, **$p < 0.01$, $^{\#}p < 0.001$.

Lipin-1 deficiency in mice was shown to lead to the accumulation of its PA acid WAT. Further PA can induce ERK1/2 (25). In order to test whether PA could be responsible for FasL-induced ERK1/2 activation and lipolysis, 3T3-L1 adipocytes were incubated with varying concentrations of PA for different time periods. Addition of 100 μM PA for 3 hours to 3T3-L1 activated ERK1/2 without effecting total ERK1/2 content (Fig. 12A). Moreover, incubation with PA for the same time period induced lipolysis, and this effect was prevented through inhibition of the MAP kinase pathway (Fig. 12B). Thus, PA induces lipolysis in 3T3-L1 adipocytes in an ERK1/2-dependent manner.

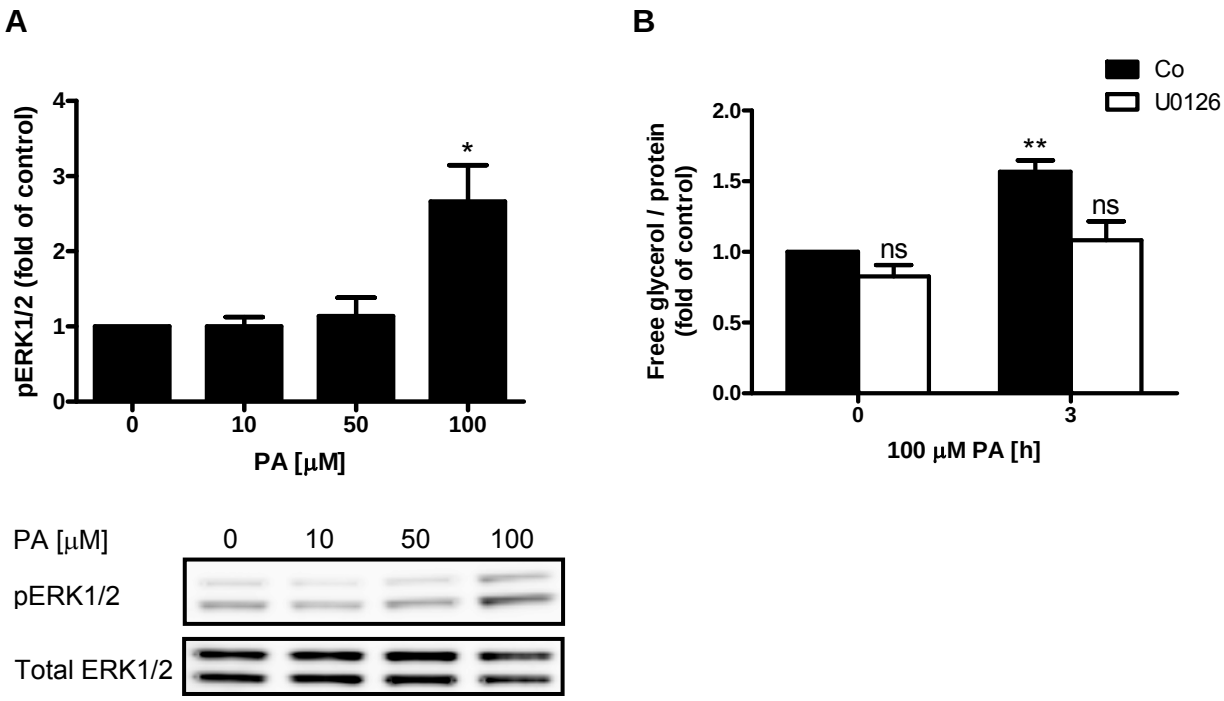

Fig. 12. Phosphatidic acid induces ERK1/2-dependent lipolysis. Cells were incubated with different concentrations of PA for 3 hours. Total cell lysates were resolved by LDS-PAGE and immunoblotted with antibodies against phospho-ERK1/2 and total ERK (A). Adipocytes were incubated with or without 100 μM PA and the MEK inhibitor U0126 for 3 hours. Glycerol release was determined after medium was removed and cells were incubated with KREBS buffer for another hour (B). Results are the mean ± SEM of 5 (A) or 4 (B) independent experiments, *p < 0.5, **p < 0.01, ns: not significant.

As a next step, we measure PA concentration in 3T3-L1 adipocytes using MS. Given the above results, we expected that incubation with FasL would increase PA concentration. However, we could not detect any differences in PA concentrations (Fig. 13), suggesting either that FasL treatment does not increase PA concentration or that we were not able to detect such potential difference.

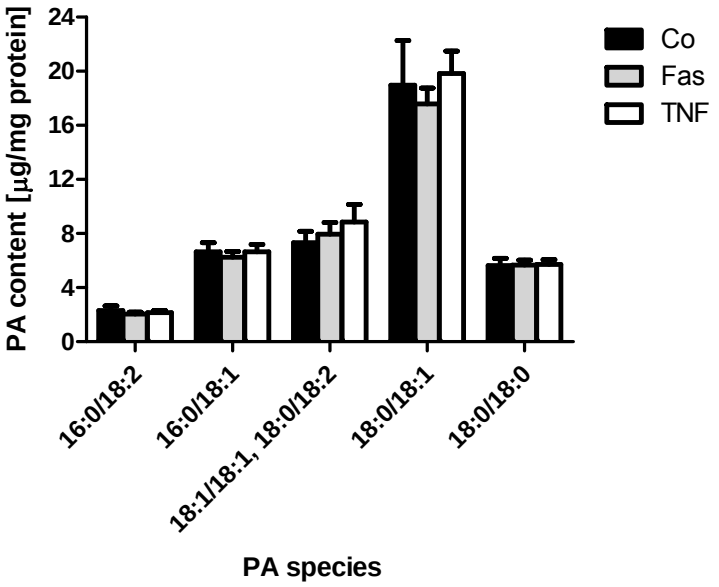

Fig. 13. Fas activation does not lead to phosphatidic acid accumulation. 3T3-L1 adipocytes were incubated with 2 ng per ml FasL or 5 nM of TNFα for 6 hours. Cells were lysed with 0.05 N NaOH and PA species were extracted with butanol and quantified using MS. Results are the mean ± SEM of 6 or 3 (18:0/18:1) independent experiments.

Calcium Signalling

Changes in intracellular calcium (Ca) concentrations are a hallmark of a broad range of signalling pathways such as muscle contraction, exocytosis and apoptosis. Increased Ca can lead to downstream signalling effects through binding to calmodulin (CaM). CaM binds 4 calcium ions but has no intrinsic enzymatic activity. By complex formation with many different enzymes CaM renders their activity Ca dependent. One of these enzymes is the calcium/calmodulin dependent protein kinase II (CaMKII). CaMKII was shown to mediate magnolol-triggered lipolysis in sterol ester-loaded 3T3-L1 preadipocytes in an ERK1/2 dependent fashion (67). We therefore postulated that FasL-induced lipolysis may be dependent on intracellular changes in Ca levels. As an initial experiment, we tested whether the extracellular Ca chelator EDTA was able to reduced Fas induced-ERK1/2 activation and lipolysis. Indeed preincubation with EDTA prevented both FasL-induced ERK-activation and lipolysis (Fig. 14).

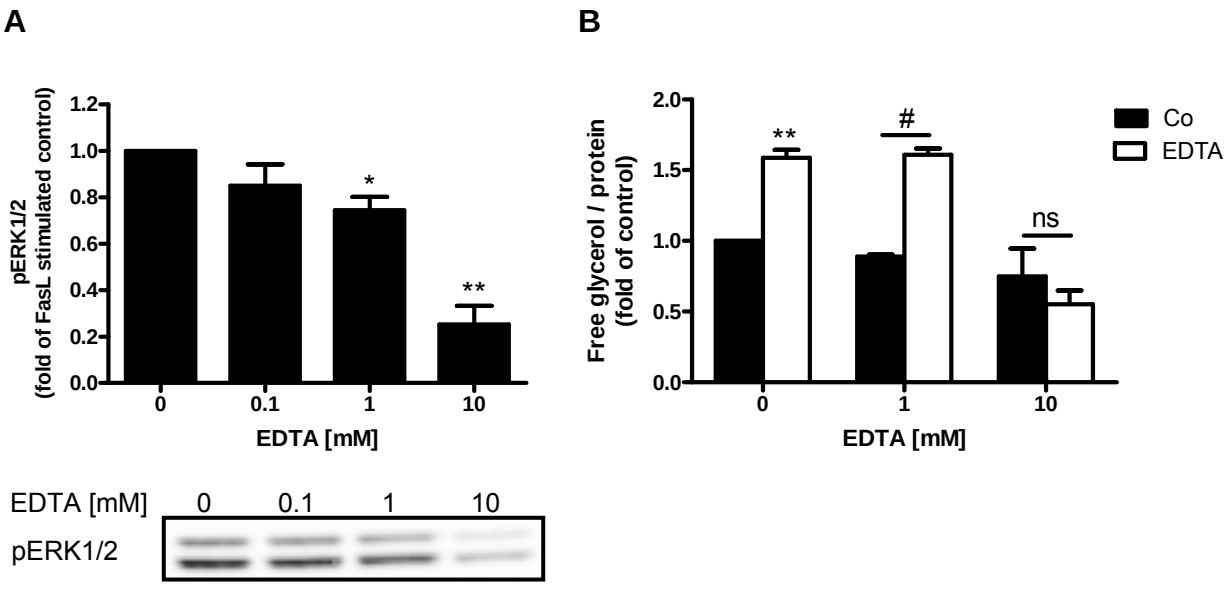

Fig. 14. EDTA reduces Fas-induced pERK1/2 and lipolysis. 3T3-L1 adipocytes were incubated with or without FasL and different concentrations of EDTA for 12 hours. Phosphorylated ERK1/2 was measured in whole cell lysate by Western blot analysis (A). Glycerol release was determined after medium was removed and cells were incubated with KREBS buffer for another hour (B). Results are the mean ± SEM of 4 independent experiments, *p < 0.5, **p < 0.01, #p < 0.001, ns: not significant (1 and 10 mM EDTA cond.: Student's t test).

However, EDTA is an unspecific Ca chelator and the effective concentrations were toxic to the cells. Thus we applied the intracellular Ca chelator BAPTA/AM to 3T3-L1 adipocytes. BAPTA/AM treatment mimicked the effects of EDTA without toxicity as depicted in Fig. 15.

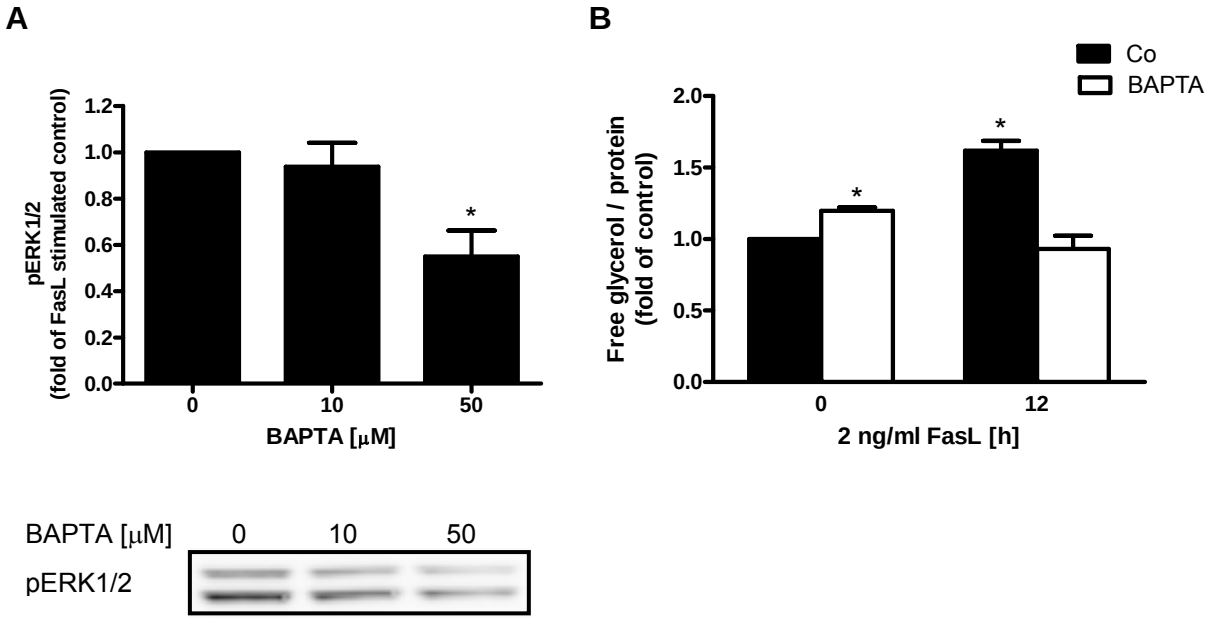

Fig. 15. BAPTA/AM reduces Fas-induced pERK1/2 and lipolysis. 3T3-L1 adipocytes were incubated with or without FasL and different concentrations of BAPTA/AM for 12 hours. Phosphorylated ERK1/2 was measured in whole cell lysate by Western blot analysis (A). Glycerol release was determined after medium was removed and cells were incubated with KREBS buffer for another hour (B). Results are the mean ± SEM of 4 (A) or 3 (B) independent experiments, *p < 0.5.

Moreover, the CaMKII inhibitor KN62 reduced FasL-mediated ERK1/2 activation as well as lipolysis suggesting the involvement of CaMKII-activation (Fig. 16).

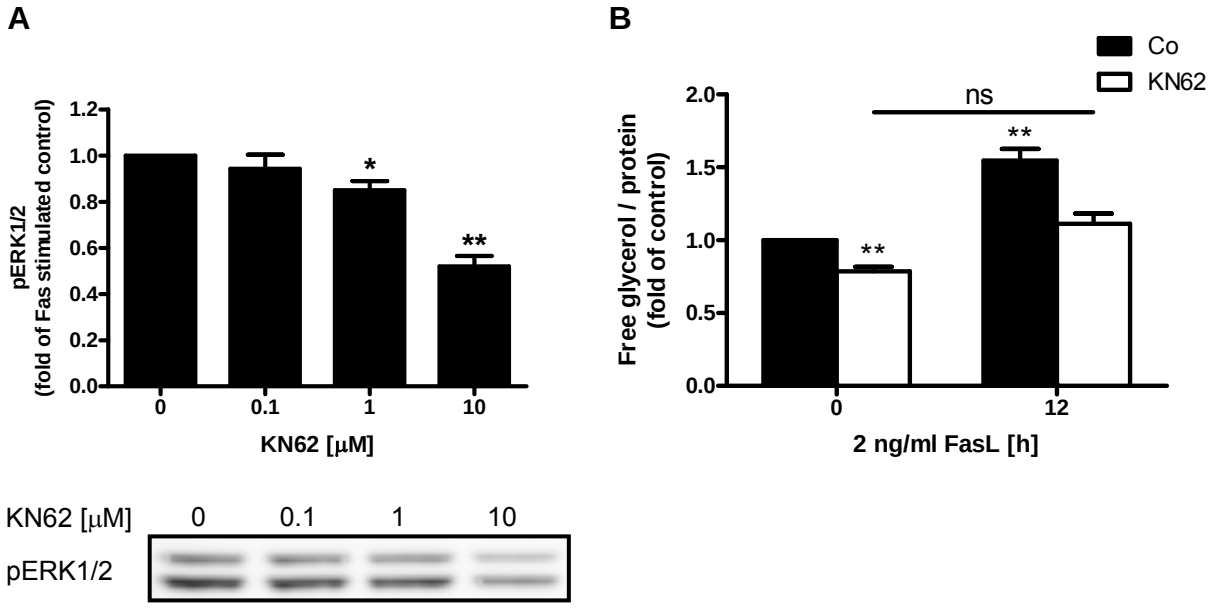

Fig. 16. The CaMKII inhibitor KN62 reduces Fas-induced pERK1/2 and lipolysis. 3T3-L1 adipocytes were incubated with or without FasL and different concentrations of the CaMKII inhibitor KN62 for 12 hours. Phosphorylated ERK1/2 was measured in whole cell lysate by Western blot analysis (A). Glycerol release was determined after medium was removed and cells were incubated with KREBS buffer for another hour. Results are the mean ± SEM of 4 (A) and 5 (B) independent experiments, *p < 0.5, **p < 0.01 (KN62 conditions (B): Student's t test).

Consequently, CaMKII activity was measured in the presence or absence of FasL treatment. As a control, we also looked at the ability other lipolytic compounds such as TNFα and isoproterenol to induce CaMKII activity. Neither pre-treatment with FasL nor with TNFα stimulated CaMKII activity (Fig. 17). Surprisingly, short-term treatment with isoproterenol activated CaMKII significantly. Use of a different lysis buffer yielded exactly the same result for 6 hours Fas and TNFα or 0.5 hour isoproterenol treatment.

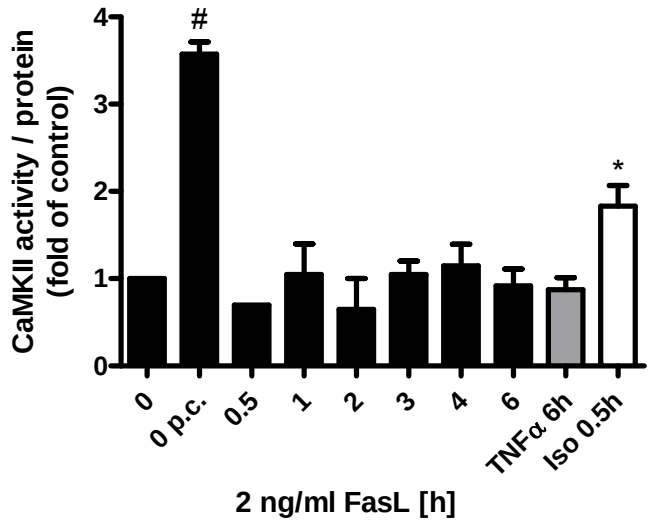

Fig. 17. Fas treatment does not induce CaMKII activation. Cells were incubated with 2 ng/ml FasL for different time periods, with 5 nM TNFα for 6 hours or with 1 μM isoproterenol for 30 minutes. Thereafter, CaMKII activity was measured. As positive control a buffer containing Ca and calmodulin was used. Results are the mean ± SEM of 2 to 8 independent experiments, *$p < 0.5$, #$p < 0.001$.

Hence, Ca signalling may meditate the lipolytic effect of FasL treatment. The lack in CaMKII activation after FasL-treatment though speaks against an involvement of the latter enzyme.

Cytokine Signalling

Adipocyte-specific Fas-knockout mice were protected from high fat diet-induced insulin resistance and this was associated with reduced adipose tissue inflammation as reflected by reduced macrophage infiltration, decreased expression of pro-inflammatory cytokines (IL-6, IL-1beta) and increased expression anti-inflammatory cytokines (IL-10). We thus hypothesized that Fas-activation increases the expression and/or secretion of pro-inflammatory cytokines. 3T3-L1 adipocytes were treated with FasL and cytokine secretion into the supernatant was determined. As expected, Fas activation increased the secretion of the chemokine KC (mouse homologue of IL-8) (2.5 fold, Fig. 18A) and of the cytokine IL-6 (1.5 fold, Fig. 18B), whereas TNFα was not detectable (data not shown), Consistent with an increased secretion, FasL induced IL-6 mRNA expression in a time-dependent manner (Fig. 18C). Furthermore, FasL treatment increased the phosphorylation of STAT3 (Fig. 18D). STAT3 is a component of the JAK-STAT signalling pathway that is activated by various cytokines, and IL-6 is a known inducer of this STAT isoform.

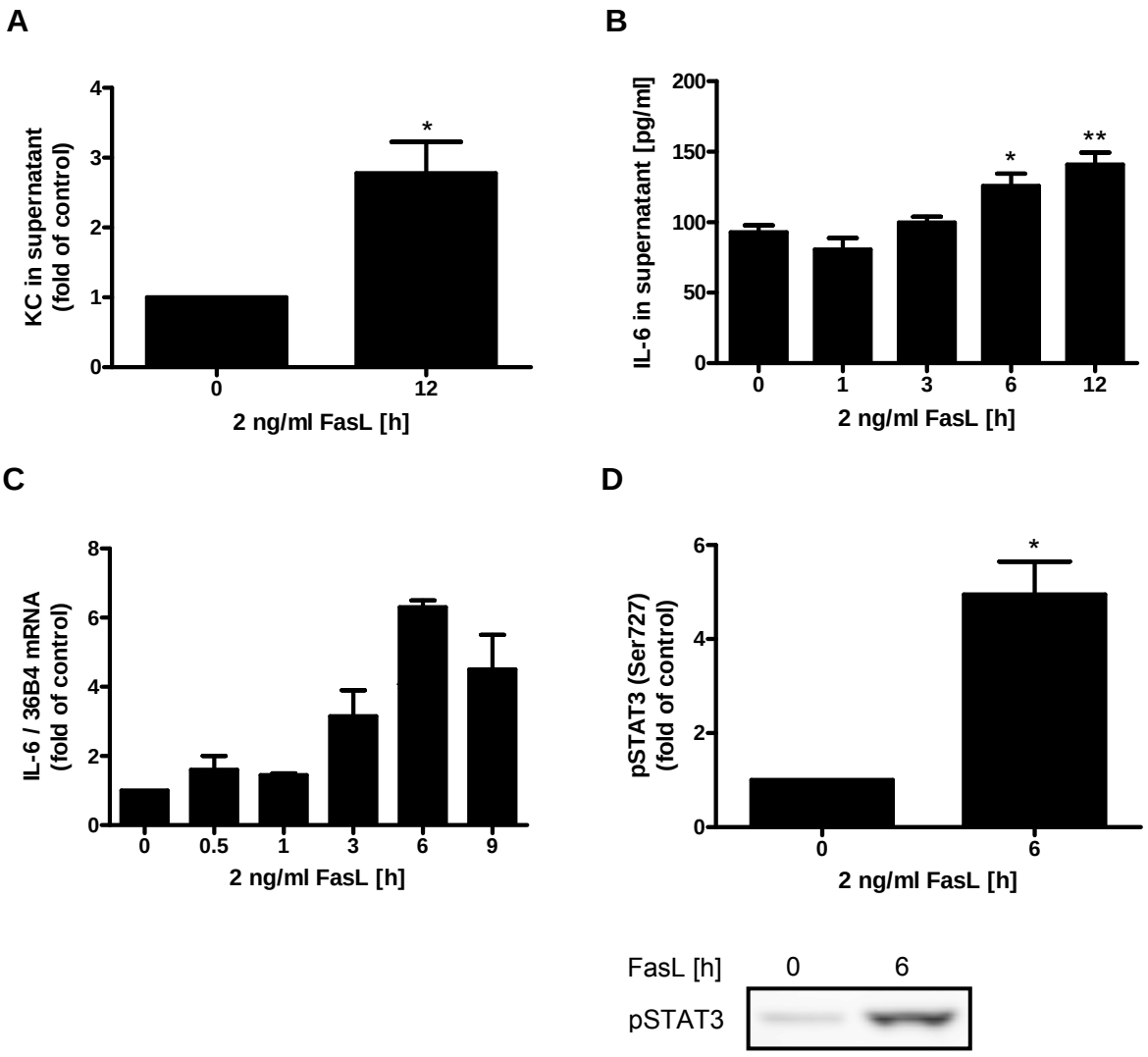

Fig. 18. FasL induces KC and IL-6 secretion, IL-6 mRNA expression and pSTAT3. Adipocytes were incubated with FasL for the indicated time periods. Cytokine release was determined after medium was removed and cells were incubated with KREBS buffer for another hour (A, B). Real-time PCR was used to determine mRNA expression of IL-6 (C). Cells were treated for 6 hours with FasL and the amount of pSTAT3 in whole cell lysates was analyzed by Western blot (D). Results are the mean ± SEM of 4 (A), 3 - 5 (B), 2 (C) or 4 (D) independent experiments, *p < 0.5, **p < 0.01.

IL-6 was previously shown to induced lipolysis (33). Since FasL treatment increased IL-6 expression, secretion and phosphorylation of STAT3, we postulated that FasL treatment may induce lipolysis via IL-6 secretion in a paracrine manner. To test this hypothesis FasL-treated 3T3-L1 adipocytes were incubated in the presence of the IL-6 receptor superantagonist 7 (Sant7). Sant7 is a modified IL-6 molecule that binds to the IL-6 receptor but does not induce signalling. Surprisingly, Sant7 did not reduce Fas-mediated phosphorylation of STAT3 (Fig. 19). On the other hand Sant7

significantly reduced the phosphorylation of ERK1/2 (Fig. 19). However, the amount of inhibition varied considerably between individual experiments.

Fig. 19. Sant7 does not affect Fas-induced pSTAT3 but down-regulates pERK1/2. Adipocytes were treated with FasL and with or without Sant7 for 6 hours. Amounts of pSTAT3 and pERK1/2 in whole cell lysates were quantified by Western blot analysis. Results are the mean ± SEM of 6 independent experiments, **p < 0.01.

To further clarify the participation of the IL-6 signalling pathway in Fas-induced lipolysis adipocytes were incubated with JAK inhibitors or a neutralising IL-6 antibody during FasL treatment. Disappointingly, treatment with the JAK2 inhibitor AG490 as well as with the JAK3 inhibitor WHI-P131 did not reduce FasL-induced phosphorylation of ERK1/2 and STAT3 (Fig. 20A). The pan-JAK inhibitor P6 had no significant effect on FasL-induced phosphorylation of ERK1/2 although it partly reduced pSTAT3 (Fig. 20B). In addition, ERK1/2 phosphorylation could not be reduced in the presence of neutralising IL-6 antibody, not even at very high concentrations (Fig. 20C).

A

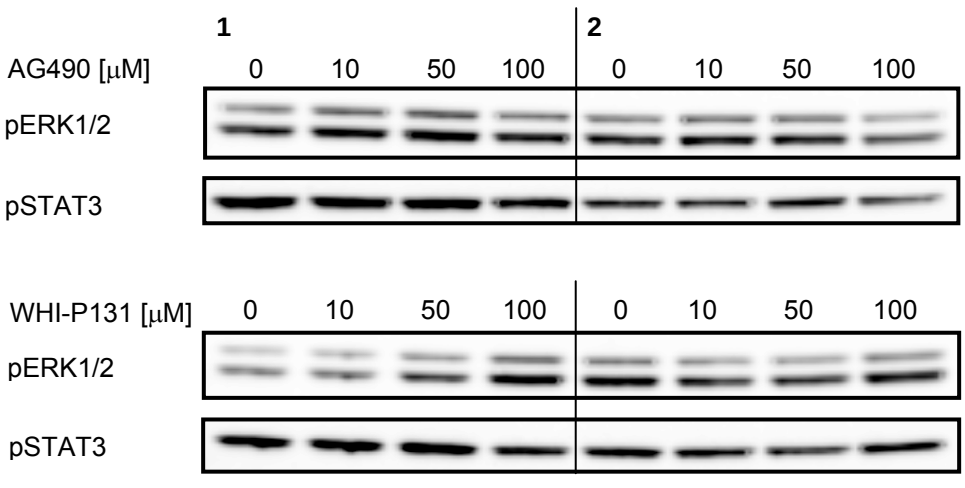

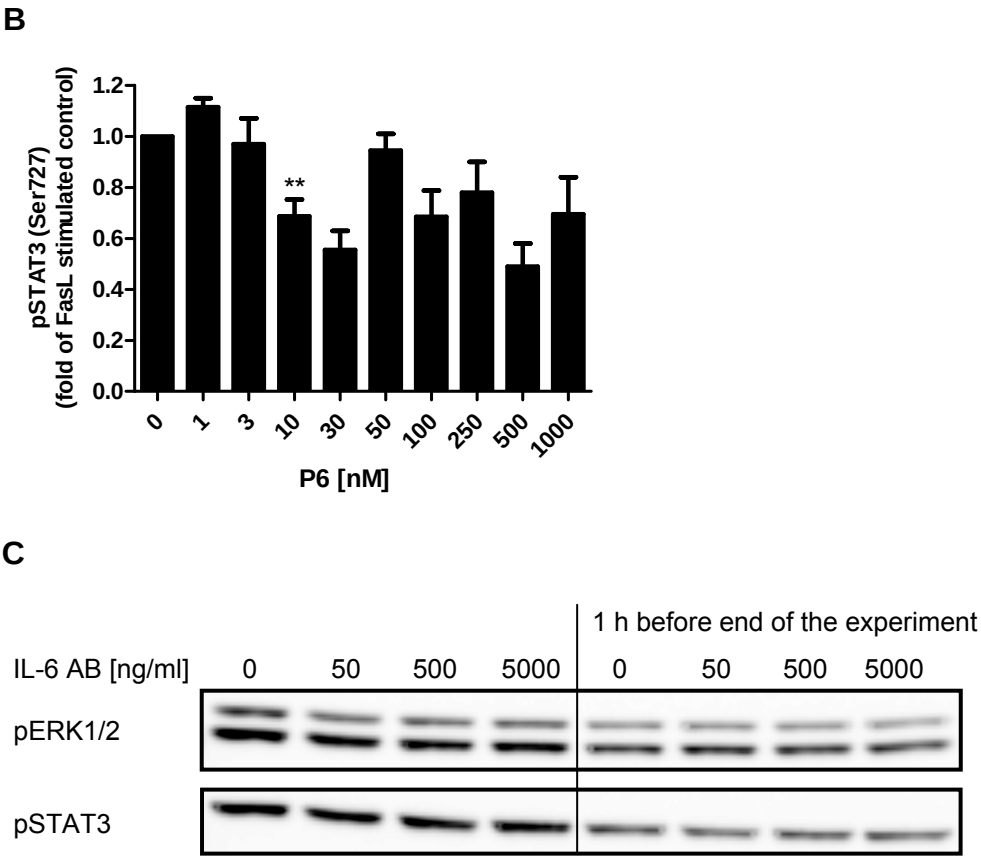

Fig. 20. Treatment with JAK inhibitors or an IL-6 antibody does not reduce Fas-induced phosphorylation of ERK1/2. Adipocytes were treated for 6 hours with FasL and with or without different concentrations of the JAK inhibitors AG490 (JAK2), WHI-P131 (JAK3) (A) and P6 (pan-JAK, B) or an IL-6 antibody (C). Amounts of pERK1/2 and pSTAT3 in whole cell lysates were quantified by Western blot analysis. Results for the experiments with P6 are the mean ± SEM of 2, 4 (100 nM) or 8 (10 nM) independent experiments, **p < 0.01.

These results suggest that increase in IL-6 secretion does not contribute to FasL-induced lipolysis, at least not to a significant extent.

Both TNFα and IL-6 are described to have lipolytic activity but could be excluded in our context. As we also measured increased KC secretion after FasL treatment and found no literature on a possible lipolytic action of the cytokine, we hypothesized that KC might induce lipolysis. 3T3-L1 adipocytes were treated with increasing dose of recombinant KC. However, as indicated in Fig. 21 no changes in glycerol release could be demonstrated.

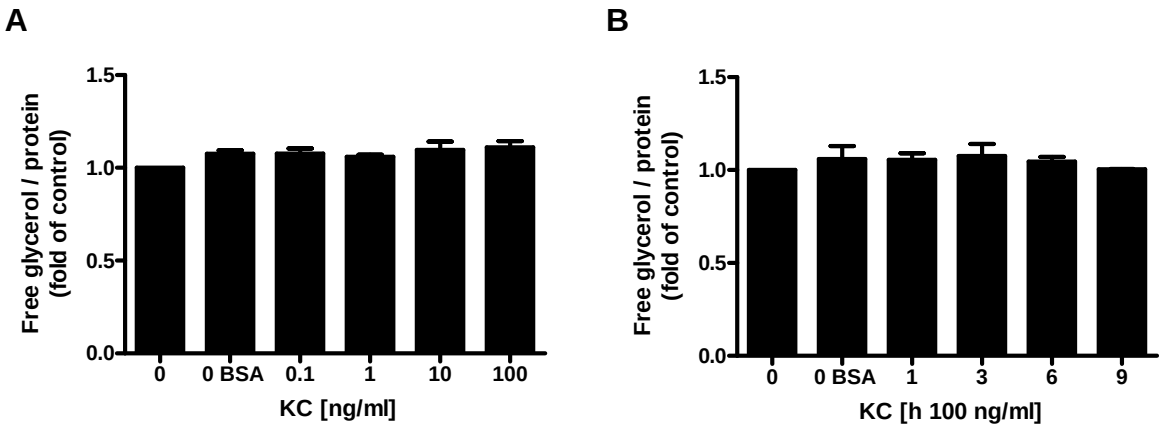

Fig. 21. Recombinant KC does not increase lipolysis in 3T3-L1 adipocytes. Adipocytes were treated with different concentrations of recombinant KC (A) or with 100 ng/ml KC for the indicated time periods (B). Glycerol release was determined after medium was removed and cells were incubated with KREBS buffer for another hour. Results are the mean ± SEM of 4 (A) or 2 (B) independent experiments.

Discussion

The term apoptosis is used in Greek to describe the falling of leaves from a tree. Working on the signalling of the Fas receptor, a well established inducer of apoptosis, has made it always difficult to determine which leaves are still green, swinging on the branches and which are dancing with the wind in orange and maroon on their way to the floor. As the induction of apoptosis results from a shift in the balance of survival and death signals to the latter, it was always hard to say which of the observed effects are due to cell death, proceed or even counteract it, or are of the kind that may be classified as non-apoptotic effects of the Fas receptor.
The aim of the current work was to elucidate the impact of Fas signalling on adipocyte physiology based on the fact that Fas deficient mice and AFasKO mice have an improved metabolic profile when fed a high fat diet.

The Fas receptor is expressed in 3T3-L1 preadipocytes, differentiating 3T3-L1 preadipocytes and mature 3T3-L1 adipocytes (Fig. 1). Initial experiments were performed to investigate the possible role of the Fas receptor in preadipocyte proliferation and differentiation. Effects on morphological features like cell size and lipid loading as well as the influence on cell number and proliferation were taken into account. Furthermore, the impact of Fas on the expression of adipogenic markers was analyzed during differentiation. Activation of the Fas receptor leads to reduced proliferation of 3T3-L1 preadipocytes after 48 hours of incubation (Fig. 2). The increased MTT metabolism at D0 in FasL treated cells can be explained as follows. The control cells are confluent at this time point and undergo growth arrest, whereas Fas treatment led to a reduction in cell number and consequently prolonged the period of cell division.
During differentiation, FasL inhibits the expression of adipogenic markers (Fig. 3). Longer incubation periods with FasL lead to cells loss and thereby less differentiated, lipid-filled adipocytes. Although some of the remaining differentiated adipocytes after FasL treatment seemed to be enlarged, a clear influence of Fas on morphological features of preadipocytes and adipocytes could not be demonstrated (data not shown). These results suggest that during high fat feeding of mice activation of Fas would act as a negative signal that inhibits the generation of new adipocytes and

thereby would favour the development of a more hyperplastic tissue. Lack of the Fas receptor on the other hand would lead to more adipocytes and a WAT that more efficiently stores excess energy. This concept seems to be verified when looking at Fas deficient mice which exhibit the same weight gain but smaller adipocytes. However, AFasKO mice show not difference in cellularity of WAT compared to wild type mice on a high fat diet. In AFasKO mice the Cre recombinase is driven by the fatty acid binding protein 4 (Fabp4) promotor. Since Fabp4 is downstream of PPARγ, Fas receptor expression is not down-regulated until during adipocyte differentiation in AFasKO mice. Thus, early adipocyte-development is unlikely to be affected in AFasKo mice, as opposed to Fas deficient mice. The reduction of preadipocyte proliferation as well as the reduction of differentiation markers and differentiated adipocytes in culture is most probably due to the apoptotic effect of Fas activation. It is however difficult to say if such an apoptotic effect on preadipocytes is present and as pronounced in vivo.

In mature 3T3-L1 adipocytes, activation of the Fas receptor influences fuel metabolism in two major aspects. First, we previously observed that Fas induces basal glucose uptake and diminishes insulin stimulated glucose uptake. Second, Fas stimulation has a time dependent influence on lipolysis and prolonged activation of Fas leads to increased release of FFAs and glycerol (Fig. 4). The time course of FFAs and glycerol release completely match each other, which indicates that the increased of these two metabolites in the buffer is not due to cell leakage.
ERK1/2 phosphorylation is induced by Fas stimulation (Fig. 5). After 15 minutes of FasL treatment the MAP kinases were induced significantly. After 30 minutes there was no difference compared to the control condition. After 3, 6 and 12 hours the kinases were again significantly activated. The shape of the graph suggests a kinetic with an acute less pronounced activation followed by a more pronounced activation after longer incubation periods. However, the little number of time points does not allow to eliminate the idea that pERK1/2 is increased gradually. In the case of a biphasic activation, we speculated that the activation seen after 15 minutes would be directly mediated by the Fas receptor whereas the activation induced after hours of incubation would be due to an indirect effect of Fas signalling. Although the signal for pERK1/2 is lower after 12 hours we can not conclude from the available data that ERK1/2 activation is again decreased gradually after 6 hours of incubation. In this

context, it is important to note that prolonged ERK1/2 activation can be linked to cell death (68). However, studies that link ERK1/2 activation to Fas triggered apoptosis show an acute and transient stimulation of the kinases (69,70).

The ERK1/2 kinases are activated by a myriad of factors. Among those are the lipolytic cytokines IL-6 and TNFα as well as the chemokine IL-8. The TNF receptors (TNF-R) belong to the same receptor superfamily as Fas. TNFα stimulates lipolysis through activation of the TNF-R1 and this effect is completely dependent on the activity of ERK1/2 (32,34,71). Indeed, Fas induced lipolysis could also be inhibited by using the MEK inhibitor U0126 (Fig. 6). This ERK1/2 dependency was further underscored by the fact the rosiglitazone pretreatment inhibited both Fas-induced ERK1/2 activation and lipolysis (Fig. 8 and 9). Since FasL treatment did not increase TNFα secretion we can conclude that the lipolytic effect of FasL is not induced indirectly through TNFα.

The glycerol assay we used also measures free glycerol-3-phosphate. As a consequence we first could not exclude the possibility that we measured a decrease in triacylglycerol synthesis instead of an increase in lipolysis. The ERK1/2 dependency of Fas induced glycerol release further supports the notion that an increase in lipolysis was actually measured.

In conclusion, prolonged Fas activation leads to an increase in lipolysis which is completely dependent on the activity of the ERK1/2 MAP kinases.

Interestingly, incubation for 2 hours with FasL resulted in a significant decrease of FFAs and glycerol release (Fig. 4). Looking at the graph of ERK1/2 activity makes room for the assumption that the kinases are activated at this time point. We aimed to clarify this conflicting result. However, work on the small decrease in lipolysis obviously requires a high number of experiments to get significant results and initial trials with the MEK inhibitor led to no conclusion. Therefore we focused on the mechanisms behind the stimulation of lipolysis by FasL.

We first aimed to investigate possible downstream consequences of the observed MAP kinase activation after FasL treatment. Like during preadipocyte differentiation Fas activation in mature adipocytes was associated with the down-regulation of the adipogenic markers C/EBPα and PPARγ (Fig. 7). This effect was very pronounced in the case of PPARγ which was reduced by 90 percent on the protein level after 12 hours of FasL incubation. Consistent with this the PPARγ targets perilipin and HSL

(63,64) were also found to be reduced (Fig. 10). MAP kinase-mediated serine phosphorylation of PPARγ was shown to reduce the activity of the transcriptional factor (65). Since PPARγ and C/EBPα positively regulate each others expression (10), a MAP kinase-induce reduction in PPARγ activity may also effect its expression. Furthermore, TNFα-induced lipolysis was shown to involve ERK1/2-dependent reduction of the lipid droplet coating protein perilipin (32). We therefore postulated that the Fas mediated reduction of PPARγ and perilipin are downstream effects of ERK1/2 activation. However, the increased activity of ERK1/2 induced by FasL treatment is not responsible for the reduction of PPARγ (data not shown) and perilipin (Fig. 10A). Nevertheless, the Fas-induced reduction of perilipin might facilitate triacylglycerol breakdown caused through ERK1/2 activation. The latter finding also suggests that Fas and TNF-R1 activation induce the same metabolic effect via different cellular mechanisms. In the context of increased lipolysis, FasL mediated reduction of HSL was a surprising finding. However, TNFα as well reduces the activity of HSL through inhibition of the enzyme's gene expression in 3T3-L1 adipocytes (72). On the other hand HSL can be activated by ERK1/2 through phosphorylation on serine 600 (66). But it is hard to hypothesize that Fas reduces the transcription of HSL like TNFα does but has the opposite effect when it comes to the enzyme's activity. Thus, it remains to be proven which lipase is responsible for the breakdown of triacylglycerols after Fas (and TNF-R1) activation.

Besides the down-regulation of perilipin and HSL we also found lipin-1 (Fig. 11) to be reduced on mRNA and protein level after FasL treatment. Lipin-1 received much attention during the last years. In adipocytes this protein acts as a phosphatase in the process of triacylglycerol synthesis as well as a transcription factor (22). Moreover, lipin-1 acts as a transcriptional co-activator involved in the maturation and maintenance of adipocytes. Transcription of lipin-1 is induced by C/EBPα. By binding to PPARγ lipin-1 increases the positive transcriptional feedback loop between C/EBPα and PPARγ (23). It is therefore not surprising that the Fas induced down-regulation of C/EBPα leads to a reduction of the lipin-1 transcript. The finding that ERK1/2 inhibition does not rescue the expression of lipin-1 (Fig. 11) suggests that ERK1/2 activation is not the cause but could rather be a downstream effect of Fas-mediated lipin-1 reduction. In this case again TNFα has a similar effect. TNFα inhibits transcription of lipin-1 and this seems to be mediated via JAK2 (73). Since TNFα

does not directly signal via JAK2 the finding suggests an inflammatory autocrine/paracrine effect of TNFα treatment. As described later in more detail, the same JAK2 inhibitor previously used in the TNFα study (73) did not influence Fas induced phosphorylation of ERK1/2 nor did it rescue Fas-induced lipin-1 protein reduction (data not shown). Hence, TNFα is claimed to reduce perilipin via ERK1/2 and to reduce lipin-1 in a JAK2 dependent but ERK1/2 independent fashion. Both signalling mechanisms seem not to be shared by the Fas receptor.

A lack of lipin-1 in WAT was shown to lead to accumulation of its substrate PA which is another inducer of the MAP kinase pathway (25). Because of the latter findings we tested the impact of PA on 3T3-L1 adipocytes. Indeed, PA induced lipolysis in adipocytes and this effect was ERK1/2-dependent (Fig. 12). It is an interesting and novel finding that this intermediate of the triacylglycerol synthesis pathway is able to enhance the breakdown of triacylglycerols. In order to measure changes in cellular PA concentrations, MS analysis was applied. So far, we have not been able to detect any increase of intracellular PA after FasL treatment so far (Fig. 13). This could be due to inappropriate extraction of PA species in our approach with butanol as a solvent. Furthermore, spatial changes in intracellular PA concentration may have an important impact which cannot be detected by our approach. Analysis with a different extraction protocol is still ongoing at the time of writing this manuscript.

Our group has previously shown that FasL treatment of 3T3-L1 adipocytes leads to the cleavage of PARP, a caspase substrate. Caspases also activate nucleases that degrade nuclear material and proteases that break-down nuclear and cytoskeletal proteins. In this context we found the transcript of AKT2 to be down-regulated by Fas treatment (data not shown). AKT is an important mediator of cell-survival signalling (74). Furthermore, PPARγ, perilipin, lipin-1 and HSL were all regulated on the transcriptional level. Based on the latter findings the reduction of the mentioned proteins could be explained by caspase-dependent DNA fragmentation which leads to reduced transcription of the respective genes. However, caspase inhibition could not correct the Fas-mediated effects on insulin stimulated glucose uptake and lipolysis (data not shown).

To summarize, we found that Fas activation leads to the down-regulation of PPARγ, C/EBPα, perilipin, lipin-1 and HSL in mature adipocytes. Perilipin and lipin-1 are ERK1/2 independently regulated and in a different fashion than by TNFα. If the down-regulation of these proteins has a causative metabolic link to the Fas-induced

increase in lipolysis and if it has to be attributed to apoptosis could not definitely be answered. Experiments with caspase inhibitors suggest that the FasL-induced alterations in glucose and lipid metabolism are caspase-independently regulated whereas the induction of apoptosis is caspase-dependent.

Secondly, we wanted to look for possible upstream mediators of the Fas-induced ERK1/2 activation. Intracellular calcium concentrations were reported to have different impacts on lipolysis. In human adipocytes that were differentiated in vitro increased intracellular calcium were found to decrease lipolysis through activation of PDE with a subsequent decrease in cAMP and HSL phosphorylation (35). The compound magnolol on the other hand was shown to induce lipolysis in sterol ester-loaded 3T3-L1 preadipocytes through CaMKII dependent ERK1/2 activation (67). Chelation of extra- and intracellular calcium indicated a role for calcium fluxes in FasL-mediated lipolysis (Fig. 14 and 15). However, we obtained conflicting results regarding the involvement of CaMKII activation. Application of the CaMKII inhibitor KN62 during FasL treatment reduced ERK1/2 activation and lipolysis (Fig. 16). Analysis of CaMKII activity on the contrary revealed that neither FasL nor TNFα stimulated the enzyme (Fig. 17). Because of the higher specificity of the activity assay and the only partial effects of the inhibitor it is appropriate to conclude that a probable calcium mediated signal is transduced via another enzyme than CaMKII. Western blot analysis revealed that Fas stimulates PKC phosphorylation in a manner that is unlikely to be responsible for the increase in lipolysis (data not shown). Hence, which downstream effectors are activated by calcium in the signalling pathway(s) leading to Fas-induced lipolysis remains elusive. Considering calcium to be involved in this metabolic change triggered by the Fas receptor one is obliged to acknowledge that calcium is involved in multiple steps of the apoptotic process (75). Based on the findings mentioned above we can not exclude that apoptosis linked calcium fluxes are responsible for at least part of the lipolytic effect of FasL treatment.

Fas activation increased the secretion of KC (mouse homologue to IL-8) and it induced IL-6 gene expression and secretion. Furthermore, it increased the phosphorylation of STAT3 (Fig. 18D). However, we could not show an influence of KC on lipolysis in 3T3-L1 adipocytes (Fig. 21). The cytokine IL-6 on the other hand is a known to induce lipolysis and STAT3 is a component of the IL-6 signalling cascade.

The increased IL-6 mRNA expression and IL-6 secretion (Fig. 18B and C) made it even more tempting to speculate that an autocrine/paracrine effect of IL-6 was responsible for the Fas-mediated activation of the MAP kinase pathway and induction of lipolysis. Yet the time course of IL-6 mRNA expression and IL-6 secretion did not match each other (Fig. 18B and C). Sant7 reduced the phosphorylation of ERK1/2 significantly but to a very varying degree in the different experiments (Fig. 19). This could be due to a lack of specificity, because Sant7 is a modification of the human IL-6 molecule. Surprisingly, Sant7 had no effect Fas-induced pSTAT3 (Fig. 19). The pan-JAK inhibitor P6 on the contrary only reduced Fas-mediated pSTAT3 and had no consistent effect on pERK1/2 (Fig. 20B). We used an antibody that is specific for phosphorylated STAT3 on serine 727, a site that is thought to be phosphorylated by the MAP kinase or the mTOR pathway (Cell Signalling product information). However, the latter findings suggest that Fas-mediated ERK1/2 and STAT3 phosphorylation are independent events. The JAK2 (and JAK3) inhibitor AG 490 and the JAK3 inhibitor WHI-P131 did not decrease the effects of FasL treatment (Fig. 20A). Taken together with the findings of the P6 experiments this suggests that the autocrine/paracrine Fas dependent signal is transduced via JAK1 or TYK2, the forth JAK isoform. The use of anti-IL-6 antibodies however further disproved the hypothesis that IL-6 is the cause of this signal (Fig. 20C). Therefore, the similar time courses of pERK induction and IL-6 mRNA expression (Fig. 5 and 18C) point towards an involvement of ERK1/2 in the regulation of IL-6 gene expression. Indeed, the MAP kinases were shown to regulated IL-6 transcription in 3T3-L1 cells (76). Therefore, it is probable that FasL treatment induces an inflammatory response in adipocytes through activation of ERK1/2 that leads to an increase in the secretion of IL-6 and other cytokines. On the other hand, the increase in IL-6 and KC secretion was significant but, by 1.5 and 2.5 fold respectively, rather low. Such small increase may be explained by the fact that apoptosis is executed without inducing an inflammatory reaction (74). However, Fas activation was shown to induce ERK1/2 dependent IL-6 secretion in human glioma cells (77) and injection of an anti-Fas antibody into the brain triggers elevated IL-6 plasma levels in mice (78). Furthermore, Fas activation induces IL-8 secretion in different cells types. In the HT-29 colon epithelial cell line this effect was shown to be independent of apoptosis and dependent on the induction of the p38 MAPK and ERK1/2 (79,80). Human rheumatoid arthritis synoviocytes also secrete more IL-8 upon Fas activation independent of apoptosis (81). In vascular

smooth muscle cells on the other hand Fas-induced apoptosis is not “silent” but connected to an inflammatory response (82). These examples illustrate that activation of the Fas receptor can induce inflammatory changes in different cellular contexts, and this aspect of Fas signalling can be independent of apoptosis and mediated by ERK1/2. Decreased Fas-mediated inflammation in adipocytes is most probably responsible for the better inflammatory profile of AFasKO mice fed a high fat diet. In conclusion, we show that Fas activation induces the production and secretion of cytokines in 3T3-L1 adipocytes. However, they do not seem to contribute to FasL-induced lipolysis.

Our data obtained from experiments with the 3T3-L1 adipocytes suggest that activation of the Fas receptor in adipose tissue has significant negative effects on the recruitment of new adipocytes as well as on the maintenance of mature adipocytes and their metabolism.

As a last thought I would like to ask myself if it would be correct to state here as a final conclusion that the Fas receptor induces something extraordinary and unexpected in 3T3-L1 adipocytes. We have some indications that Fas activation changes lipid and glucose metabolism in adipocytes independent of apoptosis. However, it is still tempting to say: “The leaves fell, and we watched them dancing.”

References

1. Walter F. Boron, E. L. B. (2005) *Medical physiology: a cellular and molecular approach - Updated ed.*, Elsevier Saunders, Philadelphia, Pennsylvania
2. Gerhard Thews, E. M., Peter Vaupel. (1999) *Anatomie, Physiologie, Pathophysiologie des Menschen*, Wissenschaftliche Verlagsgesellschaft mbH, Stuttgart
3. Kido, Y., Nakae, J., and Accili, D. (2001) *J Clin Endocrinol Metab* **86**, 972-979
4. Tamemoto, H., Kadowaki, T., Tobe, K., Yagi, T., Sakura, H., Hayakawa, T., Terauchi, Y., Ueki, K., Kaburagi, Y., Satoh, S., and et al. (1994) *Nature* **372**, 182-186
5. Withers, D. J., Gutierrez, J. S., Towery, H., Burks, D. J., Ren, J. M., Previs, S., Zhang, Y., Bernal, D., Pons, S., Shulman, G. I., Bonner-Weir, S., and White, M. F. (1998) *Nature* **391**, 900-904
6. Liu, S. C., Wang, Q., Lienhard, G. E., and Keller, S. R. (1999) *J Biol Chem* **274**, 18093-18099
7. Fantin, V. R., Wang, Q., Lienhard, G. E., and Keller, S. R. (2000) *Am J Physiol Endocrinol Metab* **278**, E127-133
8. Dugani, C. B., and Klip, A. (2005) *EMBO Rep* **6**, 1137-1142
9. Kitamura, T., Kitamura, Y., Kuroda, S., Hino, Y., Ando, M., Kotani, K., Konishi, H., Matsuzaki, H., Kikkawa, U., Ogawa, W., and Kasuga, M. (1999) *Mol Cell Biol* **19**, 6286-6296
10. Otto, T. C., and Lane, M. D. (2005) *Crit Rev Biochem Mol Biol* **40**, 229-242
11. Trujillo, M. E., and Scherer, P. E. (2006) *Endocr Rev* **27**, 762-778
12. Rosen, E. D., and MacDougald, O. A. (2006) *Nat Rev Mol Cell Biol* **7**, 885-896
13. Tang, Q. Q., Otto, T. C., and Lane, M. D. (2003) *Proc Natl Acad Sci U S A* **100**, 44-49
14. Gesta, S., Tseng, Y. H., and Kahn, C. R. (2007) *Cell* **131**, 242-256
15. Yang, X., and Smith, U. (2007) *Diabetologia* **50**, 1127-1139
16. Lelliott, C., and Vidal-Puig, A. J. (2004) *Int J Obes Relat Metab Disord* **28 Suppl 4**, S22-28
17. Heilbronn, L., Smith, S. R., and Ravussin, E. (2004) *Int J Obes Relat Metab Disord* **28 Suppl 4**, S12-21
18. Frayn, K. N., Karpe, F., Fielding, B. A., Macdonald, I. A., and Coppack, S. W. (2003) *Int J Obes Relat Metab Disord* **27**, 875-888
19. Hausman, D. B., DiGirolamo, M., Bartness, T. J., Hausman, G. J., and Martin, R. J. (2001) *Obes Rev* **2**, 239-254
20. Spalding, K. L., Arner, E., Westermark, P. O., Bernard, S., Buchholz, B. A., Bergmann, O., Blomqvist, L., Hoffstedt, J., Naslund, E., Britton, T., Concha, H., Hassan, M., Ryden, M., Frisen, J., and Arner, P. (2008) *Nature* **453**, 783-787
21. Large, V., Peroni, O., Letexier, D., Ray, H., and Beylot, M. (2004) *Diabetes Metab* **30**, 294-309
22. Reue, K., and Brindley, D. N. (2008) *J Lipid Res* **49**, 2493-2503
23. Koh, Y. K., Lee, M. Y., Kim, J. W., Kim, M., Moon, J. S., Lee, Y. J., Ahn, Y. H., and Kim, K. S. (2008) *J Biol Chem* **283**, 34896-34906
24. Peterfy, M., Phan, J., Xu, P., and Reue, K. (2001) *Nat Genet* **27**, 121-124
25. Nadra, K., de Preux Charles, A. S., Medard, J. J., Hendriks, W. T., Han, G. S., Gres, S., Carman, G. M., Saulnier-Blache, J. S., Verheijen, M. H., and Chrast, R. (2008) *Genes Dev* **22**, 1647-1661
26. Phan, J., and Reue, K. (2005) *Cell Metab* **1**, 73-83

27. Donkor, J., Sparks, L. M., Xie, H., Smith, S. R., and Reue, K. (2008) *J Clin Endocrinol Metab* **93**, 233-239
28. Ducharme, N. A., and Bickel, P. E. (2008) *Endocrinology* **149**, 942-949
29. Brasaemle, D. L. (2007) *J Lipid Res* **48**, 2547-2559
30. Arner, P. (2005) *Best Pract Res Clin Endocrinol Metab* **19**, 471-482
31. Carmen, G. Y., and Victor, S. M. (2006) *Cell Signal* **18**, 401-408
32. Souza, S. C., Palmer, H. J., Kang, Y. H., Yamamoto, M. T., Muliro, K. V., Paulson, K. E., and Greenberg, A. S. (2003) *J Cell Biochem* **89**, 1077-1086
33. Pedersen, B. K., Steensberg, A., Fischer, C., Keller, C., Ostrowski, K., and Schjerling, P. (2001) *Exerc Immunol Rev* **7**, 18-31
34. Brown, J. M., Boysen, M. S., Chung, S., Fabiyi, O., Morrison, R. F., Mandrup, S., and McIntosh, M. K. (2004) *J Biol Chem* **279**, 26735-26747
35. Xue, B., Greenberg, A. G., Kraemer, F. B., and Zemel, M. B. (2001) *FASEB J* **15**, 2527-2529
36. Fantuzzi, G. (2005) *J Allergy Clin Immunol* **115**, 911-919; quiz 920
37. Klok, M. D., Jakobsdottir, S., and Drent, M. L. (2007) *Obes Rev* **8**, 21-34
38. Yu, Y. H., and Ginsberg, H. N. (2005) *Circ Res* **96**, 1042-1052
39. Yamauchi, T., Kamon, J., Minokoshi, Y., Ito, Y., Waki, H., Uchida, S., Yamashita, S., Noda, M., Kita, S., Ueki, K., Eto, K., Akanuma, Y., Froguel, P., Foufelle, F., Ferre, P., Carling, D., Kimura, S., Nagai, R., Kahn, B. B., and Kadowaki, T. (2002) *Nat Med* **8**, 1288-1295
40. Ogden, C. L., Yanovski, S. Z., Carroll, M. D., and Flegal, K. M. (2007) *Gastroenterology* **132**, 2087-2102
41. Faeh, D., Marques-Vidal, P., Chiolero, A., and Bopp, M. (2008) *Swiss Med Wkly* **138**, 204-210
42. Lasserre, A. M., Chiolero, A., Paccaud, F., and Bovet, P. (2007) *Swiss Med Wkly* **137**, 157-158
43. Zimmermann, M. B., Gubeli, C., Puntener, C., and Molinari, L. (2004) *Swiss Med Wkly* **134**, 523-528
44. Guilherme, A., Virbasius, J. V., Puri, V., and Czech, M. P. (2008) *Nat Rev Mol Cell Biol* **9**, 367-377
45. Weisberg, S. P., McCann, D., Desai, M., Rosenbaum, M., Leibel, R. L., and Ferrante, A. W., Jr. (2003) *J Clin Invest* **112**, 1796-1808
46. Lee, D. E., Kehlenbrink, S., Lee, H., Hawkins, M., and Yudkin, J. S. (2009) *Am J Physiol Endocrinol Metab* **296**, E1210-1229
47. Gregor, M. G., and Hotamisligil, G. S. (2007) *J Lipid Res*
48. Rudich, A., Kanety, H., and Bashan, N. (2007) *Trends Endocrinol Metab* **18**, 291-299
49. Donath, M. Y., Storling, J., Maedler, K., and Mandrup-Poulsen, T. (2003) *J Mol Med* **81**, 455-470
50. Maedler, K., Schumann, D. M., Sauter, N., Ellingsgaard, H., Bosco, D., Baertschiger, R., Iwakura, Y., Oberholzer, J., Wollheim, C. B., Gauthier, B. R., and Donath, M. Y. (2006) *Diabetes* **55**, 2713-2722
51. Lambert, C., Landau, A. M., and Desbarats, J. (2003) *Apoptosis* **8**, 551-562
52. Watanabe-Fukunaga, R., Brannan, C. I., Itoh, N., Yonehara, S., Copeland, N. G., Jenkins, N. A., and Nagata, S. (1992) *J Immunol* **148**, 1274-1279
53. Lynch, D. H., Watson, M. L., Alderson, M. R., Baum, P. R., Miller, R. E., Tough, T., Gibson, M., Davis-Smith, T., Smith, C. A., Hunter, K., and et al. (1994) *Immunity* **1**, 131-136
54. Takahashi, T., Tanaka, M., Inazawa, J., Abe, T., Suda, T., and Nagata, S. (1994) *Int Immunol* **6**, 1567-1574

55. Itoh, N., Yonehara, S., Ishii, A., Yonehara, M., Mizushima, S., Sameshima, M., Hase, A., Seto, Y., and Nagata, S. (1991) *Cell* **66**, 233-243
56. Suda, T., Takahashi, T., Golstein, P., and Nagata, S. (1993) *Cell* **75**, 1169-1178
57. Wajant, H., Pfizenmaier, K., and Scheurich, P. (2003) *Cytokine Growth Factor Rev* **14**, 53-66
58. French, L. E., Hahne, M., Viard, I., Radlgruber, G., Zanone, R., Becker, K., Muller, C., and Tschopp, J. (1996) *J Cell Biol* **133**, 335-343
59. Lee, H. O., and Ferguson, T. A. (2003) *Cytokine Growth Factor Rev* **14**, 325-335
60. Houston, A., and O'Connell, J. (2004) *Curr Opin Pharmacol* **4**, 321-326
61. Salomoni, P., and Khelifi, A. F. (2006) *Trends Cell Biol* **16**, 97-104
62. Pfaffl, M. W. (2001) *Nucleic Acids Res* **29**, e45
63. Arimura, N., Horiba, T., Imagawa, M., Shimizu, M., and Sato, R. (2004) *J Biol Chem* **279**, 10070-10076
64. Deng, T., Shan, S., Li, P. P., Shen, Z. F., Lu, X. P., Cheng, J., and Ning, Z. Q. (2006) *Endocrinology* **147**, 875-884
65. Hu, E., Kim, J. B., Sarraf, P., and Spiegelman, B. M. (1996) *Science* **274**, 2100-2103
66. Greenberg, A. S., Shen, W. J., Muliro, K., Patel, S., Souza, S. C., Roth, R. A., and Kraemer, F. B. (2001) *J Biol Chem* **276**, 45456-45461
67. Huang, S. H., Shen, W. J., Yeo, H. L., and Wang, S. M. (2004) *J Cell Biochem* **91**, 1021-1029
68. Cagnol, S., and Chambard, J. C. (2009) *FEBS J*
69. Goillot, E., Raingeaud, J., Ranger, A., Tepper, R. I., Davis, R. J., Harlow, E., and Sanchez, I. (1997) *Proc Natl Acad Sci U S A* **94**, 3302-3307
70. Ulisse, S., Cinque, B., Silvano, G., Rucci, N., Biordi, L., Cifone, M. G., and D'Armiento, M. (2000) *Cell Death Differ* **7**, 916-924
71. Sethi, J. K., Xu, H., Uysal, K. T., Wiesbrock, S. M., Scheja, L., and Hotamisligil, G. S. (2000) *FEBS Lett* **469**, 77-82
72. Sumida, M., Sekiya, K., Okuda, H., Tanaka, Y., and Shiosaka, T. (1990) *J Biochem* **107**, 1-2
73. Tsuchiya, Y., Takahashi, N., Yoshizaki, T., Tanno, S., Ohhira, M., Motomura, W., Takakusaki, K., Kohgo, Y., and Okumura, T. (2009) *Biochem Biophys Res Commun* **382**, 348-352
74. Elmore, S. (2007) *Toxicol Pathol* **35**, 495-516
75. Orrenius, S., Zhivotovsky, B., and Nicotera, P. (2003) *Nat Rev Mol Cell Biol* **4**, 552-565
76. Ohashi, K., Kanazawa, A., Tsukada, S., and Maeda, S. (2005) *Biochem Biophys Res Commun* **327**, 707-712
77. Choi, C., Gillespie, G. Y., Van Wagoner, N. J., and Benveniste, E. N. (2002) *J Neurooncol* **56**, 13-19
78. Benigni, F., Sacco, S., Aloe, L., and Ghezzi, P. (1998) *Am J Pathol* **153**, 1377-1381
79. Abreu-Martin, M. T., Vidrich, A., Lynch, D. H., and Targan, S. R. (1995) *J Immunol* **155**, 4147-4154
80. O'Brien, D., O'Connor, T., Shanahan, F., and O'Connell, J. (2002) *Ann N Y Acad Sci* **973**, 161-165
81. Sekine, C., Yagita, H., Kobata, T., Hasunuma, T., Nishioka, K., and Okumura, K. (1996) *Biochem Biophys Res Commun* **228**, 14-20
82. Schaub, F. J., Han, D. K., Liles, W. C., Adams, L. D., Coats, S. A., Ramachandran, R. K., Seifert, R. A., Schwartz, S. M., and Bowen-Pope, D. F. (2000) *Nat Med* **6**, 790-796

Appendix

Paper published in *Diabetologia*

Paper published in *The Journal of Clinical Investigation*

Diabetologia (2009) 52:541–546
DOI 10.1007/s00125-008-1223-5

ARTICLE

Basal lipolysis, not the degree of insulin resistance, differentiates large from small isolated adipocytes in high-fat fed mice

S. Wueest · R. A. Rapold · J. M. Rytka · E. J. Schoenle · D. Konrad

Received: 29 October 2008 / Accepted: 4 November 2008 / Published online: 2 December 2008

Abstract
Aims/hypothesis Adipocytes in obesity are characterised by increased cell size and insulin resistance compared with adipocytes isolated from lean patients. However, it is not clear at present whether hypertrophy actually does drive adipocyte insulin resistance. Thus, the aim of the present study was to metabolically characterise small and large adipocytes isolated from epididymal fat pads of mice fed a high-fat diet (HFD).
Methods C57BL/6J mice were fed normal chow or HFD for 8 weeks. Adipocytes from epididymal fat pads were isolated by collagenase digestion and, in HFD-fed mice, separated into two fractions according to their size by filtration through a nylon mesh. Viability was assessed by lactate dehydrogenase and 3-(4,5-dimethylthiazol-2-yl)-2, 5-diphenyltetrazolium assays. Basal and insulin-stimulated d-[U-^{14}C]glucose incorporation and lipolysis were measured. Protein levels and mRNA expression were determined by western blot and real-time RT-PCR, respectively.
Results Insulin-stimulated D-[U-^{14}C]glucose incorporation into adipocytes isolated from HFD-fed mice was reduced by 50% compared with adipocytes from chow-fed mice. However, it was similar between small (average diameter 60.9±3.1 μm) and large (average diameter 83.0±6.6 μm) adipocytes. Similarly, insulin-stimulated phosphorylation of protein kinase B and AS160 were reduced to the same extent in small and large adipocytes isolated from HFD-mice. In addition, insulin failed to inhibit lipolysis in both adipocyte fractions, whereas it decreased lipolysis by 30% in adipocytes of chow-fed mice. In contrast, large and small adipocytes differed in basal lipolysis rate, which was twofold higher in the larger cells. The latter finding was associated with higher mRNA expression levels of *Atgl* (also known as *Pnpla2*) and *Hsl* (also known as *Lipe*) in larger adipocytes. Viability was not different between small and large adipocytes.
Conclusions/interpretation Rate of basal lipolysis but not insulin responsiveness is different between small and large adipocytes isolated from epididymal fat pads of HFD-fed mice.

Keywords Adipocyte size · Insulin resistance · Insulin sensitivity

Abbreviations

Akt	protein kinase B
ATGL	adipose triacylglycerol lipase
HFD	high-fat diet
HSL	hormone-sensitive lipase
ipGTT	intraperitoneal glucose tolerance test
LDH	lactate dehydrogenase
MTT	3-(4,5-dimethylthiazol-2-yl)-2,5-diphenyltetrazolium

Introduction

Adipocyte hypertrophy has been proposed to induce adipose tissue dysfunction in obesity, while cell death of

S. Wueest · R. A. Rapold · J. M. Rytka · E. J. Schoenle · D. Konrad (✉)
Department of Endocrinology and Diabetology,
University Children's Hospital,
Steinwiesstrasse 75,
CH-8032 Zurich, Switzerland
e-mail: daniel.konrad@kispi.uzh.ch

S. Wueest · R. A. Rapold · J. M. Rytka · D. Konrad
Zurich Center for Integrative Human Physiology,
University of Zurich,
Zurich, Switzerland

hypertrophic adipocytes is thought to be a driving force for macrophage infiltration into adipose tissue [1] and large adipocytes may secrete higher levels of pro-inflammatory cytokines [2]. At a more metabolic level, hypertrophic adipocytes may exhibit a reduced capacity to store and retain NEFA, leading to elevated levels of circulating NEFA [3]. In contrast, hyperplastic adipocytes may favour the deposition of NEFA and thus protect other tissues such as liver and skeletal muscle from lipotoxicity by sequestering NEFA away from them [3]. In this regard, treatment with thiazolidinediones has been shown to increase cellularity in adipose tissue by promoting pre-adipocyte differentiation and inducing apoptosis of large adipocytes, resulting in smaller and more insulin-sensitive adipocytes [4]. Yet, most studies comparing large and small adipocytes isolated them from different participants/animals (small adipocytes from lean, large adipocytes from obese) [5, 6]. Thus, differences between large and small adipocytes could have resulted from other factors that differ between lean and obese sources [5, 6] and not from genuine biological differences between large and small fat cells within the same biological context.

Thus, the aim of the present study was to metabolically characterise large versus small adipocytes isolated from the same depot of mice fed a high-fat diet (HFD) for 8 weeks. Such feeding is associated with whole-body insulin resistance, but with minimal adipocyte cell death and macrophage infiltration [1]. We hypothesised that insulin responsiveness in large adipocytes is reduced compared with small adipocytes isolated from the same fat pad.

Methods

Animals We used 6- to 8-week-old male C57BL6JOlaHsd mice, which had free access to standard rodent diet or HFD (D12331; Research Diets, New Brunswick, NJ, USA) for 8 weeks. HFD consisted of 56% of energy derived from fat, 28% from carbohydrate and 16% from protein. In total, 30 mice were used for this study. All protocols conformed to the Swiss animal protection laws and were approved by the Cantonal Veterinary Office in Zurich, Switzerland.

Intraperitoneal glucose tolerance test For the intraperitoneal glucose tolerance test (ipGTT), mice were injected intraperitoneally with 2 mg/g body weight glucose after overnight fasting. Blood glucose concentration was measured with a glucometer (Accu-Check Aviva; Roche Diagnostics, Rotkreuz, Switzerland) with blood from tail-tip bleedings [7].

Cell separation and viability assessment Adipocytes isolated from HFD-fed mice were separated into two fractions according to their size by filtration through a 60 μm nylon mesh (Millipore, Zug, Switzerland). Cells caught on the mesh (large adipocytes) were gently washed away into a separate vial. After separation, adipocyte viability was assessed with a 3-(4,5-dimethylthiazol-2-yl)-2,5-diphenyltetrazolium bromide assay (MTT) (Sigma, Buchs, Switzerland) as follows. Small and large cells were incubated with 0.5 mg/ml MTT for 1 h and salt was extracted from them with DMSO. The amount of yellow MTT reduced to purple formazan was measured spectrophotometrically (550–655 nm) with an ELISA reader. A lactate dehydrogenase (LDH) release assay using a nonradioactive cytotoxicity assay (CytoTox 96; Promega, Dübendorf, Switzerland) was also performed. LDH released into supernatant fraction was measured and normalised to cell number in incubation medium.

Glucose incorporation into isolated white adipocytes Adipocyte isolation and glucose incorporation were performed as described previously [8] with the following adaptations. Adipocytes (4-8% suspension [9]) were incubated for 60 min with D-[U-^{14}C]glucose. In this setting, most of the labelled glucose is incorporated into lipids and is therefore a readout for lipid synthesis [10]. Where indicated, cells were thereafter separated into two fractions according to their size by filtration through a 60 μm nylon net filter. Glucose incorporation was stopped by separating cells from the medium by centrifugation (about 2000 *g*) through phthalic acid dinonyl ester. Cells were then subjected to liquid scintillation counting. Cell number was determined with a Neubauer haematocytometer (Brand, Wertheim, Germany) under the light microscope.

Cell size determination Aliquots of all adipocyte fractions of each experiment were used to determine mean cell diameters. Photographs of isolated adipocytes in the haematocytometer were taken and images were analysed using ImageJ software for quantification (National Institutes of Health, Bethesda, MD, USA). At least 100 adipocytes per fraction of four independent experiments were analysed.

Lipolysis assays To assess lipolysis, cells were separated as mentioned above and incubated in the absence or presence of 100 nmol/l insulin or 1 μmol/l isoproterenol (Sigma) for 1 h. NEFA levels were measured using a method (ACS-ACOD-MEHA) from Wako Chemicals (Neuss, Germany). Glycerol content of the incubation medium was determined using a colorimetric assay, as described [11].

RNA extraction and quantitative RT-PCR Total RNA was extracted using a kit (RNeasy Lipid Tissue Mini Kit; Qiagen, Basel, Switzerland). RNA (0.5 μg) was reverse-transcribed with Superscript III Reverse Transcriptase

(Invitrogen, Basel, Switzerland) using random hexamer primer. Taqman was used for real-time PCR amplification. The following PCR primers (Applied Biosystems, Rorkreuz, Switzerland) were used: *Hsl* (also known as *Lipe*) Mm00495359_m1, *Atgl* (also known as *Pnpla2*) Mm00503040_m1. Relative gene expression was obtained after normalisation to *36B4* (also known as *Rplp0*) RNA (Applied Biosystems), using the formula $2^{-\Delta\Delta cp}$.

Western blot Isolated and separated adipocytes were homogenised in a buffer containing 150 mmol/l NaCl, 50 mmol/l Tris–HCl (pH 7.5), 1 mmol/l EGTA, 1% (vol./vol.) NP-40, 0.25% (vol./vol.) sodium deoxycholate, 1 mmol/l sodium vanadate, 1 mmol/l NaF, 10 mmol/l sodium β-glycerophosphate, 100 nmol/l okadaic acid, 0.2 mmol/l phenylmethylsulphonyl fluoride (PMSF) and a 1:1000 dilution of protease inhibitor cocktail (Sigma). Protein concentration was determined using the bicinchoninic acid (BCA) assay (Pierce, Rockford, IL, USA) and equivalent amounts of protein (40 μg) were resolved by LDS-PAGE (4–12% gel; NuPAGE; Invitrogen). Proteins were electro-transferred on to nitrocellulose membranes (0.2 μm; BioRad, Reinach, Switzerland) and immunoblotted for phosphoS473-protein kinase B (Akt), phosphoT308-Akt, phosphoAS160 (Cell Signalling, Beverly, MA, USA), anti-GLUT4 (gift from A. Klip, The Hospital for Sick Children, Toronto, ON, Canada) or anti-actin (Millipore, Zug, Switzerland). Membranes were exposed in an Image Reader and analysed with an Image Analyzer (FujiFilm, Dielsdorf, Switzerland).

Data analysis Statistical analyses were performed using either Student's *t* test or ANOVA test (Tukey's multiple comparisons test).

Results

Separation of adipocytes isolated from HFD-fed mice HFD for 8 weeks significantly impaired glucose tolerance in male C57BL6JOlaHsd mice compared with chow-fed animals as assessed by an ipGTT (Fig. 1a). Adipocytes isolated from HFD-fed mice were separated into two

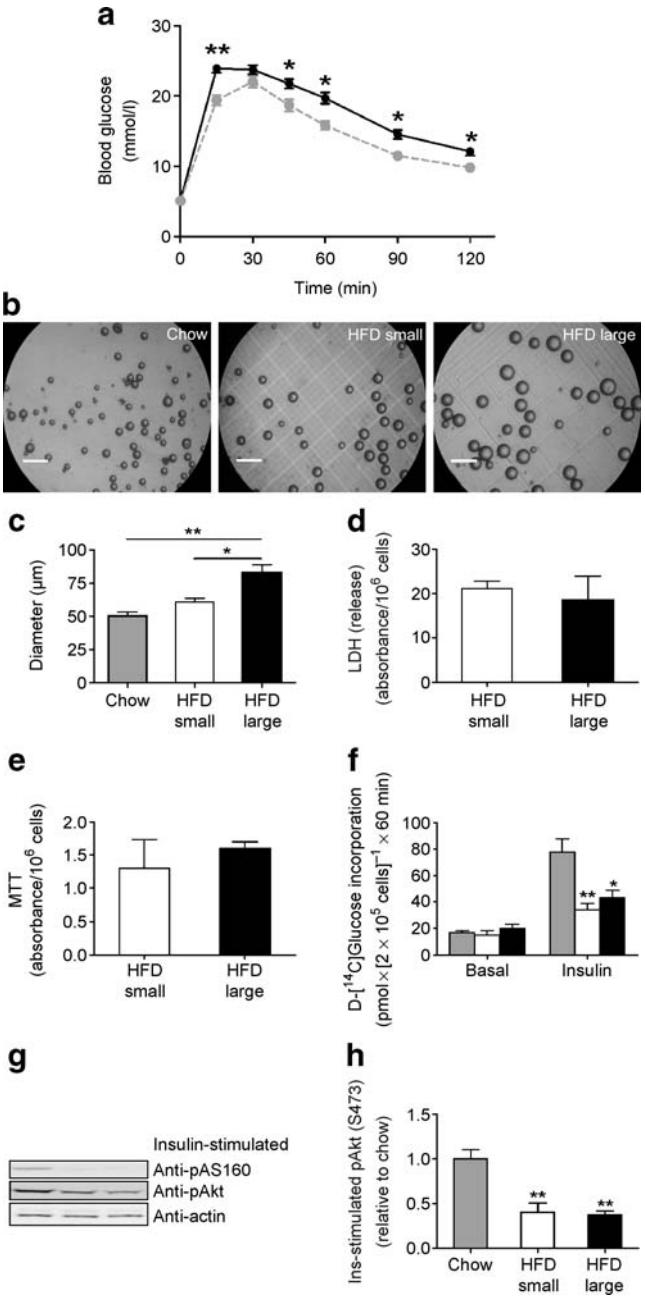

Fig. 1 Reduced insulin responsiveness in small and hypertrophic adipocytes isolated from HFD-fed mice. **a** Intraperitoneal glucose tolerance test was performed in chow-fed (grey symbols) and HFD-fed (black symbols) mice. Glucose (2 g/kg body weight) was injected intraperitoneally and blood glucose levels measured at indicated time points. Results are means±SEM of seven (chow-fed) to 24 (HFD-fed) animals per group. *$p<0.05$, **$p<0.01$ (Student's *t* test). **b** Representative photographs of adipocytes isolated from epididymal fat pads of chow-fed or HFD-fed mice (scale bar, 250 μm), with graph (**c**) showing mean adipocyte diameter of each fraction. Results represent the mean±SEM of three to four independent experiments. *$p<0.05$, **$p<0.01$ (ANOVA). **d** Adipocyte viability was assessed by an LDH and (**e**) an MTT assay. Results represent the mean±SEM of four independent experiments. **f** D-[^{14}C]Glucose incorporation into isolated adipocytes of chow-fed (grey bars), HFD-fed small (white bars) and HFD-fed large (black bars) adipocyte fractions. Results represent the mean±SEM of three to five independent experiments. *$p<0.05$, **$p<0.01$ (ANOVA) compared with insulin-stimulated glucose incorporation into adipocytes of chow-fed mice. **g** Total cell lysates were prepared from isolated adipocytes treated for 10 min with 100 nmol/l human insulin (Ins). Lysates (40 μg) were resolved by LDS-PAGE and immunoblotted with anti-phospho (p)S473-Akt, anti-pAS160 or anti-actin antibody. Representative immunoblots are shown. Membranes were exposed in an Image Reader and quantified (**h**) with Image Analyzer. Results represent the mean±SEM of three independent experiments. **$p<0.01$ (ANOVA) compared with chow-fed mice

fractions by filtration through a 60 μm nylon mesh. For each experiment, epididymal fat pads of two mice were pooled. Small adipocytes (mean diameter 60.9±3.1 μm) were significantly smaller than large fat cells (mean diameter 83.0±6.6 μm; $p<0.05$) (Fig. 1b, c). For comparison, mean diameter of adipocytes isolated from chow-fed animals was 50.7±3.3 μm, significantly ($p<0.01$) smaller only than the large adipocytes from high-fat fed mice (Fig. 1b, c). To rule out the possibility of higher occurrence of cell rupture/cell damage in one cell fraction compared with the other after filtration through the nylon mesh, cell viability was assessed by an MTT and LDH assay. As depicted in Fig. 1d and e, viability of the two adipocyte cell fractions was comparable.

No difference in insulin-stimulated glucose incorporation between small and large adipocytes isolated from HFD-fed mice In order to assess insulin responsiveness, D-[U-^{14}C] glucose incorporation into adipocytes was determined next. The fold increase in insulin-stimulated glucose incorporation into both adipocyte fractions prepared from HFD-fed mice was greatly reduced compared with adipocytes isolated from chow-fed animals (Fig. 1f), but surprisingly there was no difference in glucose incorporation between large and small adipocytes in HFD-fed mice in response to insulin (Fig. 1f). This observation held true when the fold-increase in insulin-stimulated glucose incorporation was calculated per cell surface or cell volume (data not shown). Accordingly, the insulin-stimulated increase in phosphorylation of Akt on S473 and on T308 residues as well as of AS160 was similar in both fractions, but clearly reduced compared with adipocytes isolated from chow-fed mice (Fig. 1g, h). Similarly, protein levels of GLUT4 were not different between small and large adipocytes, but was decreased by approximately 35% compared with adipocytes from chow-fed mice (data not shown).

Increased NEFA release from large epididymal adipocytes isolated from HFD-fed mice In order to evaluate lipolysis, concentrations of NEFA and glycerol were determined in the incubation medium. Basal NEFA release per cell was significantly higher in large than in small adipocytes (Fig. 2a), a difference that was not significant when controlled for surface area. This finding suggests that the elevated lipolytic activity of the large adipocytes is a direct effect of cell hypertrophy. Similar results for basal lipolysis were obtained when release of glycerol was measured (Fig. 2b). Isoproterenol-stimulated lipolysis was significantly increased compared with basal NEFA release, but not different between small and large adipocytes from HFD-fed mice (Fig. 2a). Remarkably, the ability of insulin to inhibit lipolysis was fully blunted in large and small adipocytes compared with adipocytes from chow-fed mice (in which lipolysis was inhibited by ~30%) (Fig. 2c), a finding that is consistent with the similar degree of insulin resistance observed in signalling and glucose incorporation (Fig. 1d).

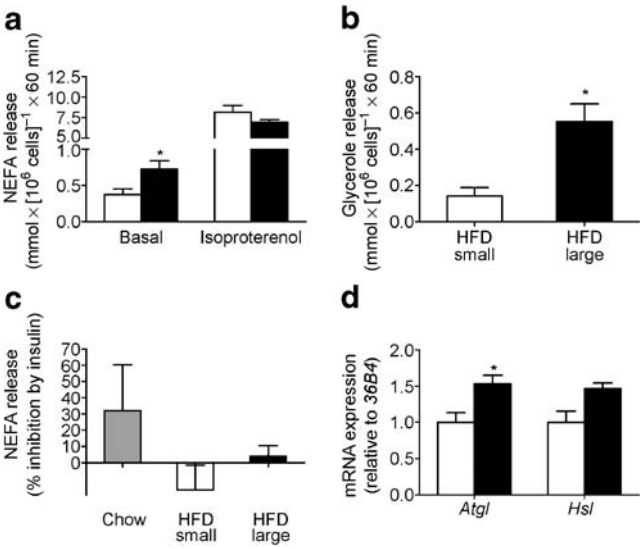

Fig. 2 Increased basal lipolysis in large adipocytes. **a** Basal and isoproterenol-stimulated NEFA release from HFD small (white bars) and HFD large (black bars) adipocytes. Results are means±SEM of five (isoproterenol) to seven (basal) independent experiments. *$p<0.05$ (Student's *t* test). **b** Basal glycerol release from HFD small and HFD large adipocytes. Results are means±SEM of three independent experiments. *$p<0.05$ (Student's *t* test). **c** Per cent inhibition of NEFA release by insulin in chow-fed, HFD-fed small and HFD-fed large adipocytes. Results represent the mean±SEM of three to five independent experiments. **d** Quantitative RT-PCR detection of *Atgl* and *Hsl* mRNA expression. The level of mRNA expression was normalised to *36B4* RNA. Results represent the mean±SEM of three independent experiments and are expressed relative to expression in the HFD-small fraction. *$p<0.05$ (Student's *t* test)

Adipose triacylglycerol lipase (ATGL) and hormone-sensitive lipase (HSL) are key players in adipocyte lipolysis. It has been suggested that ATGL and HSL may act in coordination such that ATGL is the primary lipase responsible for hydrolysing the first fatty acid from triacylglycerol and that HSL is the primary diacylglycerol lipase [12]. Alternatively, it has been proposed that HSL is the primary triacylglycerol lipase responsible for catecholamine-stimulated lipolysis from adipocytes and ATGL is the primary triacylglycerol lipase for basal lipolysis [13]. Given the differences in basal lipolysis rate between large and small adipocytes, mRNA expression levels of these two lipases were determined. There was a slight but significant increase in *Atgl* mRNA levels in large adipocytes (Fig. 2d). Similarly, *Hsl* expression tended to be higher in large adipocytes; however, this increase did not reach statistical significance.

Discussion

Adipocytes from obese persons or animals compared with those from lean persons or animals are characterised by

increased cell size and decreased insulin-stimulated glucose uptake [14, 15]. It has therefore been speculated that larger adipocytes are more insulin resistant. Although this conclusion is plausible, it is difficult to analyse the sole contribution of cell size to insulin resistance independently of other factors since cells are isolated from different individuals. It is possible that these factors, along with or independently of cell size, causatively contribute to the insulin resistance observed in adipocytes derived from the obese.

To address this point, we have characterised larger versus smaller adipocytes from the same fat depot of mice fed HFD for 8 weeks. The time span of 8 weeks of HFD was chosen to examine an early phase of obesity-induced changes in adipose tissue. Macrophage infiltration of adipose tissue and occurrence of adipocyte death may have just started at this time point [1]. Yet, 8 weeks of fat-enriched diet was already sufficient to induce whole-body insulin resistance as demonstrated by a significantly impaired ipGTT (Fig. 1a), by a reduction in insulin-stimulated glucose incorporation (Fig. 1f) and by a blunted capacity of insulin to inhibit lipolysis (Fig. 2c). Nevertheless, when comparing large to small adipocytes isolated from HFD-fed mice, we did not detect any differences in insulin responsiveness (Figs 1f and 2c). This observation was true both for insulin-mediated stimulation of glucose incorporation, as well as for the inhibition of lipolysis. It is still possible that the severity of insulin resistance differs between the extremes of adipocyte size. Yet for the cell size range of most adipocytes composing the adipose tissue of HFD mice, the data would suggest that the degree of cellular hypertrophy is not a direct determinant of severity of adipocyte insulin resistance. More probably, insulin resistance in adipocytes of HFD-fed mice could be a secondary phenomenon to alterations in the intra-fat depot environment, such as increased release of pro-inflammatory cytokines and/or NEFA. These would seem to similarly affect insulin sensitivity in larger versus smaller adipocytes within the same fat depot.

One of the main findings in the present study is the significant increase in basal lipolysis in large compared with small adipocytes (Fig. 2a, b). This finding is in accordance with a previous study showing a correlation of adipocyte size with basal rates of lipolysis [16]. The latter finding would imply increased circulating NEFA levels in patients with adipocyte hypertrophy. Indeed, enlarged adipocytes were found more frequently in patients with obesity-related metabolic disorders [17], suggesting that increased basal lipolysis of large adipocytes may directly contribute to obesity-induced metabolic alterations, potentially via deposition of lipids in liver and skeletal muscle (lipotoxicity). It would be intriguing to assess whether, by increasing local NEFA concentrations in adipose tissue, large adipocytes contribute to the insulin resistance that similarly develops in large versus small adipocytes. Intriguingly, whereas NEFA-induced insulin resistance is a well established phenomenon in skeletal muscle and liver, results in adipocytes are somewhat controversial [18, 19], leaving this putative mechanism unsettled.

In conclusion, adipocyte hypertrophy associated with diet-induced obesity does not seem to be a direct determinant of the severity of adipocyte insulin resistance. Instead, larger adipocytes have a higher basal lipolysis rate than smaller adipocytes. Hence, of the various alterations to adipose tissue in obesity, adipocyte hypertrophy may predominantly, albeit indirectly, contribute to whole-body insulin resistance, e.g. by affecting the release of secreted products like adipokines and NEFAs.

Acknowledgements This work was supported by research grants from the University of Zurich and the Swiss National Science Foundation number 310000-112275 (to D. Konrad). We would like to thank A. Rudich from the Department of Clinical Biochemistry and the S. Daniel Centre for Health and Nutrition, Ben-Gurion University, Beer-Sheva, Israel for helpful discussions.

Duality of interest The authors declare that there is no duality of interest associated with this manuscript.

References

1. Strissel KJ, Stancheva Z, Miyoshi H et al (2007) Adipocyte death, adipose tissue remodeling, and obesity complications. Diabetes 56:2910–2918
2. Skurk T, Alberti-Huber C, Herder C, Hauner H (2007) Relationship between adipocyte size and adipokine expression and secretion. J Clin Endocrinol Metab 92:1023–1033
3. Lelliott C, Vidal-Puig AJ (2004) Lipotoxicity, an imbalance between lipogenesis de novo and fatty acid oxidation. Int J Obes Relat Metab Disord 28(Suppl 4):S22–S28
4. Okuno A, Tamemoto H, Tobe K et al (1998) Troglitazone increases the number of small adipocytes without the change of white adipose tissue mass in obese Zucker rats. J Clin Invest 101:1354–1361
5. Czech MP (1976) Cellular basis of insulin insensitivity in large rat adipocytes. J Clin Invest 57:1523–1532
6. Karnieli E, Barzilai A, Rafaeloff R, Armoni M (1986) Distribution of glucose transporters in membrane fractions isolated from human adipose cells. Relation to cell size. J Clin Invest 78:1051–1055
7. Konrad D, Rudich A, Schoenle EJ (2007) Improved glucose tolerance in mice receiving intraperitoneal transplantation of normal fat tissue. Diabetologia 50:833–839
8. Rudich A, Konrad D, Török D et al (2003) Indinavir uncovers different contributions of GLUT4 and GLUT1 towards glucose uptake in muscle and fat cells and tissues. Diabetologia 46:649–658
9. Tozzo E, Shepherd PR, Gnudi L, Kahn BB (1995) Transgenic GLUT-4 overexpression in fat enhances glucose metabolism: preferential effect on fatty acid synthesis. Am J Physiol 268:E956–E964
10. Gliemann J, Gammeltoft S, Vinten J (1975) Time course of insulin-receptor binding and insulin-induced lipogenesis in isolated rat fat cells. J Biol Chem 250:3368–3374
11. Souza SC, Muliro KV, Liscum L et al (2002) Modulation of hormone-sensitive lipase and protein kinase A-mediated lipolysis

by perilipin A in an adenoviral reconstituted system. J Biol Chem 277:8267–8272
12. Zechner R, Strauss JG, Haemmerle G, Lass A, Zimmermann R (2005) Lipolysis: pathway under construction. Curr Opin Lipidol 16:333–340
13. Ducharme NA, Bickel PE (2008) Lipid droplets in lipogenesis and lipolysis. Endocrinology 149:942–949
14. Lundgren M, Svensson M, Lindmark S, Renstrom F, Ruge T, Eriksson JW (2007) Fat cell enlargement is an independent marker of insulin resistance and 'hyperleptinaemia'. Diabetologia 50:625–633
15. Molina JM, Ciaraldi TP, Brady D, Olefsky JM (1989) Decreased activation rate of insulin-stimulated glucose transport in adipocytes from obese subjects. Diabetes 38:991–995
16. Reardon MF, Goldrick RB, Fidge NH (1973) Dependence of rates of lipolysis, esterification, and free fatty acid release in isolated fat cells on age, cell size, and nutritional state. J Lipid Res 14:319–326
17. Weyer C, Foley JE, Bogardus C, Tataranni PA, Pratley RE (2000) Enlarged subcutaneous abdominal adipocyte size, but not obesity itself, predicts type II diabetes independent of insulin resistance. Diabetologia 43:1498–1506
18. Lundgren M, Eriksson JW (2004) No in vitro effects of fatty acids on glucose uptake, lipolysis or insulin signaling in rat adipocytes. Hormone Metab Res 36:203–209
19. Van Epps-Fung M, Williford J, Wells A, Hardy RW (1997) Fatty acid-induced insulin resistance in adipocytes. Endocrinology 138:4338–4345

Deletion of Fas in adipocytes relieves adipose tissue inflammation and hepatic manifestations of obesity in mice

Stephan Wueest,[1,2] Reto A. Rapold,[1,2] Desiree M. Schumann,[3] Julia M. Rytka,[1,2] Anita Schildknecht,[4] Ori Nov,[5] Alexander V. Chervonsky,[6] Assaf Rudich,[5] Eugen J. Schoenle,[1] Marc Y. Donath,[2,3] and Daniel Konrad[1,2]

[1]Division of Pediatric Endocrinology and Diabetology, University Children's Hospital, Zurich, Switzerland. [2]Zurich Center for Integrative Human Physiology, University of Zurich, Zurich, Switzerland. [3]Clinic of Endocrinology and Diabetes and [4]Institute of Experimental Immunology, University Hospital Zurich, Zurich, Switzerland. [5]Department of Clinical Biochemistry and S. Daniel Centre for Health and Nutrition, Ben-Gurion University, Beer-Sheva, Israel. [6]Department of Pathology, University of Chicago, Chicago, Illinois, USA.

Adipose tissue inflammation is linked to the pathogenesis of insulin resistance. In addition to exerting death-promoting effects, the death receptor Fas (also known as CD95) can activate inflammatory pathways in several cell lines and tissues, although little is known about the metabolic consequence of Fas activation in adipose tissue. We therefore sought to investigate the contribution of Fas in adipocytes to obesity-associated metabolic dysregulation. Fas expression was markedly increased in the adipocytes of common genetic and diet-induced mouse models of obesity and insulin resistance, as well as in the adipose tissue of obese and type 2 diabetic patients. Mice with Fas deficiency either in all cells or specifically in adipocytes (the latter are referred to herein as AFasKO mice) were protected from deterioration of glucose homeostasis induced by high-fat diet (HFD). Adipocytes in AFasKO mice were more insulin sensitive than those in wild-type mice, and mRNA levels of pro-inflammatory factors were reduced in white adipose tissue. Moreover, AFasKO mice were protected against hepatic steatosis and were more insulin sensitive, both at the whole-body level and in the liver. Thus, Fas in adipocytes contributes to adipose tissue inflammation, hepatic steatosis, and insulin resistance induced by obesity and may constitute a potential therapeutic target for the treatment of insulin resistance and type 2 diabetes.

Introduction

White adipose tissue (WAT) has been recognized as an important endocrine organ secreting different hormone-like factors (adipokines), FFAs, and cytokines, thereby regulating metabolism locally and systemically (1). In obesity, excess adipose tissue accumulation is accompanied by local inflammation, characterized by infiltration of inflammatory cells (2) and by elevated production of proinflammatory cytokines, jointly activating inflammatory pathways in adipocytes. It is proposed that the consequent alteration in the composition of secreted products from adipocytes contributes to both local and systemic insulin resistance (3–5). Particularly, liver insulin sensitivity can be impaired by obesity-induced alterations in adipokine secretion and by elevation in fat tissue–derived cytokines and fatty acids (6–9).

Fas (CD95), a member of the TNF receptor family, plays an important role in the regulation of programmed cell death (apoptosis). FasL binding to Fas assembles the death-inducing signaling complex (DISC). In turn, DISC formation leads to the activation of caspase-8 and caspase-3 and finally to apoptosis. However, like TNF-α, Fas activation can also induce non-apoptotic signaling pathways (10–12). For example, in different cell lines and tissues, Fas activation was shown to induce secretion of proinflammatory cytokines such as IL-1α, IL-1β, IL-6, IL-8 (KC), and MCP-1 (13–17), rendering it a potential key component of the inflammatory response. Although Fas was shown to be expressed in preadipocytes and adipocytes (18), little is known about non-apoptotic consequences of Fas activation in adipocytes and, particularly, its role in mediating the dysregulated metabolism that accompanies obesity, potentially via adipose tissue inflammation.

In the present study, we hypothesized that Fas mediates inflammatory signals in obesity, particularly in adipocytes, thereby contributing to adipose tissue inflammation and to metabolic dysregulation. We demonstrate that Fas expression is elevated in adipose tissue in both genetic and nutritional models of obesity in mice, as well as in patients with obesity and type 2 diabetes. Moreover, total body Fas-deficient (Fas-def) and adipocyte-specific *Fas*-KO (AFasKO) mice were partly protected from HFD-induced adipocyte and whole-body insulin resistance. In particular, AFasKO mice showed reduced adipose tissue inflammation and were protected from liver steatosis and hepatic insulin resistance, with only minimal effects on fat tissue mass and adipocyte hypertrophy. Our findings point toward an important role of adipocyte Fas expression in the development of obesity-associated fat tissue inflammation and insulin resistance.

Results

Fas expression is increased in adipocytes isolated from insulin-resistant mice and in adipose tissue of obese and diabetic patients. Fas was shown to activate inflammatory pathways in several tissues and cell lines. Since Fas is expressed in preadipocytes and adipocytes (18), and since adipose tissue inflammation may be causatively linked to insulin resistance, we hypothesized that Fas expression might modulate obesity-related fat and whole-body insulin responsiveness. First, Fas expression was determined in isolated adipocytes from insulin-resistant mice. Adipocytes were isolated from perigonadal fat pads

Conflict of interest: The authors have declared that no conflict of interest exists.
Citation for this article: *J. Clin. Invest.* **120**:191–202 (2010). doi:10.1172/JCI38388.

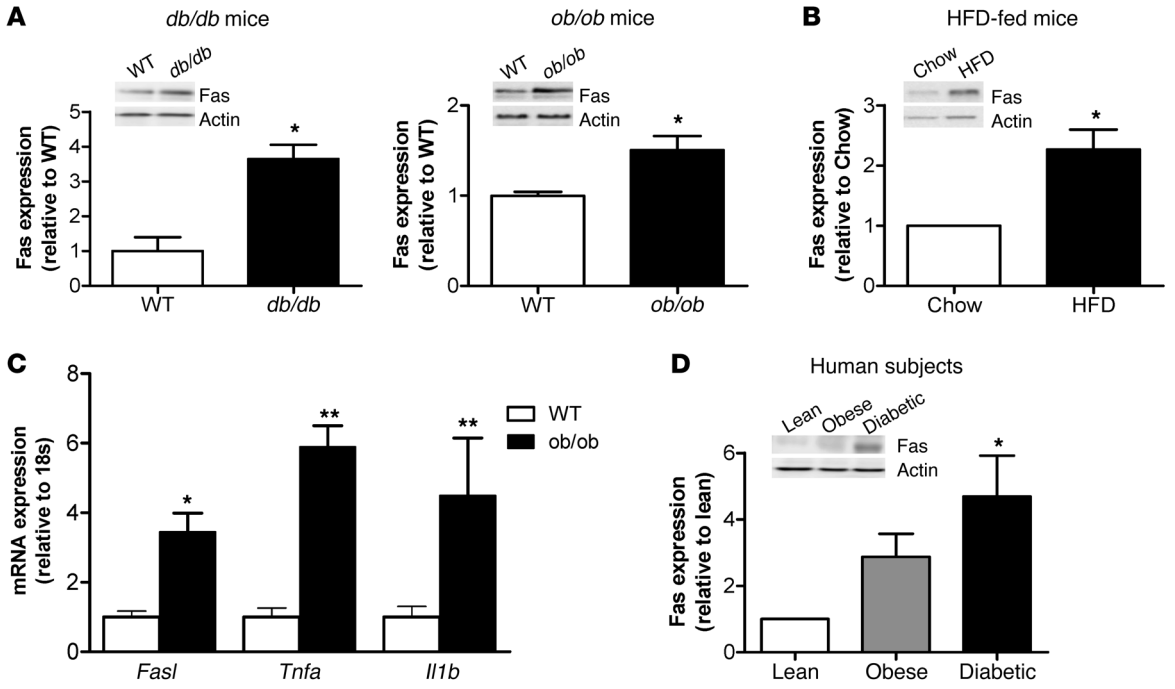

Figure 1

Fas expression is increased in adipocytes isolated from insulin-resistant mice and in adipose tissue of obese and diabetic patients. (**A**) Total cell lysates were prepared from isolated perigonadal adipocytes harvested from *db/db*, *ob/ob*, and WT control mice. Lysates were resolved by LDS-PAGE and immunoblotted with anti-Fas or anti-actin antibody. Results are mean ± SEM of 3 mice per group and normalized to actin expression. **P* < 0.05 (Student's *t* test). (**B**) Total cell lysates were prepared from isolated adipocytes of perigonadal fat pads of chow-fed and HFD-fed (8 weeks of HFD) mice. Lysates were resolved by LDS-PAGE and immunoblotted with anti-Fas or anti-actin antibody. Results are mean ± SEM of 3 mice per group and normalized to actin expression. **P* < 0.05 (1-sample *t* test). (**C**) Total RNA was extracted from perigonadal fat pads, and quantitative RT-PCR was performed. The level of mRNA expression was normalized to 18S RNA. Results represent mean ± SEM of 3 animals per group. **P* < 0.05, ***P* < 0.01 (Student's *t* test). (**D**) Tissue lysates from subcutaneous fat biopsies of lean, obese, and diabetic patients were prepared and immunoblotted with anti-Fas or anti-actin antibody. Results are mean ± SEM of 5–10 patients per group and normalized to actin expression. **P* < 0.05 (ANOVA).

of 3-month-old *ob/ob* and *db/db* mice and their WT controls. Fas protein expression was determined and normalized to actin expression (19) (Figure 1A). Fas protein levels were significantly increased in *ob/ob* as well as *db/db* mice compared with their WT controls. Similarly, Fas protein expression was increased in adipocytes isolated from perigonadal fat pads of high-fat diet–fed (HFD-fed) C57BL/6J mice compared with regular chow–fed controls (Figure 1B). In addition to Fas, we also found *Fasl*, *Tnfa*, and *Il1b* mRNA levels elevated in adipose tissue of *ob/ob* mice (Figure 1C).

In order to determine the potential relevance of increased Fas expression in adipose tissue of patients with insulin resistance, we determined Fas protein levels in adipose tissue of lean, obese, and obese type 2 diabetic patients. None of the examined patients was treated with any medications that might affect inflammatory pathways in adipose tissue or modulate insulin sensitivity (further basic clinical characteristics of the patients are provided in Supplemental Table 1; supplemental material available online with this article; doi:10.1172/JCI38388DS1). Fas expression was increased in fat tissue of obese (body mass index, >30 kg/m^2) compared with lean persons. Interestingly, Fas was further elevated in obese patient with type 2 diabetes (Figure 1D). Collectively, these data demonstrate that Fas expression is upregulated in isolated adipocytes of common genetic and nutritional mouse models of obesity and insulin resistance and in adipose tissue of obese and obese diabetic humans.

Fas-def mice are protected against HFD-induced insulin resistance. To start assessing a putative metabolic role for increased adipocyte Fas expression under insulin-resistant conditions, we analyzed glucose tolerance in total body Fas-def mice (20). Fas-def or WT mice were fed regular chow or HFD for 6 weeks. Total body weight gain on HFD was similar in Fas-def and WT mice (Figure 2A). However, perigonadal fat pad weight was significantly lower in HFD-fed Fas-def mice compared with WT mice (Figure 2B), and adipocyte size distribution was shifted to the left, reflecting smaller mean adipocyte size in Fas-def mice (Figure 2C). Adipocyte number was similar in HFD-fed WT and Fas-def mice (data not shown), suggesting that fat pads in Fas-def mice are smaller due to the smaller size of adipocytes. Six weeks of HFD was sufficient to significantly impair glucose tolerance in WT mice (Figure 2D), though the degree of impairment was less than reported following a longer duration of HFD feeding (20 weeks), reflecting early metabolic adaptation to HFD feeding. Remarkably, Fas-def mice were protected against HFD-induced glucose intolerance (Figure 2D). Further, consistent with Fas involvement in the induction of insulin resistance, fasting insulin levels increased significantly in WT mice fed HFD compared with chow-fed controls, whereas in Fas-def mice, there was no diet-induced change in fasting insulin levels (Figure 2E). Concurrently, isolated adipocytes from HFD-fed WT mice exhibited a marked reduction in insulin-stimulated glucose incorpora-

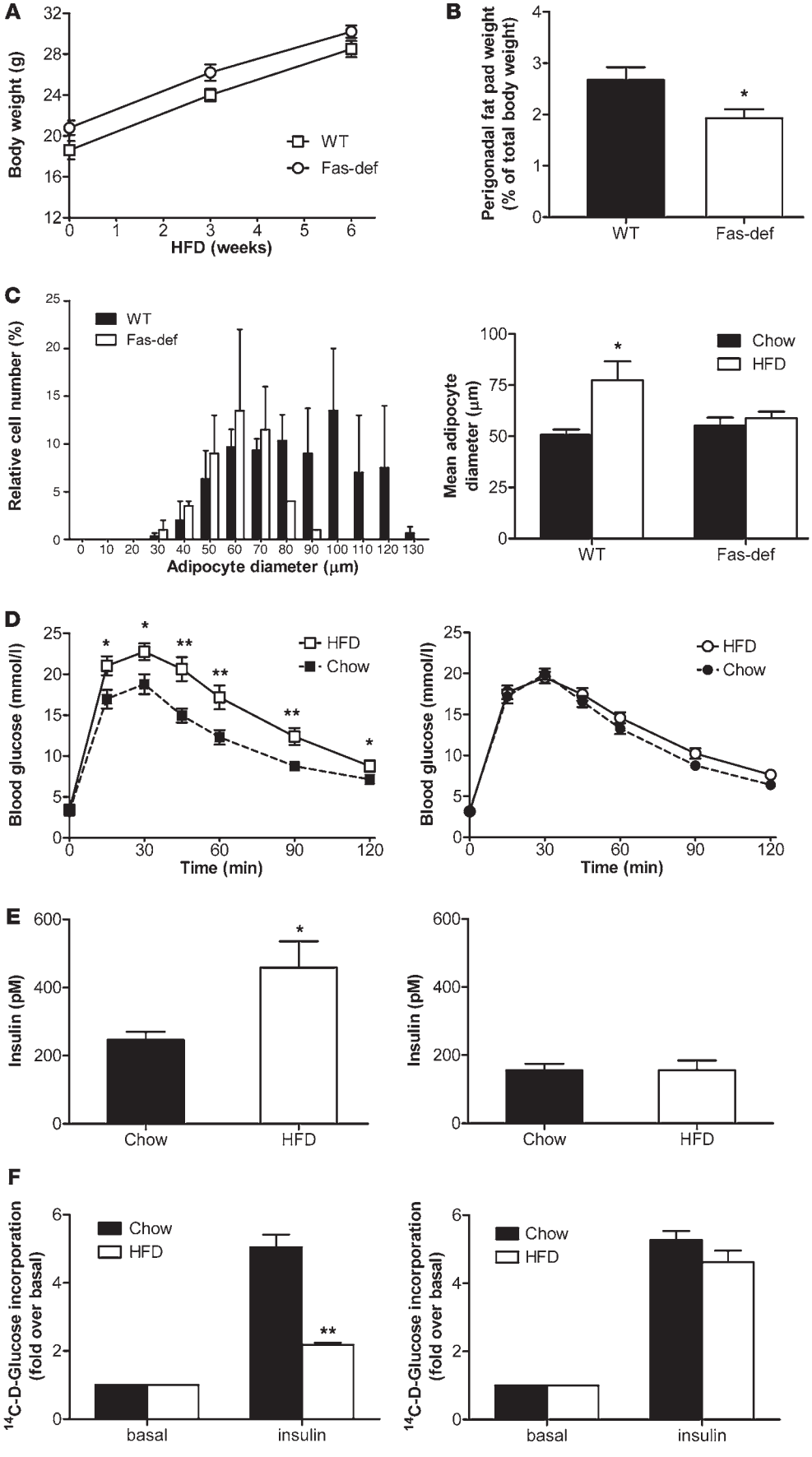

Figure 2

Fas-def mice are protected from HFD-induced changes in adipose tissue and glucose homeostasis. (**A**) Weight gain was analyzed in HFD-fed WT and Fas-def mice. Results are mean ± SEM of 10 animals per group. (**B**) Perigonadal fat pads were harvested and weighed. Results are expressed relative to total body weight and represent mean ± SEM of 10–15 mice group. *$P < 0.05$ (Student's *t* test). (**C**) Left: Relative size distribution of adipocyte diameter after 6 weeks of HFD. Results represent mean ± SEM of 6 mice per group. Right: Mean adipocyte diameter of chow- or HFD-fed Fas-def and WT mice. Results represent mean ± SEM of 6 mice per group. *$P < 0.05$ (Student's *t* test). (**D**) Intraperitoneal glucose tolerance tests in WT (left) and Fas-def (right) mice. Results are mean ± SEM of 12–18 animals per group. *$P < 0.05$, **$P < 0.01$ (Student's *t* test). (**E**) Fasting insulin levels were determined in WT (left) and Fas-def (right) mice after 8 hours of food withdrawal. Results are mean ± SEM of 4–5 animals per group. *$P < 0.05$ (Student's *t* test). (**F**) ^{14}C-D-glucose incorporation into isolated adipocytes from chow- and HFD-fed mice was determined in the absence or presence of insulin. Left: Fold glucose incorporation in WT mice. Right: Fold glucose incorporation in Fas-def mice. Results represent mean ± SEM of 6 experiments. **$P < 0.01$ (Student's *t* test).

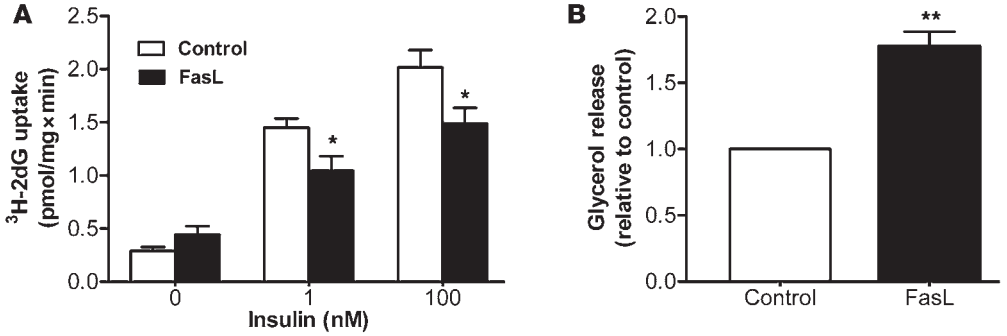

Figure 3

Fas activation in 3T3-L1 adipocytes decreases insulin sensitivity and stimulates lipolysis. Mature 3T3-L1 adipocytes were incubated with 2 ng/ml FasL for 12 hours. (**A**) ^{3}H-2dG glucose uptake was determined after treatment with or without insulin at different concentrations. Shown are absolute values of ^{3}H-2dG uptake in untreated or FasL-treated 3T3-L1 adipocytes. Results are mean ± SEM of 5–9 independent experiments. *$P < 0.05$ (ANOVA). (**B**) Glycerol release was determined after medium was removed and cells were incubated with KREBS buffer for another hour. Results represent mean ± SEM of 4 independent experiments. **$P < 0.01$ (1-sample *t* test).

tion (largely reflecting lipogenic glucose flux; ref. 21) compared with chow-fed mice, whereas adipocytes from Fas-def mice were almost entirely protected against diet-induced adipocyte insulin resistance (Figure 2F). Similarly, insulin significantly reduced FFA release in adipocytes isolated from Fas-def mice, whereas it had no effect in WT adipocytes (Supplemental Figure 1). Thus, total body deficiency of Fas resulted in protection against adipose tissue expansion and adipocyte hypertrophy as well as whole-body and adipocyte insulin resistance induced by 6 weeks of HFD feeding.

Given the seemingly complex effect of Fas on adipose tissue development and on fat cell metabolism in response to HFD, we wanted to verify that Fas activation, even as an isolated factor, modulates insulin sensitivity in adipocytes. 3T3-L1 adipocytes were stimulated with 2 ng/ml membrane-bound FasL for 12 hours. Such treatment had no negative effect on cell viability and did not increase apoptosis rate as assessed by MTT and TUNEL assays, respectively (Supplemental Figure 2 and data not shown). Yet Fas activation significantly reduced insulin-stimulated glucose uptake (Figure 3A) and stimulated lipolysis (Figure 3B). Lower FasL concentrations (0.02, 0.5, and 1.0 ng/ml) had no effect on insulin-stimulated glucose uptake (Supplemental Figure 3). These findings support the proposition that adipocyte Fas may regulate fat cell metabolism by mechanisms unrelated to Fas-induced cell death, potentially contributing to obesity-related insulin resistance.

AFasKO mice are protected against HFD-induced adipocyte insulin resistance and total body insulin resistance. To better investigate the specific role of Fas expression in adipocytes in the development of insulin resistance in response to HFD feeding, we generated an adipocyte-specific *Fas*-KO mouse (AFasKO) using the Cre-lox system (*Fas$^{fl/fl}$;Fabp4-Cre$^{+/-}$*). As a control, floxed Fas mice that do not express Cre recombinase (Cre) were used (*Fas$^{fl/fl}$;Fabp4-Cre$^{-/-}$*), referred to below as WT. As expected, Fas expression was greatly diminished in isolated white adipocytes of AFasKO mice (Figure 4A); decreased in white and brown adipose tissue, which also includes non-adipocyte cell types (Figure 4B); but was not decreased in other tissues (Figure 4C) (an unexplained consistent increase in Fas expression was observed in lysates from lung tissue).

It was previously claimed that fatty acid binding protein 4 (Fabp4)/aP2 expression was induced in activated macrophages (22). Given the fact that Cre expression in our mice is under the regulation of the Fabp4 promoter, Fas expression might have been decreased in activated macrophages in addition to adipocytes, thereby influencing adipose tissue biology. However, Cre was expressed in adipocytes of AFasKO mice, whereas it was undetectable in macrophages (Figure 4D), consistent with previous studies using the same *Fabp4-Cre* strain (19, 23). Moreover, in both resident (naive) macrophages isolated from the spleen and in activated peritoneal macrophages harvested after thioglycollate injection, Fas protein expression was not decreased in AFasKO mice (Figure 4E). Although it still remains possible that a small subpopulation of activated macrophages within adipose tissue express decreased levels of Fas in the AFasKO mice, this novel mouse model exhibits greatly diminished Fas expression in adipocytes but not in other tissues and cell types, including resident and activated peritoneal macrophages. Moreover, since previous studies using the same *Fabp4-Cre* mouse line found no effect of the Cre allele in the first 6 months of life (23), AFasKO mice seemed to be a useful model to study the in vivo role of Fas expression specifically in adipocytes.

To investigate the functional significance of adipocyte-specific Fas deletion, AFasKO mice were fed normal chow or HFD for up to 6 weeks. Total body weight gain was similar in AFasKO and Cre-negative littermates fed normal chow (data not shown) and HFD (Figure 4F). After 6 weeks of HFD, inguinal, perigonadal, and retroperitoneal fat pad weights in the AFasKO mice were comparable to those in WT mice, whereas mesenteric fat pad weight was slightly, but significantly, lower in AFasKO mice (Figure 4G). Importantly, and in contrast to total body Fas-def mice, adipocyte size was similar in the 2 groups (Figure 4H).

Blood glucose levels were significantly higher in WT mice after a 7-hour fasting period, whereas insulin, FFA, triglyceride (TG), and glycerol levels did not differ between WT and AFasKO mice (Table 1). Moreover, adipocytes isolated from AFasKO mice exhibited improved insulin-stimulated glucose incorporation, compared with adipocytes from WT mice after 6 weeks of HFD (Figure 5A). Further, consistent with improved adipocyte insulin sensitivity in the absence of Fas expression in adipocytes, insulin still had a significant antilipolytic effect in isolated adipocytes of HFD-fed AFasKO mice, compared with adipocytes of WT mice (49% ± 19% vs. 26% ± 7%), whereas basal FFA release was not different in the 2 groups. Thus, specific ablation of Fas expression in adipocytes was associated with protection against the metabolic effects of HFD feeding in adipocytes, without affecting adipocyte size.

To examine whether improved insulin responsiveness of adipocytes conferred by adipocyte-specific Fas deletion had systemic consequences, we assessed glucose metabolism. There were no differences in glucose and insulin tolerance test results between chow-fed 3-month-old AFasKO and WT littermates (data not shown). In contrast, after 6 weeks of HFD, AFasKO mice exhibited mildly but

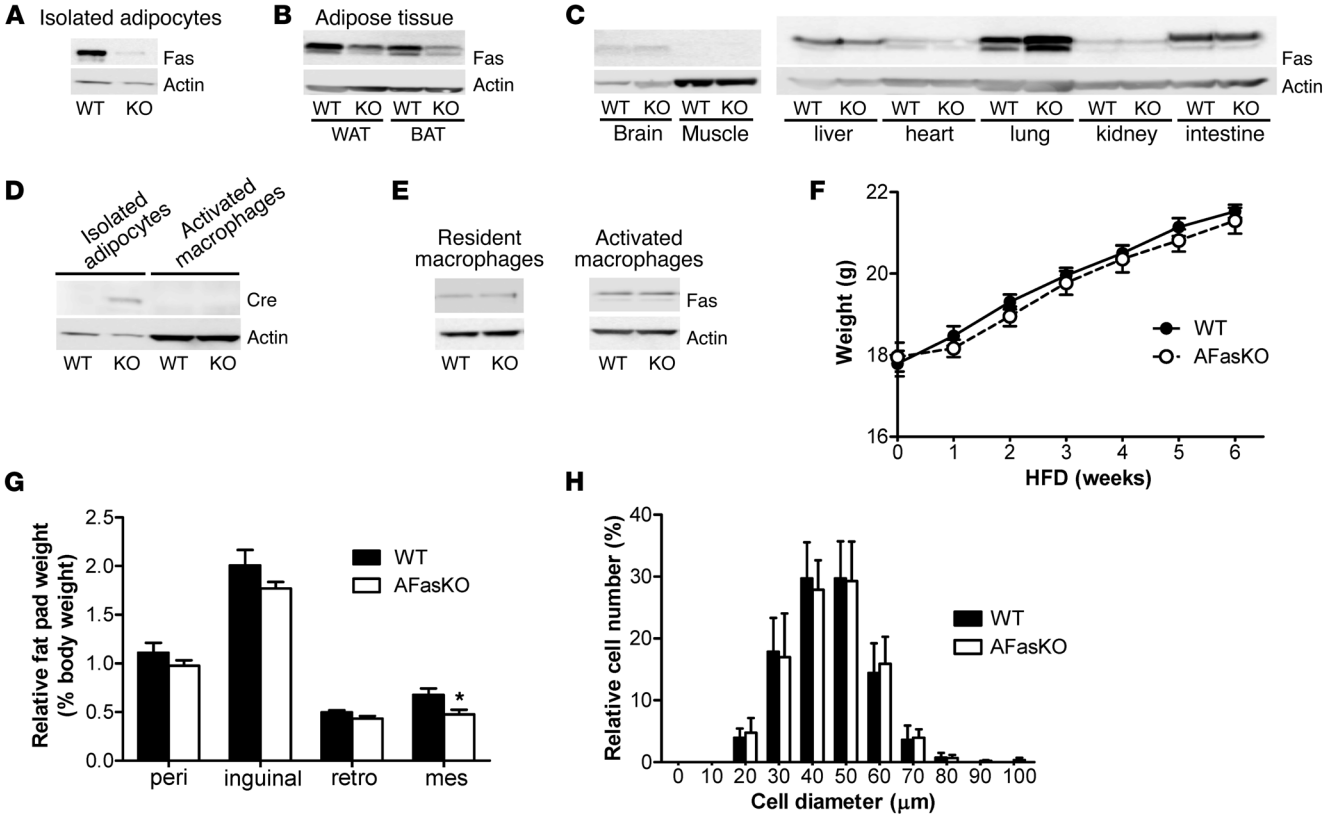

Figure 4

Characterization of AFasKO mice. (**A**) Total cell lysates were prepared from isolated adipocytes of WT (*Fas*$^{fl/fl}$*;Fabp4-Cre*$^{-/-}$) and AFasKO (*Fas*$^{fl/fl}$*; Fabp4-Cre*$^{+/-}$) mice. Lysates were resolved by LDS-PAGE and immunoblotted with anti-Fas or anti-actin antibody. (**B** and **C**) Tissue lysates were prepared and resolved by LDS-PAGE and immunoblotted with anti-Fas or anti-actin antibody. (**D**) Total cell lysates (80 μg) from adipocytes and macrophages were prepared, resolved by LDS-PAGE, and immunoblotted with anti-Cre or anti-actin antibody. (**E**) Total cell lysates from resident and activated macrophages were prepared, resolved by LDS-PAGE, and immunoblotted with anti-Fas or anti-actin antibody. (**F**) Weight gain was analyzed in WT and AFasKO mice. Results are mean ± SEM of 14–15 animals per group. (**G**) Different fat pads were harvested and weighed. Results are expressed relative to total body weight and represent mean ± SEM of 14 mice per group. **P* < 0.05. peri, perigonadal; retro, retroperitoneal; mes, mesenteric. (**H**) The size of isolated perigonadal adipocytes was analyzed. For each mouse, at least 100 adipocytes were analyzed. Images were analyzed using NIH ImageJ software for quantification. Results represent mean ± SEM of 4–5 mice per group.

significantly improved glucose tolerance compared with Cre-negative littermates (Figure 5B). Moreover, AFasKO mice were significantly more insulin sensitive as assessed by insulin tolerance test (Figure 5C). Finally, under hyperinsulinemic-euglycemic clamp, glucose infusion rate was significantly increased in AFasKO mice compared with WT littermates (see Figure 5D for the steady-state glucose infusion rates and Supplemental Figure 4 for the detailed time course), confirming improved whole-body insulin sensitivity. In vivo lipolysis determined during hyperinsulinemic-euglycemic clamp showed no difference in basal FFA levels, but insulin had a significant effect in reducing circulating FFA in AFasKO mice, while this effect was blunted in WT littermates (Figure 5E). Based on the results presented herein, we describe an adipocyte-specific *Fas*-KO mouse model that is protected against adipocyte and whole-body insulin resistance induced by HFD feeding.

Fas deletion in adipocytes may prevent adipocyte and whole-body insulin resistance by interfering with adipose tissue inflammatory circuits induced by HFD feeding. Given that Fas may be involved in inflammatory processes, we next assessed its potential involvement in adipose tissue inflammation. mRNA levels of major inflammatory markers were assessed in adipose tissue of HFD-fed WT versus AFasKO mice. In the KO mice, fat mRNA levels of *Il6*, *Cd11b*, *Mcp1*, and resistin were significantly decreased, whereas *Il10* and arginase 1 levels were increased (Figure 6A and Supplemental Table 2). Since adipose tissue is proposed to be a major source of circulating levels of cytokines such as MCP-1 and IL-6 (24, 25), we measured their levels in the circulation. Whereas circulating MCP-1 levels were not significantly different between WT and AFasKO mice after 6 weeks of HFD, IL-6 levels were approximately 40% lower in the KO mice (Figure 6B and Table 1), and KC levels (murine IL-8 equivalent) tended to be decreased (Table 1). Circulating levels of the adipokines adiponectin, resistin, and leptin were not affected (Table 1), the latter finding being further consistent with a lack of a significant effect of adipocyte-specific Fas deletion on whole-body fat mass. These results suggest that the proinflammatory profile of secreted products from adipose tissue of AFasKO mice in response to HFD feeding is diminished compared with WT mice.

To further confirm a role for Fas activation, even as an isolated factor, in propagating adipocyte inflammatory response, we used 3T3-L1 adipocytes. Fas activation by incubation of cells for 12 hours with FasL increased the release of IL-6 and KC into the medium by 1.5 ± 0.1–fold and 2.8 ± 0.5, respectively ($P < 0.05$ for both

Table 1
Plasma levels of glucose, insulin, FFAs, TG, glycerol, adipokines, and cytokines of HFD-fed WT and AFasKO mice

	WT	AFasKO
Blood glucose (mmol/l)	10.6 ± 0.3	9.4 ± 0.4[A]
Insulin (pmol/l)	98.5 ± 17.7	89.1 ± 7.8
FFAs (mmol/l)	1.36 ± 0.06	1.33 ± 0.04
TG (mg/dl)	85.9 ± 4.1	85.9 ± 6.5
Glycerol (mg/dl)	6.72 ± 0.37	6.52 ± 0.38
Adiponectin (μg/ml)	52.9 ± 5.7	56.4 ± 4.4
Resistin (pg/ml)	4,465 ± 516	5,251 ± 730
Leptin (pg/ml)	1,270 ± 305	1,240 ± 209
MCP-1 (pg/ml)	47.5 ± 12.9	35.1 ± 7.8
IL-6 (pg/ml)	7.6 ± 0.9	4.6 ± 1.0[A]
KC (pg/ml)	481 ± 139	278 ± 54
TNF-α	ND	ND

Results are mean ± SEM of 5–9 independent experiments. ND, not detectable (limit of detection, 3 pg/ml). [A]$P < 0.05$ (Student's t test).

cytokines compared with unstimulated cells; Figure 7A). Moreover, according to an in vitro macrophage-adipocyte adherence assay, macrophages adhered significantly more readily to FasL-treated 3T3-L1 adipocytes (25% ± 9% increase in macrophages adherent to adipocytes, $P < 0.05$; Figure 7B). These findings are consistent with the observation that AFasKO mice on a HFD had decreased expression of adipose tissue CD11b (probably reflecting decreased infiltrating leukocytes) (Figure 6A and Supplemental Table 2) and collectively suggest a role for Fas as an activator of adipocyte-derived inflammation under HFD.

Fas ablation in adipocytes protects against liver steatosis and insulin resistance induced by HFD. Adipose tissue inflammation has been linked to hepatic manifestations of obesity. In particular, the degree of adipose tissue macrophage infiltration correlated with histopathological changes in the liver (26). Moreover, JNK1 deficiency specifically in adipocytes was recently shown to cause increased hepatic insulin sensitivity (19). Hence, we next addressed the possibility that adipocyte Fas deletion protects from hepatic insulin resistance and steatosis along with diminished adipose tissue inflammation. Histological examinations and biochemical determination of total hepatic lipid content revealed that the livers of AFasKO mice were protected against liver steatosis induced by HFD (Figure 8A). Furthermore, AFasKO mice had significantly decreased liver ceramide levels, whereas diacylglycerol levels were similar in AFasKO and WT mice (Figure 8B and data not shown). Moreover, mRNA levels of the fatty acid transporter *Cd36* were reduced by 27% ($P < 0.05$) in livers of AFasKO mice, whereas mRNA levels of genes involved in gluconeogenesis, β-oxidation, and lipogenesis were similar (Figure 8C). Consistent with decreased steatosis in AFasKO livers, protein content of the lipid droplet protein adipose differentiation related protein (ADRP) and the lipogenic transcription factor PPARγ were decreased in AFasKO compared with WT mice (Figure 8D) (27). In addition, liver steatosis was associated with activation of the NF-κB signaling pathway (28). Intriguingly, activation of NF-κB was reduced to 35% in livers of AFasKO mice compared with WT mice, as assessed by phosphorylation of the p65 subunit of NF-κB (Figure 8E).

Molecularly, liver resistance to insulin actions was suggested to be mediated by increased Ser307 phosphorylation on IRS1 and by increased expression of SOCS3 (19). Interestingly, AFasKO mice had 50% lower levels of IRS1 phosphorylation on Ser307 (Figure 9A). In addition, expression of *Socs3* mRNA levels (relative to 18S) was reduced by 25%. Circulating glucose levels following a pyruvate load suggested that AFasKO mice had lower gluconeogenic flux compared with WT mice on HFD (Supplemental Figure 5). Moreover, during a hyperinsulinemic-euglycemic clamp, insulin-induced suppression of hepatic glucose production was blunted in HFD-fed WT mice but was clearly evident in AFasKO mice (Figure 9B).

To further support a role for adipocyte-expressed Fas in the development of HFD-induced liver insulin resistance, we performed experiments with conditioned medium. 3T3-L1 adipocytes were treated with or without FasL, and conditioned medium was then collected. Hepatocytes incubated with FasL-conditioned medium developed insulin resistance, as shown by decreased insulin-stimulated phosphorylation of Akt (Figure 9C).

Collectively, these studies demonstrate that in the absence of Fas in adipocytes, mice are protected against hepatic steatosis and liver insulin resistance induced by HFD.

Discussion

In the present study, we demonstrate that both total body Fas-deficient mice and a novel adipocyte-specific *Fas*-KO model were significantly protected against insulin resistance induced by HFD feeding, at the adipocyte, liver, and whole-body levels. Our findings suggest that Fas-mediated pathways in adipocytes play a role in obesity-associated insulin resistance by modulating adipose tissue inflammatory cascades.

Our finding of reduced fat pad weight and lack of an increase in adipocyte size under HFD in Fas-def mice (Figure 2C) hints at a role of Fas in modulating adipocyte development and/or differentiation, as Fas is not expressed in preadipocytes and adipocytes of Fas-def mice. Thus, the metabolic effect of Fas may be secondary to its effect on adipocyte differentiation. In contrast, since Fabp4 is downstream of PPARγ, Cre is only expressed during late stages of adipocyte differentiation in the AFasKO mice, as was previously shown (23). Consistent with such a notion, adipocyte size of AFasKO mice did not differ from WT mice after 6 weeks of HFD (Figure 4H). Thus, early adipocyte development was unlikely to be affected in AFasKO mice, as opposed to Fas-def mice, and the hypertrophic response of adipocytes to HFD remained similar to that in control mice. Moreover, we assessed the potential influence of Fas stimulation on preadipocyte differentiation by treating 3T3-L1 (pre)adipocytes with FasL during differentiation. We found that markers of differentiation such as C/EBPβ, C/EBPα, and PPARγ were reduced (Supplemental Figure 6). Furthermore, it is possible that Fas expression in other cells is indirectly involved in adipocyte growth/differentiation, as was previously shown for macrophages (29), explaining the observation that adipocytes were affected to a greater extent in the Fas-def model than in the AFasKO model. Similar to the reduction in markers of differentiation in FasL-treated 3T3-L1 adipocytes (Supplemental Figure 6), PPARγ was significantly reduced in WAT of WT compared with AFasKO mice upon 6 weeks of HFD, whereas C/EBPα showed a trend toward lower expression levels in WT mice (Supplemental Figure 7).

Additional support for the involvement of Fas in obesity-related adipose tissue inflammation was initially gained by finding increased expression of Fas in both common genetic and nutritional mouse obesity models and in obese humans. Interestingly,

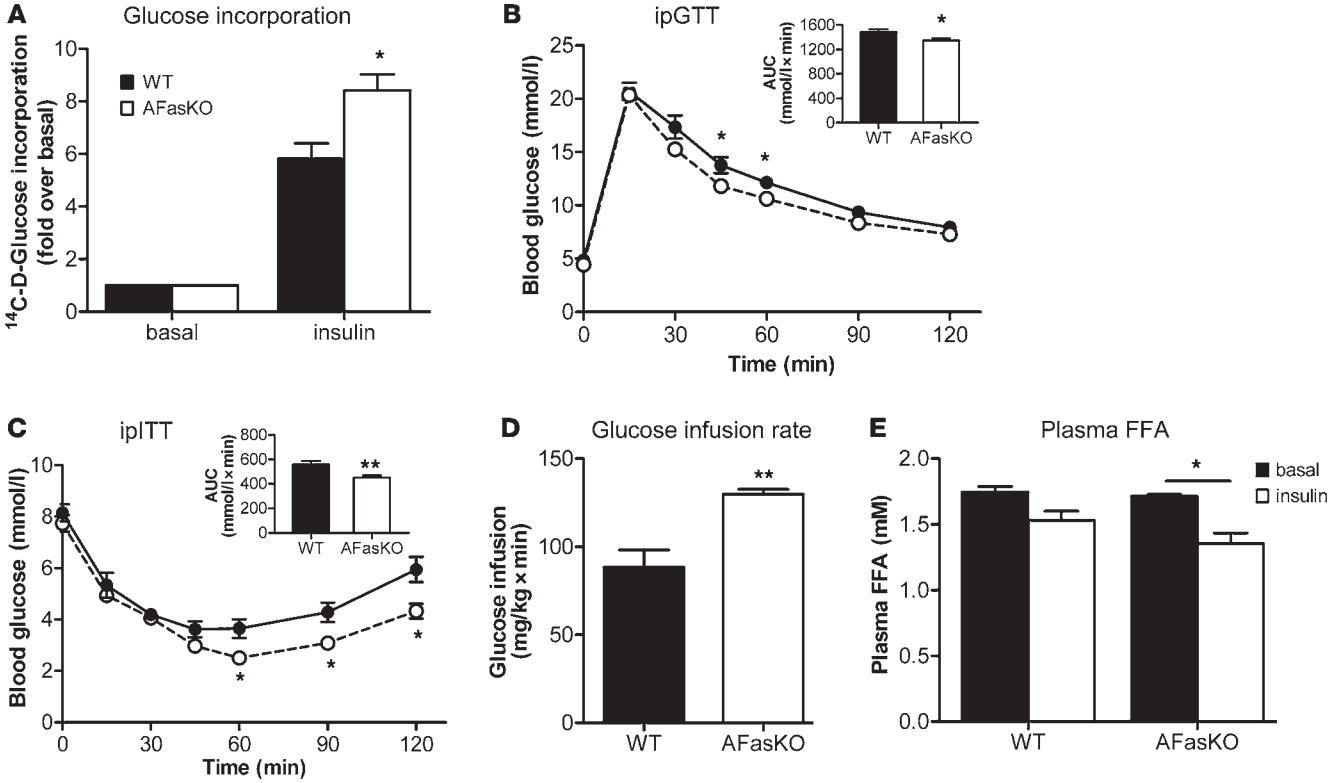

Figure 5

AFasKO mice are protected from HFD-induced deteriorations in glucose metabolism. (**A**) ^{14}C-D-glucose incorporation into isolated perigonadal adipocytes from WT (*Fas$^{fl/fl}$;Fabp4-Cre$^{-/-}$*) and AFasKO (*Fas$^{fl/fl}$;Fabp4-Cre$^{+/-}$*) mice was determined in the absence or presence of insulin. Results are expressed relative to basal uptake and represent mean ± SEM of 5 independent experiments performed in triplicate. **P* < 0.05 (Student's *t* test). Intraperitoneal glucose (**B**) and insulin (**C**) tolerance tests (ipGTT and ipITT) were performed in WT (filled circles) and AFasKO (open circles) mice. Inset graphs in **B** and **C** depict the respective analysis of the area under the curve. Results are mean ± SEM of 8–10 animals per group. **P* < 0.05, ***P* < 0.01 (Student's *t* test). (**D**) Steady-state glucose infusion rates during hyperinsulinemic-euglycemic clamps. Results are mean ± SEM of 3–4 animals per group. ***P* < 0.01 (Student's *t* test). (**E**) Plasma FFA levels in HFD-fed WT and AFasKO mice before and at the end of a euglycemic-hyperinsulinemic clamp are depicted. Results are mean ± SEM of 3 animals per group. **P* < 0.05 (Student's *t* test).

4 days of HFD feeding was sufficient to upregulate Fas expression in adipocytes (Supplemental Figure 8). This finding suggests that upregulation of Fas in adipocytes reflects an early adaptation step to HFD. To further establish a functional role for adipocyte Fas in adipose tissue inflammation in obesity, we established the AFasKO mouse, which displays a specific deletion of Fas in adipocytes. Adipose tissue inflammation in obesity is characterized by increased infiltration of bone-derived immune cells, particularly proinflammatory macrophages, and elevated expression and secretion of proinflammatory cytokines, with decreases in IL-10 and arginase 1 (30). Intriguingly, HFD-fed AFasKO mice exhibited decreased leukocyte infiltration (evidenced by lower expression of CD11b), diminished expression of IL-6, and increased expression of IL-10 and arginase 1 compared with WT controls (Figure 6A and Supplemental Table 2). Moreover, in support of the hypothesis that Fas acts as an isolated factor to promote macrophage infil-

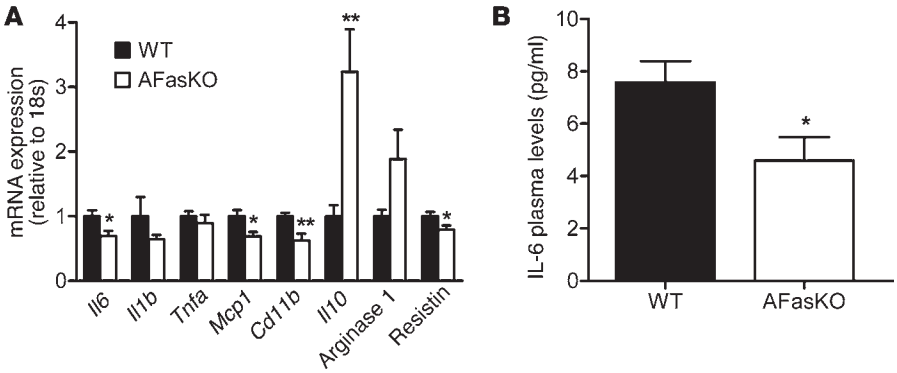

Figure 6

Reduced inflammatory profile in HFD-fed AFasKO mice. (**A**) Quantitative RT-PCR detection of mRNA expression in WAT. The level of mRNA expression was normalized to 18S RNA. Results are mean ± SEM of 5–9 animals per group. **P* < 0.05, ***P* < 0.01 (Student's *t* test). (**B**) Plasma concentration of IL-6. Results represent mean ± SEM of 5 animals per group. **P* < 0.05 (Student's *t* test).

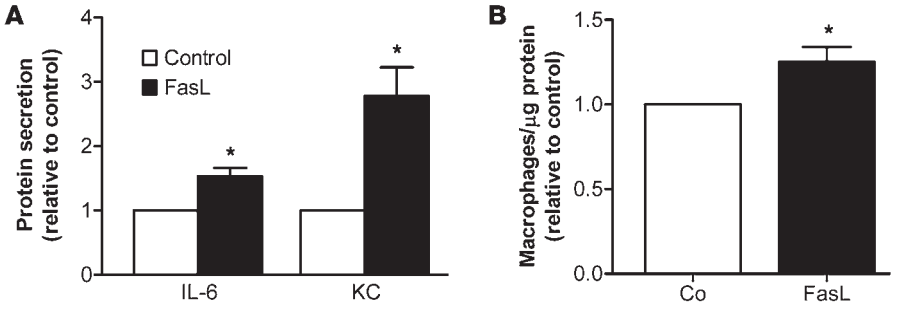

Figure 7

Increased secretion of immunoattractant cytokines and higher macrophage adherence in FasL-treated 3T3-L1 adipocytes. (**A**) Fas ligation increases expression of proinflammatory cytokines in 3T3-L1 adipocytes. Mature 3T3-L1 adipocytes were incubated in the presence or absence of 2 ng/ml FasL for 12 hours. Medium was removed, and cells were incubated with KREBS buffer. Cytokine levels were then determined in the supernatant. Shown are results normalized to untreated cells. Results represent mean ± SEM of 4–5 independent experiments. $^*P < 0.05$ (1-sample *t* test). (**B**) Mature 3T3-L1 adipocytes were incubated in the presence or absence (control [Co]) of 2 ng/ml FasL for 12 hours. Thereafter, adipocytes were incubated with ^{3}H-labeled macrophages for 1 hour at 37°C. Cells were washed and lysed (0.05N NaOH). Finally, radioactivity of lysates was determined by a beta counter. Results represent mean ± SEM of 7 independent experiments. $^*P < 0.05$ (1-sample *t* test).

tration, macrophages adhered more readily to 3T3-L1 adipocytes stimulated with FasL (Figure 7B). Thus, adipocyte Fas plays a role in modulating adipose tissue inflammatory response to obesity.

What is the mechanism for increased adipocyte Fas expression in obesity? We observed that Fas expression was higher in larger compared with smaller adipocytes isolated from the same fat depot of HFD-fed WT mice (Supplemental Figure 9). Yet given that adipocyte size in AFasKO mice on HFD was comparable to that in controls, it is unlikely that the increased adipose tissue Fas expression is the consequence of higher abundance of hypertrophied adipocytes in this mouse model. Rather, studies in 3T3-L1 adipocytes suggest that TNF-α and IL-1β, two key proinflammatory cytokines arising early in the inflammatory process, induce Fas expression (see Supplemental Figure 10). Moreover, at later stages of adipose tissue inflammation, adipose tissue is infiltrated by inflammatory cells, such as T cells and macrophages, which express and secrete FasL (10). Intriguingly, we found *Fasl* mRNA to be upregulated in WAT of *ob/ob* mice (Figure 1C). Thus, it is very likely that the trigger to upregulate Fas expression and activation in adipose tissue in obesity is the increased production of proinflammatory cytokines and FasL. Intriguingly, a similar regulation was previously shown for TNF, i.e., expression of TNF receptor was shown to be upregulated by different cytokines as well as by TNF (31, 32). Thus, like many other inflammatory mediators that participate in feed-forward loops to enhance the inflammatory response, Fas appears to be both the target and a positive mediator of the proinflammatory cascade of adipose tissue in obesity.

Enhanced Fas expression and activation in adipose tissue have functional consequences at the level of both adipose tissue and, indirectly, the liver. Fas is well characterized as a proapoptotic factor, and adipocyte hypertrophy in obesity was proposed to promote adipocyte cell death, possibly with some apoptotic characteristics (33). It is therefore conceivable that enhanced adipocyte Fas expression sensitizes adipocytes to FasL-induced apoptosis. In addition, Fas activation may exert direct metabolic/endocrine effects unrelated to cell death, reminiscent of the metabolic/endocrine effects of TNF-α (34).

Adipose tissue inflammation was previously correlated with hepatic steatosis (26). Consistent with this finding, ablation of Fas specifically in adipocytes was associated with decreased hepatic steatosis and hepatic insulin resistance (Figures 8 and 9). Moreover, cultured medium from FasL-treated 3T3-L1 adipocytes induced insulin resistance in cultured hepatocytes (Figure 9C), supporting a potential role of adipocyte-expressed Fas in the induction of perturbed adipocyte-hepatocyte crosstalk that results in hepatic insulin resistance. A possible candidate mediating the link between adipose tissue inflammation and hepatic steatosis/insulin resistance is IL-6. Indeed, IL-6 treatment of hepatocytes induced insulin resistance in vitro (35), and it seems to be generally accepted that IL-6 causes hepatic insulin resistance (24). Particularly, IL-6 was shown to induce phosphorylation of IRS1 on Ser307 residue and to activate the negative insulin signaling regulator SOCS3 in C57BL/6J mice (36, 37). Accordingly, IL-6 expression in adipose tissue and circulating IL-6 levels were reduced in HFD-fed AFasKO mice, and their livers exhibited decreased Ser307 phosphorylation of IRS1 and decreased mRNA levels of *Socs3* compared with those of WT mice.

Besides IL-6, elevated portal delivery of FFAs or resistin may lead to hepatic steatosis and/or hepatic insulin resistance in rodents (38, 39). Of note, insulin-induced inhibition of lipolysis was maintained in AFasKO but not in HFD-fed WT mice (in vivo and in vitro), suggesting that postprandial hyperlipidemia could be prevented by adipocyte-specific Fas deletion. Likewise, mRNA levels of the fatty acid transporter *Cd36* were significantly increased in livers of HFD-fed WT mice, suggesting increased hepatic fatty acid uptake (40). In turn, increased delivery of FFAs to the liver might contribute to higher ceramide levels in WT compared with AFasKO livers (Figure 8B) and subsequently to hepatic insulin resistance (41). Moreover, hepatic glucose production was lower in HFD-fed AFasKO mice (as assessed by hepatic glucose production during clamp studies). Interestingly, mRNA expression levels of gluconeogenic enzymes were not different in AFasKO and WT mice. This apparent contradiction might be due to the fact that liver samples were obtained in randomly fed mice. Moreover, similar findings with differences in gluconeogenic flux but without differences in mRNA levels of *Pck1* and *G6pc* were previously reported by others (42). In addition, expression levels of PEPCK and G6Pase may not always accurately reflect gluconeogenesis flux (43, 44). Thus, adipocyte-specific Fas deletion protects the liver from developing insulin resistance and hepatic steatosis by interfering with Fas-mediated adipose tissue inflammation and/or metabolic dysregulation.

The relevance of our studies to human obesity are suggested by our finding that Fas is upregulated in adipose tissue of obese patients and even more so in obese diabetic patients. This finding may hint at a role of Fas in the development of obesity-induced insulin resistance in humans. Intriguingly, recent studies in humans revealed an association of promoter alterations in the Fas and FasL gene with type 2 diabetes and insulin resistance (45), further supporting such a notion.

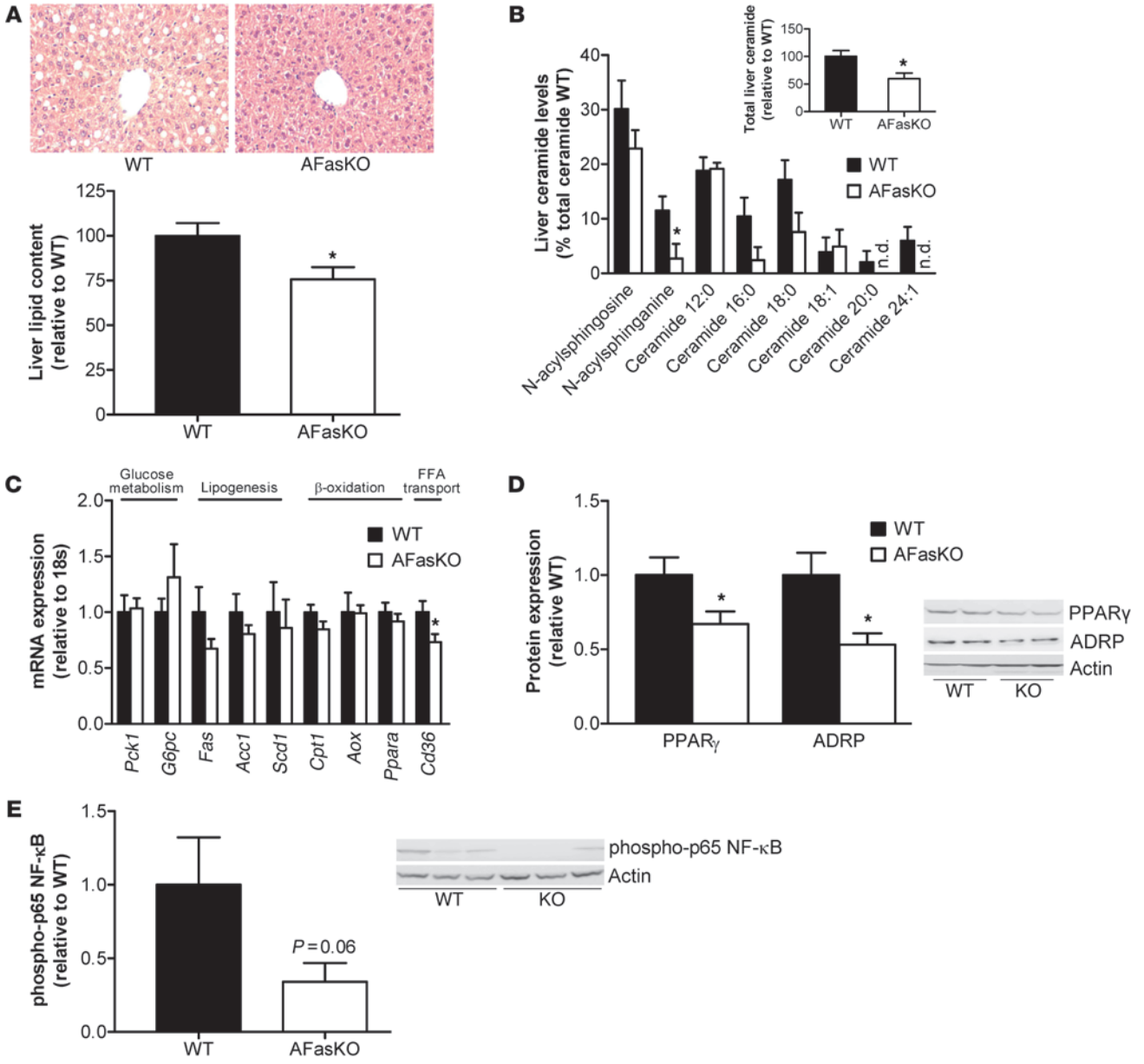

Figure 8

Reduced hepatic steatosis in HFD-fed AFasKO mice. (**A**) H&E-stained liver sections from WT (*Fas*$^{fl/fl}$*;Fabp4-Cre*$^{-/-}$) and AFasKO (*Fas*$^{fl/fl}$*;Fabp4-Cre*$^{+/-}$) mice (original magnification, ×40). Total liver lipids were determined and expressed relative to lipid content in WT mice. Results represent mean ± SEM of 8 mice of each group. *$P < 0.05$ (Student's *t* test). (**B**) Levels of detected liver ceramide species are shown. Results are mean ± SEM of 6–8 animals per group and are expressed relative to total lipids in WT mice. *$P < 0.05$ (Student's *t* test). n.d., not detected. (**C**) mRNA expression of indicated markers in liver tissue of WT and AFasKO mice was analyzed. Results are mean ± SEM of 5–9 mice per group, expressed relative to WT and normalized to expression of 18S. *$P < 0.05$ (Student's *t* test). (**D** and **E**) Liver lysates were prepared from WT and AFasKO mice and resolved by LDS-PAGE. (**D**) Lysates were immunoblotted with ADRP, PPARγ, or actin antibodies. Results are mean ± SEM of 4–6 animals per group and expressed relative to protein expression in WT mice. *$P < 0.05$ (Student's *t* test). (**E**) Lysates were immunoblotted with anti–phospho–p65 NF-κB or anti-actin antibody. Expression levels of phospho-p65 are normalized to expression of actin. Results are mean ± SEM of 5–6 mice and expressed relative to WT.

In conclusion, our findings suggest that Fas activation in adipocytes contributes to the increased production and secretion of inflammatory cytokines in obesity and thus contributes to the development of insulin resistance. Based on these findings, it would seem important to determine whether inhibition of Fas expression/activation in adipocytes constitutes a potential new therapeutic target in the treatment of insulin resistance and type 2 diabetes.

Methods

Human samples. Fat biopsy samples were taken from women undergoing elective laparoscopic abdominal surgery at the Soroka University Medical

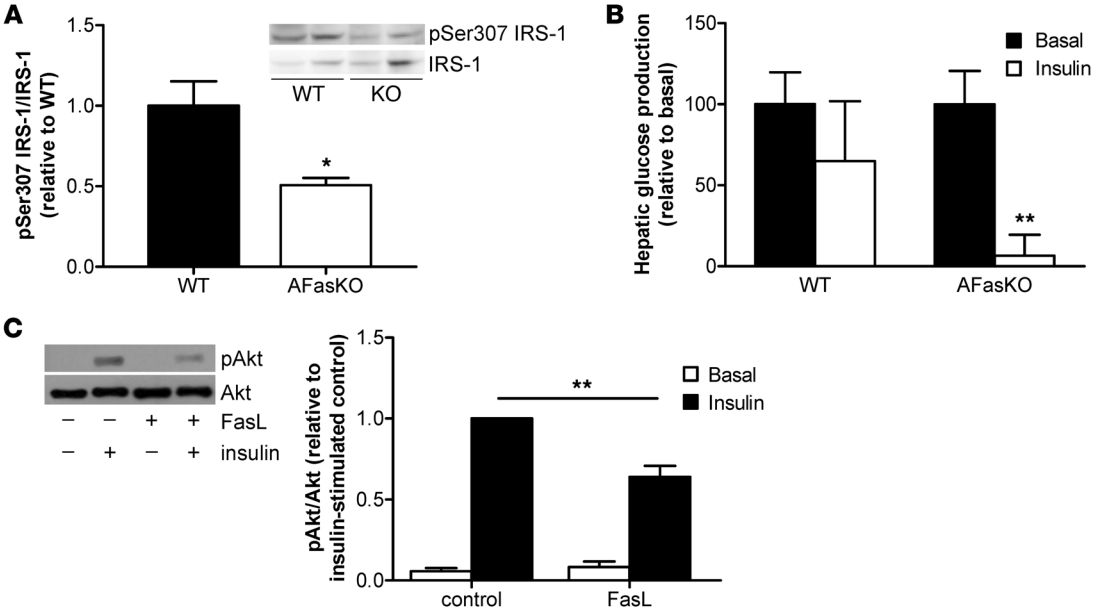

Figure 9

Improved hepatic insulin sensitivity in AFasKO mice. (**A**) Lysates were immunoblotted with anti–phospho-IRS1 (Ser307) and total IRS1 antibody. Expression levels of pSer307 are normalized to expression of total IRS1. Results are mean ± SEM of 4 mice and expressed relative to WT. *$P < 0.05$ (Student's *t* test). (**B**) Hepatic glucose production was calculated in the basal period and in response to insulin infusion during the hyperinsulinemic-euglycemic clamp study. Results are mean ± SEM of 3–4 animals per group and expressed relative to basal hepatic glucose production. **$P < 0.01$ (Student's *t* test). (**C**) 3T3-L1 adipocytes were incubated with or without FasL for 12 hours, and subsequently, supernatant was collected for 24 hours. Hepatoma cells (Fao) were incubated with the conditioned medium for 24 hours. Total cell lysates were prepared and resolved by LDS-PAGE and immunoblotted with anti–phospho-Akt or Akt antibody. Results are mean ± SEM of 7–9 independent experiments. **$P < 0.01$ (ANOVA).

Center (Beer-Sheva, Israel) as described and characterized elsewhere (46, 47). All procedures were approved in advance by the Soroka University Medical Center Institutional Review Committee. Patients gave written informed consent for all procedures.

Animals. C57BL/6J WT and Fas-def mice backcrossed for more than 10 generations onto this same C57BL/6J inbred strain background (B6.MRL^{lpr}) were obtained from The Jackson Laboratory. Mice with exon 9 of Fas flanked with *loxP* sites were produced as described previously (48). Animals with Cre recombinase controlled by the *Fabp4* promoter [B6.Cg-Tg(Fabp4-cre)1Rev/J] were purchased from The Jackson Laboratory. All mice were genotyped by PCR with primers amplifying the Cre transgene and Fas, generating 319-bp WT and 399-bp floxed allele products. C57BL/6J WT (C57BL/6JOlaHsd), *ob/ob* (C57BL/6OlaHsd-Lep<ob>), and *db/db* (BKS.Cg-+Leprdb/+Leprdb/OlaHsd) mice were purchased from Harlan.

All mice were housed in a specific pathogen–free environment on a 12-hour light/12-hour dark cycle and fed ad libitum a regular chow diet (Provimi Kliba) or HFD (58 kcal% fat with sucrose Surwit Diet, D12331, Research Diets). All protocols conformed to Swiss animal protection laws and were approved by the Cantonal Veterinary Office (Zurich, Switzerland).

Harvesting of naive splenic macrophages. Splenocytes were isolated in PBS by smashing the spleen through a metal grid with a syringe plunger. After removal of residual tissue, cells were washed and resuspended in 0.4 ml MACS buffer (1× PBS, 2% FCS, 5 mM EDTA). Twenty microliters of appropriate beads (anti-CD11b; Miltenyi Biotec) was added, and the suspension was incubated on ice for 15 minutes. Upon washing, cells were applied to the MACS magnetic separator according to the manufacturer's protocol. To elute the appropriate cells, MACS buffer was pushed through the column with a plunger. For FACS analysis (before and after MACS), about 3×10^6 splenocytes were resuspended in FACS buffer (1× PBS, 2% FCS, 0.2% sodium azide, 0.02 M EDTA) and stained with anti-CD11b–PE (BD Biosciences — Pharmingen) labeled antibody. After washing of the cells with FACS buffer, cells were analyzed immediately using FlowJo software (Tree Star).

Induction of activated peritoneal macrophages by thioglycollate. Three months before use, 30 g thioglycollate medium (Difco, Chemie Brunschwig AG) was rehydrated in 1 l H_2O and autoclaved. For induction of activated peritoneal macrophages, mice were injected i.p. with 1 ml thioglycollate suspension. Seventy-two hours later, the mice were sacrificed, and the peritoneum was flushed with cold PBS in order to harvest the macrophages.

Intraperitoneal glucose, insulin, and pyruvate tolerance tests. For the intraperitoneal glucose tolerance test mice were fasted overnight; for the intraperitoneal insulin and pyruvate tolerance tests, mice were fasted for 3 hours. Glucose (2 g/kg body weight), human recombinant insulin (0.75 U/kg or 1 U/kg body weight), or pyruvate (2 g/kg body weight) was injected intraperitoneally (49).

Glucose incorporation into isolated white adipocytes. Adipocyte isolation was performed as described previously (21, 50). To determine glucose incorporation, adipocytes were incubated with D-[U-^{14}C]glucose (final glucose concentration, 0.89 mmol/l) for 60 minutes in the presence or absence of 100 nM insulin. Glucose incorporation was stopped by separating cells from the medium by centrifugation through phthalic acid dinonyl ester and then subjecting them to liquid scintillation counting.

Adipocyte size determination. Aliquots of adipocyte fractions were used to determine mean cell diameters. Photographs of isolated adipocytes in the hemocytometer were taken, and images were analyzed using NIH ImageJ software for quantification (http://rsbweb.nih.gov/ij/). At least 100 adipocytes per mouse were analyzed.

Determination of plasma insulin, adipokine, FFA, TG, and glycerol levels. Plasma insulin and FFA levels were determined as described previously (49). Plasma adipokine and cytokine levels were determined with mouse LINCOplex kits from Linco Research Inc. (Labodia). TG and glycerol concentrations were determined using a colorimetric assay (Sigma-Aldrich).

Total liver lipid extraction. Liver tissue (30 mg) was homogenized in PBS, and lipids were extracted in a chloroform/methanol (2:1) mixture. Total liver lipids were determined by a sulfo-phospho-vanillin reaction as previously described (51).

Ceramide and diacylglycerol analysis in liver tissue. Extraction of lipids from liver tissue (30 mg) was performed by the method of Bligh and Dyer (52) with 50 mM potassium phosphate buffer in the aqueous layer and β-sitosterol (2 μg; Sigma-Aldrich) as internal standard. Lipid extracts were analyzed on a Q-TOF Ultima spectrometer (Waters) equipped with a NanoMate HD (Adrion Biosciences Ltd.) by direct infusion of the samples. Ammonium acetate (final concentration, 7.5 mM) was added to the extracts prior to analysis to induce ionization. Data were analyzed using MassLynx (version 4.1, Waters), and targeted lipids were identified based on their exact mass. Relative quantities of all lipids were reported as background corrected intensity ratios relative to the internal standard β-sitosterol.

RNA extraction and quantitative RT-PCR. Total RNA from fat pads was extracted with the RNeasy Lipid Tissue Mini Kit (QIAGEN) and analyzed with a Bioanalyzer (Agilent Technologies). RNA (0.75 μg) was reverse transcribed with Superscript III Reverse Transcriptase (Invitrogen) using random hexamer primer (Invitrogen). TaqMan system (Applied Biosystems) was used for real-time PCR amplification. Relative gene expression was obtained after normalization to 18s RNA (Applied Biosystems), using the formula $2^{-\Delta\Delta cp}$ (53). The following primers were used: TNF-α, Mm00443258_m1; IL-6, Mm00446190_m1; KC, Mm00433859_m1; IL-1β, Mm0043422/8_m1; FasL, Mm00438864_m1; cd11b, Mm00434455_m1; MCP-1, Mm00441242_m1; resistin, Mm00445641_m1; SOCS3, Mm00545913_s1; CD36, Mm00432403_m1; ArgI, Mm00475988_m1; IL-10, Mm00439614_m1; adiponectin, Mm00456425_m1; PPARγ, Mm00440945_m1; PEPCK, Mm0044636_m1; G6Pase, Mm00839363_m1; FAS, Mm00662319_m1; ACC-1, Mm01304289_m1; SCD-1, Mm01197142_m1; CPT-1, Mm00550438_m1; PPARα, Mm00627559_m1; AOX, Mm00443579_m1 (Applied Biosystems).

Glucose clamp studies. Glucose turnover rate was assessed in freely moving mice after 6 weeks of HFD during a euglycemic-hyperinsulinemic clamp. Briefly, mice were anesthetized with isoflurane, and a catheter (MRE 025, Braintree Scientific) was inserted into the left jugular vein and exteriorized at the back of the neck. After 7 days of recovery, only mice that had regained greater than 95% of their preoperative weight were studied. After a fasting period of 5 hours, 3-[^{3}H]glucose (0.1 μCi/min; PerkinElmer) was infused for 80 minutes, and blood was collected from tail tip for basal turnover calculation. After basal sampling, insulin (18 mU/kg/min) was infused for 2 hours. Euglycemia was maintained by periodically adjusting a variable infusion of 20% glucose with a syringe pump (TSE Systems). The glucose infusion rate was calculated as the mean of the steady-state infusion (60–90 minutes) after 1 hour of insulin infusion. A blood sample was collected from tail tip after steady-state infusion. The glucose turnover rate was calculated by dividing the rate of 3-[^{3}H]glucose infusion by the plasma 3-[^{3}H]glucose–specific activity. Hepatic glucose production was calculated by subtracting the glucose infusion rate from the glucose turnover rate.

Western blot analysis. Cell lysates and tissue samples were homogenized in a buffer containing 150 mM NaCl, 50 mM Tris-HCl (pH 7.5), 1 mM EGTA, 1% NP-40, 0.25% sodium deoxycholate, 1 mM sodium vanadate, 1 mM NaF, 10 mM sodium β-glycerophosphate, 100 nM okadaic acid, 0.2 mM PMSF, and a 1:1,000 dilution protease inhibitor cocktail (Sigma-Aldrich). For isolation of total membranes, 3T3-L1 adipocytes were lysed and homogenized in a buffer containing 20 mM HEPES, 250 mM sucrose, 5 mM NaN_3, 1 mM EDTA, 0.2 mM PMSF, and a 1:1,000 dilution protease inhibitor cocktail. Lysates were centrifuged at 229,000 *g* for 90 minutes at 4°C, and the pellet was resuspended in homogenization buffer.

Protein concentration was determined using BCA assay (Pierce), and equivalent amounts of protein (20–50 μg) were resolved by LDS-PAGE (4%–12% gel; NuPAGE, Invitrogen). Proteins were transferred to a nitrocellulose membrane (0.2 μm; Bio-Rad) and blocked for 1 hour in 5% nonfat dry milk (Bio-Rad) resolved in Tris-buffered saline, containing 1% Tween-20. Membranes were incubated overnight at 4°C on a rocking platform with respective primary antibodies. The following primary antibodies were used: anti-GLUT4 (gift of A. Klip, The Hospital for Sick Children, Toronto, Ontario, Canada), anti-Fas, anti–phospho-IRS1 (Ser307) (Upstate), anti-Fas (human), anti-IRS1, anti-PPARγ, anti-C/EBPα and anti-C/EBPβ (Santa Cruz Biotechnology Inc.), anti-ADRP (Novus Biologicals), anti-Cre and anti-actin (Millipore), anti–phospho-Akt (Ser473), anti-Akt and anti–phospho–NF-κB p65 (Cell Signaling Technology). Subsequently, membranes were incubated with secondary antibody (HRP-conjugated; Santa Cruz Biotechnology and Alexis Biochemicals) for 1 hour at room temperature. Bands were detected after 5-minute incubation with Lumi-Light substrate (Roche). Membranes were exposed in an Image Reader and analyzed with Image Analyzer (FujiFilm).

Determination of 2-deoxy-^{3}H-D-glucose uptake and lipolysis in 3T3-L1 cells. 3T3-L1 cells were grown and differentiated into adipocytes as described previously (50). Uptake and lipolysis of 2-deoxy-^{3}H-D-glucose (^{3}H-2dG) were measured in mature 3T3-L1 adipocytes as previously reported (50, 54).

Macrophage adherence assay. Thioglycollate-activated macrophages (as described above) were labeled with ^{3}H-2dG (55) by incubation with HEPES-buffered saline containing 2.5 mM D-glucose and 5 μCi/ml ^{3}H-2dG for 1 hour at 37°C. Glucose uptake was stopped by 2 washes with cold HEPES-buffered saline. Labeled macrophages were resuspended in HEPES-buffered saline and added to mature 3T3-L1 adipocytes, treated with or without 2 ng/ml FasL for 12 hours in advance. After 1 hour of incubation at 37°C, cells were washed and lysed (0.05N NaOH). Finally, radioactivity of lysates was determined by a beta counter.

Experiments with conditioned medium. Mature 3T3-L1 adipocytes were incubated without or with 2 ng/ml FasL for 12 hours. Cells were rinsed with PBS, and fresh medium (DMEM) was added and collected after 24 hours. Thereafter, hepatoma cells (Fao) were incubated for 24 hours with conditioned medium from untreated or FasL-treated adipocytes. Fao cells were rinsed and stimulated with insulin (100 nM) for 7 minutes. Lysates were prepared and subjected to Western blot analysis using respective antibodies.

Statistics. Data are presented as mean ± SEM and were analyzed by 2-tailed Student's *t* test, 1-sample *t* test, or ANOVA with a Tukey correction for multiple group comparisons. *P* values less than 0.05 were considered significant.

Acknowledgments

This work was supported by Swiss National Science Foundation grant 310000-112275 and by a "Forschungskredit" from the University of Zurich (both to D. Konrad). We gratefully acknowledge Maggy Arras for expert veterinary advice and Kurt Bürki for advice regarding the breeding of *Lox* and *Cre* mice. We are indebted to Paolo Cinelli for his advice regarding mRNA preparation and determination, to Oliver Tschopp for technical advice regarding determination of hepatic lipid content, and to Giatgen Spinas for continuous support. We thank Endre Laczko of the Functional Genomics Center Zurich (FGCZ) for technical support and assistance regarding ceramide and diacylglycerol analysis.

Received for publication December 19, 2008, and accepted in revised form September 30, 2009.

Address correspondence to: Daniel Konrad, University Children's Hospital, Division of Pediatric Endocrinology and Diabetology, Steinwiesstrasse 75, CH-8032 Zurich, Switzerland. Phone: 41-44-266-7966; Fax: 41-44-266-7983; E-mail: daniel.konrad@kispi.uzh.ch.

1. Scherer PE. Adipose tissue: from lipid storage compartment to endocrine organ. *Diabetes.* 2006; 55(6):1537–1545.
2. Wellen KE, Hotamisligil GS. Inflammation, stress, and diabetes. *J Clin Invest.* 2005;115(5):1111–1119.
3. Park SY, et al. Unraveling the temporal pattern of diet-induced insulin resistance in individual organs and cardiac dysfunction in C57BL/6 mice. *Diabetes.* 2005;54(12):3530–3540.
4. Poirier H, Shapiro JS, Kim RJ, Lazar MA. Nutritional supplementation with trans-10, cis-12-conjugated linoleic acid induces inflammation of white adipose tissue. *Diabetes.* 2006;55(6):1634–1641.
5. Zick Y. Ser/Thr phosphorylation of IRS proteins: a molecular basis for insulin resistance. *Sci STKE.* 2005;(268):pe4.
6. Kanda H, et al. MCP-1 contributes to macrophage infiltration into adipose tissue, insulin resistance, and hepatic steatosis in obesity. *J Clin Invest.* 2006; 116(6):1494–1505.
7. Klover PJ, Zimmers TA, Koniaris LG, Mooney RA. Chronic exposure to interleukin-6 causes hepatic insulin resistance in mice. *Diabetes.* 2003; 52(11):2784–2789.
8. Parekh S, Anania FA. Abnormal lipid and glucose metabolism in obesity: implications for nonalcoholic fatty liver disease. *Gastroenterology.* 2007; 132(6):2191–2207.
9. Xu A, et al. The fat-derived hormone adiponectin alleviates alcoholic and nonalcoholic fatty liver diseases in mice. *J Clin Invest.* 2003;112(1):91–100.
10. Peter ME, et al. The CD95 receptor: apoptosis revisited. *Cell.* 2007;129(3):447–450.
11. Schumann DM, et al. The Fas pathway is involved in pancreatic beta cell secretory function. *Proc Natl Acad Sci U S A.* 2007;104(8):2861–2866.
12. Wajant H, Pfizenmaier K, Scheurich P. Non-apoptotic Fas signaling. *Cytokine Growth Factor Rev.* 2003;14(1):53–66.
13. Faouzi S, et al. Anti-Fas induces hepatic chemokines and promotes inflammation by an NF-kappa B-independent, caspase-3-dependent pathway. *J Biol Chem.* 2001;276(52):49077–49082.
14. Farley SM, et al. Fas ligand-induced proinflammatory transcriptional responses in reconstructed human epidermis. Recruitment of the epidermal growth factor receptor and activation of MAP kinases. *J Biol Chem.* 2008;283(2):919–928.
15. Imamura R, et al. Fas ligand induces cell-autonomous NF-kappaB activation and interleukin-8 production by a mechanism distinct from that of tumor necrosis factor-alpha. *J Biol Chem.* 2004; 279(45):46415–46423.
16. Miwa K, et al. Caspase 1-independent IL-1beta release and inflammation induced by the apoptosis inducer Fas ligand. *Nat Med.* 1998;4(11):1287–1292.
17. Schaub FJ, et al. Fas and Fas-associated death domain protein regulate monocyte chemoattractant protein-1 expression by human smooth muscle cells through caspase- and calpain-dependent release of interleukin-1alpha. *Circ Res.* 2003; 93(6):515–522.
18. Fischer-Posovszky P, Tornqvist H, Debatin KM, Wabitsch M. Inhibition of death-receptor mediated apoptosis in human adipocytes by the insulin-like growth factor I (IGF-I)/IGF-I receptor autocrine circuit. *Endocrinology.* 2004; 145(4):1849–1859.
19. Sabio G, et al. A stress signaling pathway in adipose tissue regulates hepatic insulin resistance. *Science.* 2008;322(5907):1539–1543.
20. Pisetsky DS, Caster SA, Roths JB, Murphy ED. Ipr gene control of the anti-DNA antibody response. *J Immunol.* 1982;128(5):2322–2325.
21. Wueest S, Rapold RA, Rytka JM, Schoenle EJ, and Konrad D. Basal lipolysis, not the degree of insulin resistance, differentiates large from small isolated adipocytes in high-fat fed mice. *Diabetologia.* 2009;52(3):541–546.
22. Makowski L, et al. Lack of macrophage fatty-acid-binding protein aP2 protects mice deficient in apolipoprotein E against atherosclerosis. *Nat Med.* 2001;7(6):699–705.
23. He W, et al. Adipose-specific peroxisome proliferator-activated receptor gamma knockout causes insulin resistance in fat and liver but not in muscle. *Proc Natl Acad Sci U S A.* 2003;100(26):15712–15717.
24. Carey AL, Febbraio MA. Interleukin-6 and insulin sensitivity: friend or foe? *Diabetologia.* 2004; 47(7):1135–1142.
25. Sartipy P, Loskutoff DJ. Monocyte chemoattractant protein 1 in obesity and insulin resistance. *Proc Natl Acad Sci U S A.* 2003;100(12):7265–7270.
26. Cancello R, et al. Increased infiltration of macrophages in omental adipose tissue is associated with marked hepatic lesions in morbid human obesity. *Diabetes.* 2006;55(6):1554–1561.
27. Inoue M, et al. Increased expression of PPARgamma in high fat diet-induced liver steatosis in mice. *Biochem Biophys Res Commun.* 2005;336(1):215–222.
28. Cai D, et al. Local and systemic insulin resistance resulting from hepatic activation of IKK-beta and NF-kappaB. *Nat Med.* 2005;11(2):183–190.
29. Nishimura S, et al. Adipogenesis in obesity requires close interplay between differentiating adipocytes, stromal cells, and blood vessels. *Diabetes.* 2007; 56(6):1517–1526.
30. Lumeng CN, Bodzin JL, Saltiel AR. Obesity induces a phenotypic switch in adipose tissue macrophage polarization. *J Clin Invest.* 2007;117(1):175–184.
31. Bradley JR. TNF-mediated inflammatory disease. *J Pathol.* 2008;214(2):149–160.
32. Winzen R, Wallach D, Kemper O, Resch K, Holtmann H. Selective up-regulation of the 75-kDa tumor necrosis factor (TNF) receptor and its mRNA by TNF and IL-1. *J Immunol.* 1993; 150(10):4346–4353.
33. Cinti S, et al. Adipocyte death defines macrophage localization and function in adipose tissue of obese mice and humans. *J. Lipid Res.* 2005; 46:2347–2355.
34. Hotamisligil GS. Role of endoplasmic reticulum stress and c-Jun NH2-terminal kinase pathways in inflammation and origin of obesity and diabetes. *Diabetes.* 2005;54(suppl 2):S73–S78.
35. Senn JJ, Klover PJ, Nowak IA, Mooney RA. Interleukin-6 induces cellular insulin resistance in hepatocytes. *Diabetes.* 2002;51(12):3391–3399.
36. Senn JJ, et al. Suppressor of cytokine signaling-3 (SOCS-3), a potential mediator of interleukin-6-dependent insulin resistance in hepatocytes. *J Biol Chem.* 2003;278(16):13740–13746.
37. Weigert C, et al. Direct cross-talk of interleukin-6 and insulin signal transduction via insulin receptor substrate-1 in skeletal muscle cells. *J Biol Chem.* 2006;281(11):7060–7067.
38. Muse ED, et al. Role of resistin in diet-induced hepatic insulin resistance. *J Clin Invest.* 2004; 114(2):232–239.
39. Yang X, Smith U. Adipose tissue distribution and risk of metabolic disease: does thiazolidinedione-induced adipose tissue redistribution provide a clue to the answer? *Diabetologia.* 2007;50(6):1127–1139.
40. Koonen DP, et al. Increased hepatic CD36 expression contributes to dyslipidemia associated with diet-induced obesity. *Diabetes.* 2007;56(12):2863–2871.
41. Summers SA. Ceramides in insulin resistance and lipotoxicity. *Prog Lipid Res.* 2006;45(1):42–72.
42. Pennisi P, et al. Recombinant human insulin-like growth factor-I treatment inhibits gluconeogenesis in a transgenic mouse model of type 2 diabetes mellitus. *Endocrinology.* 2006;147(6):2619–2630.
43. Burgess SC, et al. Cytosolic phosphoenolpyruvate carboxykinase does not solely control the rate of hepatic gluconeogenesis in the intact mouse liver. *Cell Metab.* 2007;5(4):313–320.
44. Samuel VT, et al. Fasting hyperglycemia is not associated with increased expression of PEPCK or G6Pc in patients with Type 2 Diabetes. *Proc Natl Acad Sci U S A.* 2009;106(29):12121–12126.
45. Nolsoe RL, et al. Association of a microsatellite in FASL to type II diabetes and of the FAS-670G>A genotype to insulin resistance. *Genes Immun.* 2006; 7(4):316–321.
46. Bashan N, et al. Mitogen-activated protein kinases, inhibitory-kappaB kinase, and insulin signaling in human omental versus subcutaneous adipose tissue in obesity. *Endocrinology.* 2007; 148(6):2955–2962.
47. Harman-Boehm I, et al. Macrophage infiltration into omental versus subcutaneous fat across different populations: effect of regional adiposity and the comorbidities of obesity. *J Clin Endocrinol Metab.* 2007;92(6):2240–2247.
48. Stranges PB, et al. Elimination of antigen-presenting cells and autoreactive T cells by Fas contributes to prevention of autoimmunity. *Immunity.* 2007;26(5):629–641.
49. Konrad D, Rudich A, Schoenle EJ. Improved glucose tolerance in mice receiving intraperitoneal transplantation of normal fat tissue. *Diabetologia.* 2007;50(4):833–839.
50. Rudich A, et al. Indinavir uncovers different contributions of GLUT4 and GLUT1 towards glucose uptake in muscle and fat cells and tissues. *Diabetologia.* 2003;46(5):649–658.
51. Knight JA, Anderson S, Rawle JM. Chemical basis of the sulfo-phospho-vanillin reaction for estimating total serum lipids. *Clin Chem.* 1972;18(3):199–202.
52. Bligh EG, Dyer WJ. A rapid method of total lipid extraction and purification. *Can J Biochem Physiol.* 1959;37(8):911–917.
53. Pfaffl MW. A new mathematical model for relative quantification in real-time RT-PCR. *Nucleic Acids Res.* 2001;29(9):e45.
54. Souza SC, et al. Modulation of hormone-sensitive lipase and protein kinase A-mediated lipolysis by perilipin A in an adenoviral reconstituted system. *J Biol Chem.* 2002;277(10):8267–8272.
55. Fukuzumi M, Shinomiya H, Shimizu Y, Ohishi K, Utsumi S. Endotoxin-induced enhancement of glucose influx into murine peritoneal macrophages via GLUT1. *Infect Immun.* 1996;64(1):108–112.